1-1-2016

Hot-melt extrusion: A versatile pharmaceutical technology

Hemlata Patil
University of Mississippi

HOT-MELT EXTRUSION: A VERSATILE PHARMACEUTICALTECHNOLOGY

Dissertation

presented in partial fulfillment of requirements

for the degree of Doctor of Philosophy

in the Department of Pharmaceutics and Drug Delivery

The University of Mississippi

by

HEMLATA PATIL

December 2016

ABSTRACT

Hot-melt extrusion (HME) is a promising technology for the production of new Chemical entities in the developmental pipeline and for improving products already on the market. The first objective of this research work was to describe a continuous process for the production of solid lipid nanoparticles (SLN) as drug-carrier systems via hot-melt extrusion (HME) using Quality by Design (QbD) principles. Fenofibrate SLN were prepared by combining two processes: HME technology for melt-emulsification and high-pressure homogenization (HPH) for size reduction. Varying the process parameters enabled the production of SLN below 200 nm. At the end of a 5-h *in-vitro* dissolution study, a SLN formulation released 92– 93% of drug, whereas drug release was approximately 65% and 45% for the marketed micronized formulation and crude drug, respectively. The second objective of this research work was to develop pH-independent/dependent sustained release (SR) tablets of ondansetron HCl dihydrate (OND). The *in-vitro* release study demonstrated sustained release for 24 h with 90% of drug release in formulations using stearic acid in combination with ethyl cellulose, whereas 100% drug release in 8 h for stearic acid-hydroxypropylcellulose matrices. The third objective of this research work was apply a QbD approach based on design of experiments as a risk-based proactive approach to achieve predictable critical quality attributes (CQAs) to develop a dry-granulation process for controlled release formulation of OND SR tablets by twin-screw extruder. The effect of screw speed, feed rate and amount of fumaric acid on the particle size and flow properties of the granules and time required for complete and controlled release of the drug

from the dosage was optimized by 2^3 factorial design. Based on the design of experiment (DOE) results, a formulation comprising of 2.5 % (w/w) fumaric acid extruded at high screw speed (100 rpm) and low feed rate (1%) was found to fulfill requisites of an optimum formulation. The fourth objective was to understand the dehydration behavior of OND during HME process. Hydrates of active pharmaceutical ingredients may undergo dehydration during the manufacturing process and/or storage. This can affect the physiochemical properties of the formulation including solubility, dissolution rate, bioavailability and stability.

DEDICATION

Dedicated to my lovely family for their continuous support and trust in me.

ACKNOWLEDGMENTS

I am extremely grateful to my advisor Dr. Michael A. Repka, to thank him words would not be sufficient, for his expert guidance and scholarly supervision during the course of my graduate study. His scrupulous supervision, cordial advice and feats of knowledge have casted a spell on me and will serve as a beacon star to my path ahead. He has instilled in me self-confidence and patience, which made me to accomplish the research problems successfully. I would also like to thank my committee members, Dr. Soumyajit Majumdar, Dr. Seongbong Jo, and Dr. Samir A. Ross for their valuable time, critical reviews and suggestions regarding my research work at OleMiss.

I would like to acknowledge my family, who always motivated me in my life and career path. I would like to specially mention my husband Roshan Tiwari, because of his continuous support and understanding helped me to achieve my target on time, thanks for your love and care

I acknowledge with thanks, the valuable suggestion, criticism and co-operation from my friends and lab colleagues.

I would like to thank School of Pharmacy, The University of Mississippi for giving me an opportunity to do research.

TABLE OF CONTENTS

LIST OF TABLES

LIST OF FIGURES

CHAPTER I

HOT-MELT EXTRUSION TECHNOLOGY

1.1 Introduction

Hot-melt extrusion (HME) processing was established in the early 1930s, and during that time, it rapidly became the most widely applied processing technology in the plastic, rubber, and food industries. The application of HME expanded to the pharmaceutical industry at the beginning of the 1970s and was used in formulation and product development as well as manufacturing. The first application of HME as a manufacturing tool in the pharmaceutical industry was investigated by El-Egakey *et al.* (1971) using poly (vinyl acetate-co-methacrylic acid) and epoxy resin containing a secondary amine as a polymeric carrier [1]. HME is a continuous pharmaceutical process that involves pumping polymeric materials with a rotating screw at temperatures above their glass transition temperature (Tg) and sometimes above the melting temperature (Tm) to achieve molecular level mixing of the active compounds and thermoplastic binders, polymers, or both. This molecular mixing converts the components into an amorphous product with a uniform shape and density, thereby increasing the dissolution profile of the poorly water-soluble drug. Additionally, HME has been utilized for the delivery of water soluble drugs with several applications such as taste masking [2]. This exciting yet challenging technology may offer several advantages over conventional pharmaceutical manufacturing processes such as shorter and more efficient time to achieve the final product environmental advantages due to the elimination of solvent use, and increased efficiency of drug

delivery to the patient. As a result, HME has emerged as an alternative "platform technology" to other traditional techniques for manufacturing pharmaceutical dosage forms such as tablets, capsules, films, and implants for drug delivery *via* oral, transdermal, and transmucosal routes. The introduction of HME to pharmaceutical formulation development has made sophisticated equipment such as the extruder, customized downstream auxiliary equipment, and monitoring tools available for application in the evaluating the performance and product quality. This enhanced availability has supported the growth of this innovative technique in pharmaceutical manufacturing processes utilizing both single and twin-screw extruders.

To date, several research articles have been published describing the use of HME as the novel technique of choice in dealing with the day-to-day formulation challenges of new active pharmaceutical ingredients (APIs). Moreover, numerous aspects of the HME technology have been extensively cited in the literature. Additionally, the number of patents based on HME techniques has risen steadily worldwide in recent decades [3-11].

Regulatory bodies continue to encourage the investment in the use of quality by design (QbD) and process analytical technology (PAT), which are already essential tools in the HME process, to enhance product and process understanding. As a continuous process, HME fits perfectly within this framework. PAT tools including Raman and near infrared (NIR) spectroscopy play an important role in real–time quality evaluation and understanding of the extrusion process in the production pharmaceutical dosage forms.

1.2. Hot-Melt Extrusion: Equipment and Process

1.2.1. Equipment

Pharmaceutical-class extruders have evolved and adapted to mix APIs with carriers, plasticizers, or with other processing aids to develop various solid dosage forms. The major

difference between the pharmaceutical-class extruder and a ″plastic extruder″ are the contact parts, which are specifically configured to meet the current regulatory norms of manufacturing dosage forms [4]. The HME process is implemented using the equipment that mainly consists of an extruder, ancillary equipment for the extruder, downstream processing equipment, and other controlling tools used for performance and product quality evaluation. The extruder generally consists of a feeding hopper that is the opening through which material enters the barrel, a conveying section that is comprised of barrels and single or twin screws, the die for shaping the extrudates and a screw-driving unit. The ancillary equipment for the extruder consists of a heating/cooling device for the barrels, a conveyer belt to cool down the product and a solvent delivery pump for cooling, cutting, and/or collecting the finished product [12]. The controlling devices on the equipment include temperature gauges, a screw-speed controller, an extrusion torque monitor, and pressure gauges.

Different types of screw extruders are available such as single or multi-screw extruders. Multiscrew extruders can involve either two screws (twin screw design) or generally up to four. Single screw extruders (SSE) are still utilized within the plastics field; however, their use in pharmaceuticals is limited. SSE consists of one rotating screw inside a stationary cylindrical barrel subdivided into three distinct zones: feeding zone, compressing zone, and metering zone. The barrel is generally manufactured in sections, which are either bolted or clamped with each other. The three primary functions of SSE are conveying, melting, and pumping polymers into a desired shape. The shape of the extruded product depends on the type of die connected to the end of the barrel [3]. Mechanical simplicity and a low cost of investment and minimal maintenance make SSE a good choice for the manufacturing of plastic extruded products. However, it has some limitations, such as poor mixing capability, and, therefore, it is not the preferred option for

the manufacturing of most of the pharmaceutical formulations where high kneading and dispersing capacities are required. To overcome the stated limitations of SSE, multiscrew extruders were developed. The first twin-screw extruder (TSE) was developed in the late 1930s in Italy. The TSE has two agitator assemblies mounted on parallel shafts. Different types of TSE are available with each type having distinct operating principles and applications in processing. The two main types of TSE are either co-rotating (rotate in the same direction) or counter-rotating (the opposite direction). These two types of TSE can further be classified as either fully intermeshing or non-intermeshing [13, 14]. Schematic presentation of a TSE setup is provided in Figure 11.1.

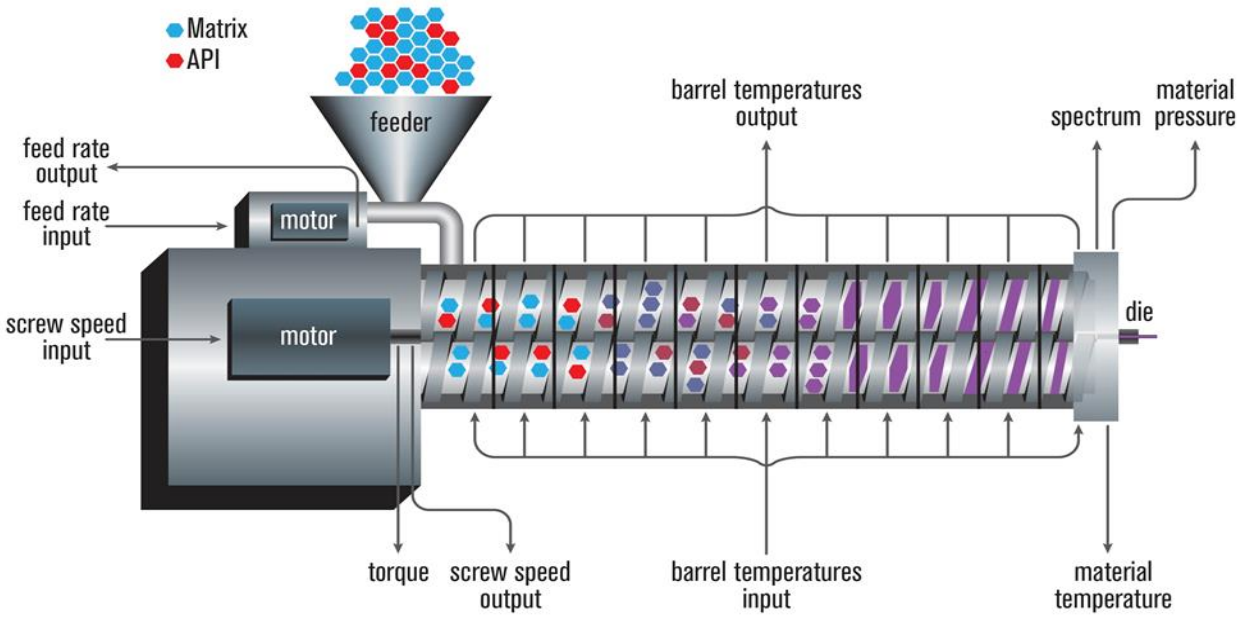

Fig 1.1: Schematic diagram of twin-screw extruder

The difference between SSE and multiscrew extruders is their mode of operation. In an SSE, friction between the material and the rotating screw allows the material to rotate with the screw, and the friction between the rotating material and the barrel pushes the material forward,

which results in the generation of heat. Therefore, for achieving high throughput in SSE by increasing screw speed results in the increase in frictional heat and therefore higher temperatures. Whereas, intermeshing screws of TSEs pushes the material forward with the relative motion of the flight of one screw inside the channel of the other. In TSEs, heat is therefore controlled independently from an outside source and is not influenced by screw speed. This difference in the operation becomes important when processing a thermos labile drug.

When compared with SSE, intermeshing corotating TSEs generally provides better mixing to produce a homogeneous solid containing finely distributed and dispersed active compounds, better melt temperature control therefore less tendency to overheat, little dependence on the materials friction coefficients, and short transit time due to relatively fast melting [13, 14].

1.2.2. Process

Although HME is considered as a unit operation, for a theoretical understanding, the process can be categorized into the following sub processes:[3, 4, 12-14]

1. Material feeding of the extruder with assistance of a hopper.

2. Conveying of mass.

3. Flow through the die.

4. Finally, extrudates from the die and subsequent downstream processing.

1. *Material feeding*: Active compounds, carriers, plasticizers, or other processing excipients can be used as a preblend or can be introduced as an individual feed stream with the aid of a hopper(s) through feeding zone of the extruder by using either gravimetric (loss-in-weight) or

volumetric feeders. The preblend must have good flow. Feed rate, feed type, and oscillation in feeding rate affects the degree of fill, which influences the homogeneity, thermal, and mechanical energy input into the formulation.

2. *Conveying of mass*: The material enters the feeder onto the rotating screws and is transported toward the die in the conveying section. This section includes several operations, such as melting, mixing, grinding, reduction in particle size, venting, and kneading. Therefore, the conveying process is mainly dependent upon screw speed and filling level, melting point of the individual components, particle size of the components, residence time, and screw configuration [15]. Modified screw designs are used when high shear is required to prepare an extrudate. Different types of screw elements to achieve desired results are shown in Figure 1.2.

3. *Flow through the die*: At the end of barrel, a die is attached to the extruder in order to extrude the material. After the conveying section, the next step within the extrusion process is to pump the molten mass into the die. Different shapes of a die are available and are used depending on the desired end product shape.

4. *Extrusion from the die and following downstream processing*: Just before the die, high pressure is generally incurred, which allows nearly 100 % screw fill level and ensures a constant melt flow through the die to provide an even shaping. Once the molten mass exit from the die, downstream processing plays a role into finishing, shaping, and analyzing the extruded product. The finishing process entails different downstream ancillary components are involved, such as conveyor belts that transfer the extruded product from the die to the end of the processing line. The molten extrudates are often cooled by chill rolls and then either milled into powder or cut into rods by a strand-cutter. Sometimes pelletizers are also used to cut the extrudates into smaller units.

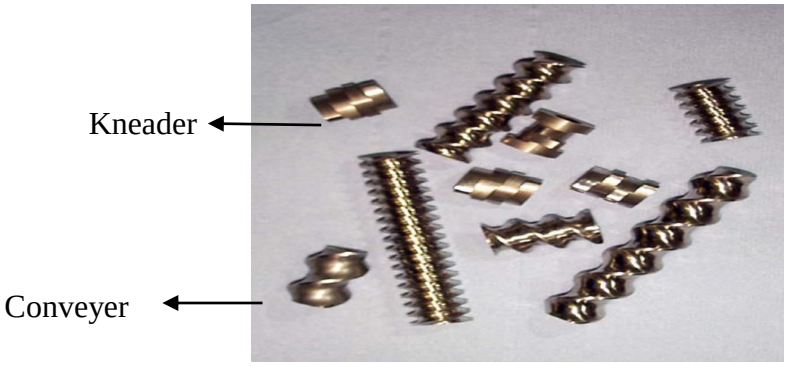

Fig1.2: Modular screws design

1.3. Advantages and Disadvantages of Hot-Melt Extrusion

HME offers several distinct advantages over conventional pharmaceutical formulation techniques [2-4, 11-14]

1. HME is a continuous and efficient process, which thus enables high throughput, online monitoring, minimal and controlled processing, and manageable process variables.

2. Solvent free techniques also reduce the number of processing steps and eliminate the time consuming drying step. Also, there is no need to handle potentially dangerous solvents, resulting in the absence of residual solvents in the final formulation.

3. HME increases the solubility and potential bioavailability of poorly water-soluble and insoluble compounds, mainly by molecular dispersion of the drug within the final dosage form.

4. This processing technique may not require major downstream processing such as compression (tablets, etc.).

5. Uniform dispersion of fine particles resulting from the intense mixing and agitation imposed by the rotating screw, which cause de-aggregation of suspended particles in the molten polymer, is another attribute of this technology.

6. Properly processed, one can achieve good stability at various pHs and moisture levels.

7. Wide array of pharmaceutical dosage forms such as pellets, granules, sustained/controlled release, oral fast dissolving system, targeted release such as transdermal, transmucosal, and transungual delivery system and implants. HME has also recently been used for taste-masking and drug-abuse deterrent products.

8. Fortunately, the equipment has a wide range of screw geometries available for processing.

9. HME technology is useful for low compressibility index APIs. Poorly compactable material can be easily compressed into tablets by this technique.

10. Compared to other techniques, hot-melt extruded solid solutions are thermodynamically stable if proper planning of the process is utilized.

Even though HME offers several advantages, like any pharmaceutical processing technique, it entails a few disadvantages, which includes the following. However, some of these can be managed and minimized:

1. HME may require high processing temperatures, which tend to limit its applicability in processing of thermolabile compounds. Thus, it is not suitable for relatively high heat sensitive molecules such as proteins and microbial species.

2. There are a finite number of heat-stable polymers.

3. The process requires high energy input.

CHAPTER II

CONTINUOUS PRODUCTION OF FENOFIBRATE SOLID LIPID NANOPARTICLES BY HOT-MELT EXTRUSION TECHNOLOGY: A SYSTEMATIC STUDY BASED ON A QUALITY BY DESIGN APPROACH

2.1. Abstract

This contribution describes a continuous process for the production of solid lipid nanoparticles (SLN) as drug-carrier systems via hot-melt extrusion (HME). Presently, HME technology has not been used for the manufacturing of SLN. Generally, SLN are prepared as a batch process, which is time consuming and may result in variability of end-product quality attributes. In this study, using Quality by Design (QbD) principles, we were able to achieve continuous production of SLN by combining two processes: HME technology for melt-emulsification and high-pressure homogenization (HPH) for size reduction. Fenofibrate (FBT), a poorly water-soluble model drug, was incorporated into SLN using HME-HPH methods. The developed novel platform demonstrated better process control and size reduction compared to the conventional process of hot homogenization (batch process). Varying the process parameters enabled the production of SLN below 200 nm. The dissolution profile of the FBT SLN prepared by the novel HME-HPH method was faster than that of the crude FBT and a micronized marketed FBT formulation. At the end of a 5-h *in vitro* dissolution study, a SLN formulation

released 92–93% of drug, whereas drug release was approximately 65 and 45% for the marketed micronized formulation and crude drug, respectively. Also, pharmacokinetic study results demonstrated a statistical increase in Cmax, Tmax, and AUC0–24 h in the rate of drug absorption from SLN formulations as compared to the crude drug and marketed micronized formulation. In summary, the present study demonstrated the potential use of hot-melt extrusion technology for continuous and large-scale production of SLN.

2.2. Introduction:

Quality by design (QbD) is a holistic, systematic, risk-based proactive approach aimed at final product quality. This approach begins with predefined objectives to ensure predictable product quality. The main purpose of QbD is to identify and control critical parameters which affect product quality [16-18]. QbD has been promoted by the United States Food and Drug Administration (US FDA) as a way to enhance pharmaceutical development through design efforts from product conceptualization to commercialization [19]. Formulation of drugs, which are poorly water soluble, is the most challenging problem with respect to their biopharmaceutic quality, because slow and erratic dissolution prevents these compounds from being rapidly and completely absorbed from the gastrointestinal tract [20]. Several nanosized formulations were developed recently to overcome these problems [21]**.** In these nanosized formulations, solid lipid nanoparticles (SLN) are one of the potential drug delivery systems and have been reported for controlled drug delivery, bioavailability enhancement by modification of dissolution rate and/or by improving tissue distribution and, targeting of drugs by using various application routes. SLN are mainly formulated by non-solvent or solvent-based techniques. The solvent-based technique utilizes organic solvents to dissolve the solid lipid; the solvent is then evaporated from the emulsion to obtain SLN. In the non-solvent technique, the solid lipid is liquefied over its melting

point and is subsequently converted to nanoemulsions through common techniques such as high-pressure homogenization, in which cooling further results in SLN [5].

For more than two decades, fibrates played an important role in the treatment of hyperlipidemia. Fenofibrate (FBT) is one of the most commonly used fibrate worldwide. FBT is a pro-drug of fenofibric acid, approved to treat hypertriglyceridemia because it reduces low-density lipoprotein (LDL), and very-low-density lipoprotein (VLDL) while increasing the level of high-density lipoprotein (HDL) [22, 23]. It belongs to BCS II, which means that it is lipophilic with a logP value of 5.6 and practically insoluble in water [22, 24, 25]. The major drawback of FBT is its low bioavailability when taken under fasting conditions. Thus, there is a need to develop a new formulation/process in order to increase the FBT dissolution rate and improve its oral bioavailability.

High pressure homogenization (HPH) has emerged as a reliable and powerful technique for the preparation of SLN [25]. HPH (hot and cold homogenization) have been explored for the feasibility in scaling-up. However, these methods for SLN preparation needs a preparatory step that involves the drug incorporation into the bulk lipid which in-turn involves multistep processes such as melting of lipid, dispersion or dissolution of drugs in melted lipid, preparation of aqueous dispersions and finally size reduction, which makes this as a batch process. The pharmaceutical industry prefers a continuous process over a batch process as the continuous process is economical, it decreases the cost of production by less need of space, labor and resources as well as provides high efficacy and more desired product quality. On the other hand batch processes require careful and complex procedures and controls to prevent variations in the final product. During the manufacturing of SLN, emulsion preparation is often an essential step. Emulsion preparation is a batch process, while size reduction by high pressure homogenization is

a continuous process. Thus, the development of a continuous emulsion preparation process is an essential aspect to allow a fully continuous SLN production line. Therefore, new approaches are essential to both increase the quality of the product and to reduce the production time.

Hot-melt extrusion (HME) is an innovative technology for the production of a variety of dosage forms. HME technology may offer several advantages over conventional pharmaceutical manufacturing processes. Shorter and more efficient times to the final product, environmental advantages due to elimination of solvents in processing and increased efficiency of drug delivery to the patient make HME an exciting challenge for the pharma scientists and executives. Thus, HME has emerged as an alternative "platform technology" to other traditional techniques for pharmaceutical dosage forms, such as tablets, capsules, films and implants for drug delivery via oral, transdermal and transmucosal routes. HME technology is a potential continuous process of pumping raw materials at high temperatures and pressures resulting in a product of uniform shape and density [2, 3, 12]. To date several research articles have been published describing the use of HME as a novel technique of choice to deal with day-to-day formulation challenges of new active pharmaceutical ingredients (API). To the best of our knowledge, HME has not been reported in the literature for the manufacturing of SLN and this study utilizes HME technology for the manufacturing of drug-loaded SLN. The purpose of this current work was to develop a continuous process for SLN production using hot-melt extrusion for preparing a pre-emulsion and high pressure homogenization for further size reduction using the poorly water-soluble drug FBT as a model drug. In the present work, we will propose an improved method i.e HME-HPH method for the continuous production of FBT SLN, using Quality by Design (QbD) principles and a design of experiment (DOE) approach. We have used a Plackett-Burmen design in our present study to prepare FBT SLN.

2.3 Materials and Methods:

2.3.1. Materials:

Fenofibrate was purchased from Ria International (East Hanover, NJ, USA). Dynasan® 114 (trimyristin) and Imwitor® 900 K (Glyceryl stearate) were offered from Sasol Germany GmbH (Witten, Germany). Stearic acid, Compritol® 888 ATO (Glyceryl Dibehenate EP) and Precirol® ATO 5 (Glycerol Distearate (Type I) EP) was a kind gift from Gattafosse (USA). Cremophore EL and Tween 80 were purchased from Sigma-Aldrich (St. Louis, MO, USA). Lofibra® (200 mg micronized FBT capsule) was a commercial product produced by Global Pharmaceuticals (Chalfont, PA, USA). HPLC grade Acetonitrile was obtained from Fisher Scientific (USA). D.I water was used throughout the study. All other chemicals were of analytical grade.

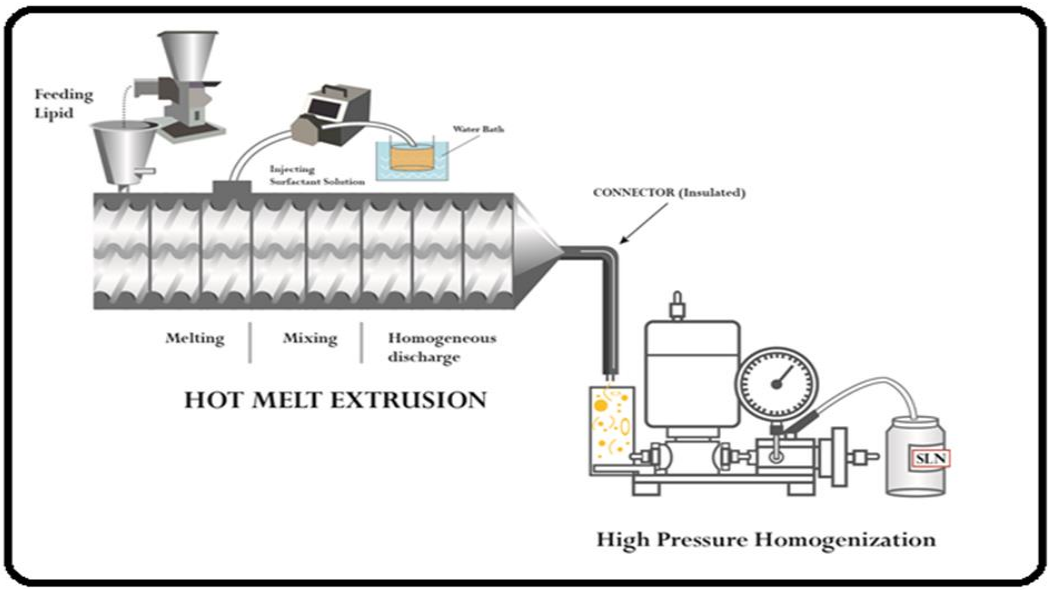

Fig 2.1: Schematic representation of Continuous Preparation of SLNs using Hot Melt Extrusion connected to High Pressure Homogenizer

2.3.2 Experimental set up:

A schematic illustration of SLN formation by HME-HPH system is shown in Fig 2.1. Briefly, it consists of two parts, a hot melt extruder and high pressure homogenizer. Extruder is typically consisting of a motor, which act as a drive unit, feeding hopper, an extrusion barrel, a rotating screw and an extrusion die. An electronic control unit is connected to the extruder which controls the screw speed, temperature, pressure, and feed rate. Generally one or two rotating screws are used inside a stationary cylindrical barrel. Here we are using two rotating screws inside the stationary cylindrical barrel. For this study we are using two different types of screw configuration i.e standard configuration and modified configuration (Fig. 2.2). Extruder barrel consist of 8 zones. First zone is used for the drug-lipid physical mixture feeding and either zone 3 or zone 4 was used for the addition of surfactant aqueous solution. The first part that is extruder is connected to the second part high pressure homogenizer via connector which is insulated to prevent the loss of heat.

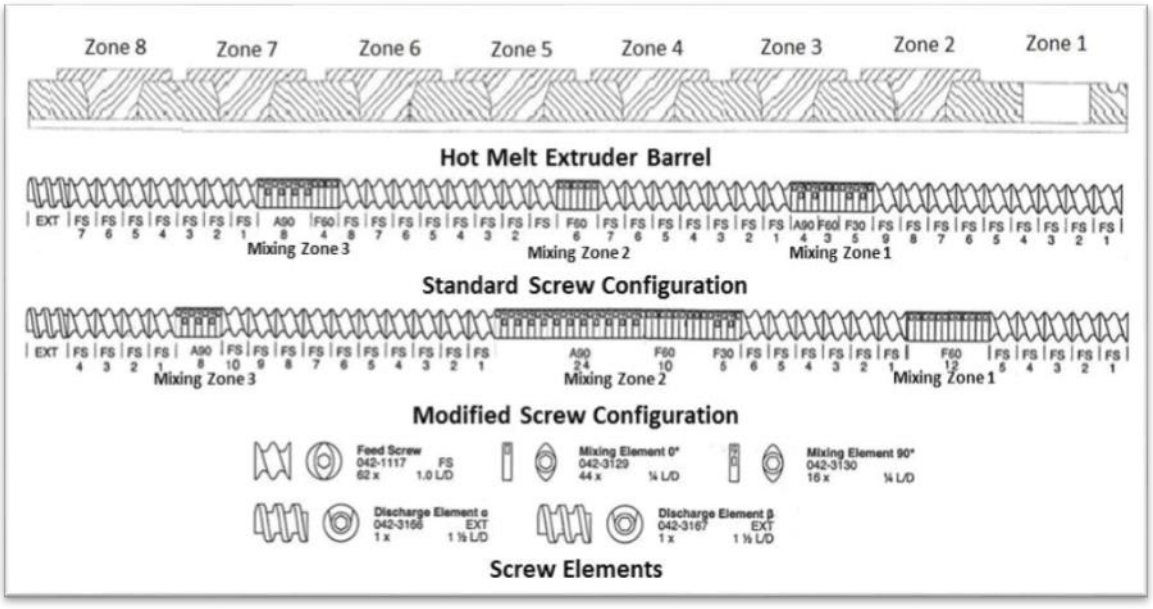

Fig 2.2: Screw Configuration and Mixing zones used in the preparation of SLNs by HME

2.3.3. Preparation of Fenofibrate SLN:

2.3.3.1 Solubility Studies:

Solubility studies were performed to identify suitable lipids for the development of the FBT SLN. The lipid used in the system should have high solubilization capacity for the drug, ensuring the solubilization of the drug in the resultant dispersion. The screening of lipids was performed by evaluating the solubility of FBT (10-25 % w/w with respect to lipid mass) in different lipids such as Stearic acid, Compritol® 888 ATO, Precirol® ATO 5, Dynasan 114 and Imwitor® 900 K. Measured 10 – 25 mg of FBT was added into each vial containing 100 mg of selected excipient. Then, the mixture was heated at 90 °C in a water bath to facilitate the solubilization and the melt of drug and lipid were physically observed to confirm the presence or absence of insoluble drug crystals.

2.3.3.2 Preliminary study:

Preliminary study was conducted to identify process variables to be used for the preparation of FBT SLN. In the preliminary study formulation variables for SLN such as drug concentration, lipid concentration, surfactant concentration, different lipid and different surfactant were optimized to obtain SLN with particle size below 200 nm with maximum entrapment efficiency. Further, process variables such as screw configuration, barrel temperature, zone of liquid addition and screw speed were optimized. Ishikawa diagram (also known as fish-bone diagrams, or cause-and-effect diagrams) were constructed to identify the potential risks and corresponding causes was created to identify quality attributes for the better performance of developed FBT SLN by HME-HPH technique (Fig. 2.3). Particle size, polydispersibility index, zeta potential and entrapment efficiency were found to be critical quality attributes of the FBT SLN. Factors responsible for these quality attributes were identified as critical process parameters. Plackett-

Burmen screening experimental design was commonly used to identify these CPP that influence product critical quality attributes.

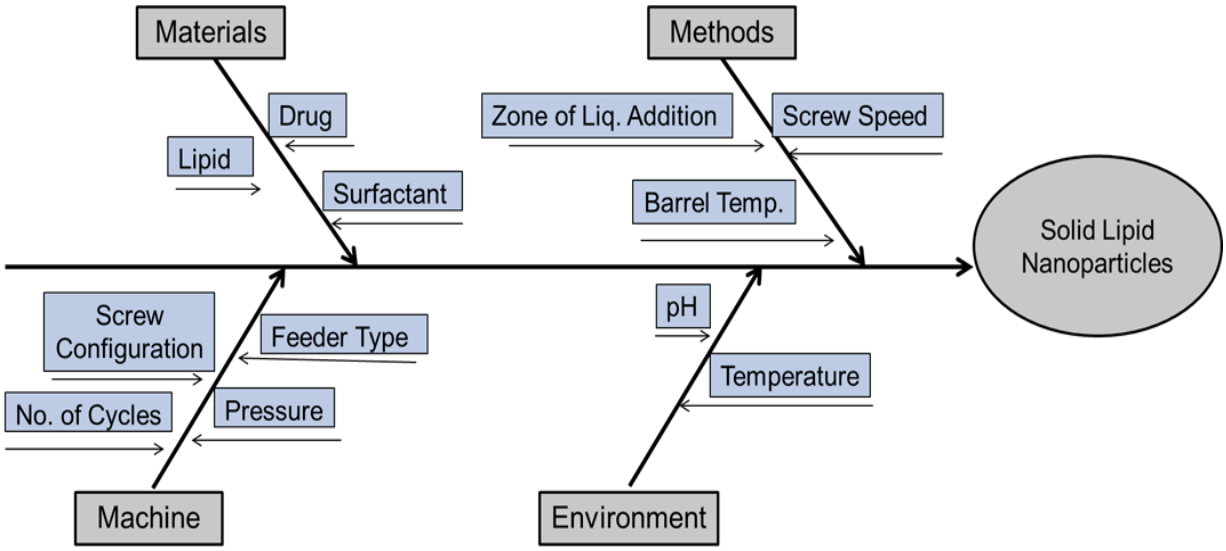

Fig 2.3: Modified Ishikawa Diagram

2.3.3.3 Formulation of FBT SLN:

SLN were prepared by mixing a lipid and aqueous phase containing surfactant inside the extruder barrel at temperatures 10-15 °C above the melting point of the lipid which results in the formation of an emulsion. The selected lipids (Compritol® 888 ATO/Precirol® ATO 5) and FBT geometric mixture was fed into the co-rotating twin-screw extruder (11 mm Process 11, Thermo-Fisher Scientific Karlsruhe, Germany) using a volumetric feeder. Different concentrations of a surfactant Cremophore EL (Sigma Aldrich, USA) /Pluronic® F 68(BASF,USA) aqueous solution, equivalent to the extrusion temperature, was injected into the extruder barrel either zone 3 or zone 4 through an injection port using a peristaltic pump. The barrel temperature for zone 2 was either 150 °C or 120 °C; Zone 3 and the rest of the zones including the die temperature were kept at 90 °C. Screw speed for all of the formulations was either 160 rpm or 240 rpm. The hot

pre-emulsion resulted from hot-melt extrusion was passed through an insulated tube connecting to the HME die and sample holder of the high pressure homogenizer (Avestin Emulsiflex C5, Canada) for size reduction. The HPH was performed at 85 °C and 1000 bar pressure with two repeated cycles to reduce the particle size of pre-emulsion resulting from melt extrusion. The HPH parameters were constant for all of the batches. Further, the size-reduced emulsion was cooled at room temperature to obtain SLN. The melt extrusion was performed by varying the formulation parameters such as drug concentration (DC), surfactant concentration (SC), lipid concentration (LC), surfactant (ST), lipid (LT) and by varying process parameters such as screw speed (SS), barrel temperature (BT) and zone of liquid addition (ZA).

2.3.3.4. Design of Experiment:

A set of Plackett-Burmen (PB) screening design was adopted to study the effect of critical process parameters on FBT SLN performance and characteristics. PB design is one of the most commonly used designs of experiment. They are the resolution three designs so they can be used when only main effects are of interest to be investigated. PB designs involve a large number of variables and relatively fewer runs. A total of 12 experimental trials with PB design were constructed using design expert stat-ease software version 9. Multilinear regression analysis and one way ANOVA were performed to test the significance of the model and the factor coefficients. The experimental runs (formulations) were prepared in triplicate. The dependent variables were average particle size (Y1), polydispersibility index (Y2), zeta potential (Y3), entrapment efficiency (Y4). The linear equation of the model is as follows:

$$Y = b0 + b1X1 + b2X2 + b3X3 + b4X4 + b5X5 + \cdots + bnXn \quad \text{eq. 1}$$

Where Y is the response, b0 is the constant and b1, b2. . .bn is the coefficient of factor X1, X2. . .Xn (representing the effect of each factor ordered within −1, +1).

2.3.3.5. HPLC analysis of fenofibrate *in-vitro*:

A Waters HPLC-UV system (Waters Corp, Milford, MA, USA) and UV detector set at wavelength of 286 nm. The separation of fenofibrate was performed on a Symmetry Shield RP 18 (5 µm) 4.6 × 250 mm column at 35 °C, eluted with acetonitrile and phosphoric acid in water (pH = 2.8) at a ratio of 85:15 (v/v). The mobile phase flow rate was maintained at 1.0 mL/min. Fenofibrate retention time was 7 min under these conditions. Injection volume was 20 µL. All of the HPLC data was analyzed using Empower V. software (Milford, MA, USA). The calibration curve was linear with a correlation coefficient of 0.9998 over the range of 0.5-50 µg/ml. The within-day and between-day coefficients of variations did not exceed 3%. The limit of detection (LOD) value for fenofibrate was 15ng/ml, and the limit of quantitation (LOQ) value was 50ng/ml, respectively. The accuracy of the method was verified with recovery values of 98-102%.

2.3.4. Characterization of FBT SLN:

2.3.4.1 Micromeritics measurement:

The mean particle size and polydispersity index (PDI) of the developed SLN were determined by using Zetasizer Nano ZS (Malvern, USA). Dynamic Light Scattering technique was used to measure particle size. This technique measures the diffusion of particles moving under Brownian motion, and converts this to size and a size distribution using the Stokes-Einstein relationship. The mean value of three repeated measurements for each sample was reported as the final measurement. SLN sample was diluted with sufficient water and diluted sample were directly

placed into cuvette and mean particle size and polydispersibility index were measured [26-28]. Zeta potential measurement was carried out with the same instrument Zetasizer Nano ZS. All results are an average of three measurements, which are calculated based on an average of 10 runs. Zeta potential is defined as a measure of degree of repulsion between charged particles. These repulsive forces prevent the particle aggregation and are therefore an indicator of physical stability of the formulation. According to the literature dispersion with the zeta potential more than ± 20 mV is physically stable [29]. The parameters for zetasizer were set as scattering angle was 173°, refractive index was 1.33, viscosity was 0.89 cP and the temperature was 25 °C.

2.3.4.2 Encapsulation efficiency measurement:

For the determination of the percentage entrapment efficiency, the SLN were first separated from the aqueous suspension medium by ultrafiltration-centrifugation using centrifugal filters (Amicon Ultra – 0.5 with 50 kDa cut-off, Millipore, USA) at 12000 rpm for 20 min at the room temperature. The percent entrapment efficiency was determined in triplicate indirectly by determining the amount of free FBT in the aqueous phase of the dispersion. The analysis of FBT was performed amount of free FBT in aqueous phase was measured by validated HPLC method at wavelength 288 nm. The separation of FBT was performed on a 250 × 4.6 mm BDS hypersil C18 column at 40 °C, eluted with water and acetonitrile (25:75; pH adjusted to 2.6 with o-phosphoric acid) at a flow rate of 1.0 ml/min. The FBT entrapment efficiency (EE) of SLN was calculated from the amount of drug determined by the HPLC analysis using the following equations,

$$\text{Entrapment efficiency} = \frac{\text{Total amount of FBT loaded} - \text{Free FBT in supernatant}}{\text{Total amount of FBT loaded}} \times 100$$

2.3.5. Quantification of drug release *in-vitro*:

Dissolution tests for the crude FBT and the marketed micronized FBT formulation (200 mg) were performed with a dissolution apparatus using the paddle method. The accurately weighed amount of crude FBT (200 mg filled in gelatin capsules) and marketed FBT formulation were placed in 900ml phosphate buffer pH 7.4 containing 0.3% sodium lauryl sulfate (SDS) at 37 °C and 75 rpm. An aliquot of 1.5 ml release media was withdrawn at intervals of 5, 10, 15, 30, 45, 60, 90, 120, 180, 240 and 300 min, and then replaced by 1.5 ml of fresh dissolution fluid. Each sample was passed through a 0.45 µm syringe filter and determined by HPLC (see section 2.3.5). The drug release from SLN formulations was performed by using the dialysis bag technique. This is the most exclusively used method reported in the literature to estimate drug release from the SLN. We are using dialysis bag method as previously used for studying drug release kinetics of nanoparticulate systems by Luo et al. [30] with some modifications. Phosphate buffer pH 7.4 containing 0.3% SDS was used as the release medium. The dialysis bag retains nanoparticles and allows the free drug into the dissolution media with a cut-off of 10–14 kDa. The bags were soaked in double-distilled water for 12 h before use. Two milliliters of SLN dispersion was poured into the bag with the two ends fixed by clamps and immersed in 50 mL of pre-heated release medium in conical flask. The conical flasks were placed into a reciprocal shaking water batch manufactured by Precision (Cat. No 51221080) at 37 °C at a rate and 150 rpm. At fixed time intervals (Same time points which used for the dissolution of crude FBT and marketed formulation), the medium in the conical flask was removed and filtered for analysis and fresh dissolution medium was then added to maintain sink condition. The amount of drug in the filtrate was analyzed by HPLC method as described above. Measurements for all three crude FBT, marketed formulation and SLN formulation were performed in triplicate and averages are reported here.

2.3.6. Comparison between the SLN prepared by conventional method and novel HME-HPH method:

From PB design, three optimized formulations PB 7, PB 8 and PB 9 were selected and prepared by a conventional method as described earlier by Shengpeng et al [31]. Briefly, in conventional method lipid and drug heated up to temperature 10-15 °C above the melting point of lipid and drug. Surfactants were dissolved in beaker with water, and then added into melted drug and lipid drop by drop over 70–80 ºC water bath. The obtained pre-emulsion was passed through a high pressure homogenizer. These three formulations were compared for characteristics such as PS PDI and ZP when prepared by conventional and by novel HME-HPM techniques.

2.3.7. In-vivo pharmacokinetic study:

All animal care and experimental studies were approved by the Institutional Animal Care and Use Committee (IACUC) with protocol no. 14-013. Jugular vein cannulated male Wistar rats (body weight 250 ± 10 g, Harlan laboratories, Indiana, USA) were housed in cages for a minimum of at least three days prior to begin of the study and had free access to food and water. Rats were randomly divided into three groups of six animals each. The rats were fasted for 12 h prior to experiments and after 2 h of dosing of formulations gave access to food. The oral dose of FBT was 12.5 mg/animal, thus 0.5 ml formulation was administered to each rat. The crude FBT drug was suspended in 0.1% SLS aqueous solution and the commercial micronized FBT formulation was diluted 1:10 with saline prior to administration by gavage. The SLN formulation was administered undiluted. Serial blood samples (200 µl) was taken from the cannulated jugular vein, pre-dose and at time points of, 0.5, 1, 2, 4, 6, 8, 10, 24 h post-dosing. The whole blood was collected into heparin coated tubes and centrifuged at 4 °C at 12,000 rpm for 5min to obtain plasma. The plasma samples were kept frozen at -80 °C until analysis.

2.3.7.1. Plasma processing and HPLC analysis:

Fenofibric acid was determined by an HPLC-UV method as describe above. The sample preparation of the plasma samples was based on the procedure described by Hanafy et al. [20] with a little modification. An aliquot of 100 µl plasma and 400 µl methanol was transferred to Eppendorf tubes and vortexed for 1 min, followed by the centrifugation at 12,000 rpm for 10 min at 4 °C. An aliquot of 20 µl supernatant was injected into the HPLC system and the fenofibric acid was detected. The standard calibration curve was prepared in plasma similarly as described above. The standard curve was obtained, with a correlation coefficient of 0.9998 over the concentration range from 0.11 µg/ml to 123.68 µg/ml. The recovery by the described procedure was more than 92% in the investigated concentration range.

2.3.7.2. Data and statistical Analysis:

The pharmacokinetic parameters were calculated based on a non-compartmental model. The area under the concentration-time curve from time zero to time t (AUC_{0-t}) was calculated using trapezoidal method. Peak concentration (C_{max}) and time of peak concentration (T_{max}) were obtained directly from the concentration-time profiles. Differences between batches were analyzed by one-way analysis of variance (ANOVA) followed by Tukey test. $P < 0.05$ was considered statistically significant. All values were reported as mean of four findings.

2.3.8. Stability Study:

The stability of the developed SLN formulation was conducted for 6 months as per International Conference on Harmonization (ICH) Q1A (R2) guidelines. The optimized formulation (PB 9 design) was selected for the stability study. Briefly, samples were stored in the sealed amber

colored glass vials at 4 °C and at 25 °C. After 1, 3 and 6 months, the samples were characterized with respect to particle size, ZP, PDI, and EE.

2.4. Results and Discussion:

2.4.1. Solubility of FBT in lipids:

The assessment of solubility of drug in the lipid material is the first step in the selection of lipids for the formulation of SLN dispersions as solubility of the drug in the lipid is one of the most important factors for determining entrapment efficiency (EE) of the SLN. Four lipids with different physicochemical properties were selected and results from the solubility studies are shown in Table 2.1. Among five lipids, FBT was not completely soluble in Stearic acid, Dynasan® 116 and Imwitor® 900K whereas no drug crystals were observed when FBT was heated together with Precirol® ATO 5 for all three concentrations tested (10-20 mg). Also when FBT was heated with Compritol® ATO 888, no drug crystals were observed for all four concentrations tested (10-25mg). This study indicated that EE of FBT in Compritol® ATO 888 and Precirol® ATO 5 might be more than Dynasan® 116 and Imwitor® 900K. Thus Compritol® ATO 888 and Precirol® ATO 5 were selected for the preparation of SLN.

Table 2.1: Screening of lipids based on solubility of Fenofibrate ('+' indicates no drug crystal and '–' indicates drug crystal seen at the end of test)

Lipid	mg Fenofibrate/100 mg solid lipid			
	10	15	20	25
Stearic acid	+	-	-	-
Compritol ATO 888	+	+	+	+
Precirol	+	+	+	-
Dynasan 114	+	+	-	-
Imwitor 900K	+	-	-	-

2.4.2. Formulation of FBT SLN:

From the preliminary studies, formulation parameters such as DC, SC, LC, ST and LT were found to have significant effects on characteristics of the SLN. Also process parameters such as screw configuration, BT, ZA and SS were found to have substantial effects. A modified screw configuration was selected to prepare all SLN formulations. To study the effect of formulation and process parameters, PB design approach was used. Experimental factors and their levels are given in Table 2.2 and the experimental design is shown in Table 2.3.

Table 2.2: Experimental factors and their levels

Factor	Factor Significance	Unit	Level (-1)	Level (+1)
X1	Drug Concentration	**% w/w**	0.5	1
X2	Lipid Concentration	**% w/w**	6	8
X3	Surfactant concentration	**% w/w**	1.5	3
X4	Surfactant	**--**	Cremophore EL	Tween80
X5	Screw speed	**RPM**	160	240
X6	Barrel Temperature	**°C**	120	150
X7	Zone of Liquid addition	**--**	3	4
X8	Lipid	--	Compritol® ATO 888	Precirol® ATO 5

Table 2.3: Experimental Design

PB	X1	X2	X3	X4	X5	X6	X7	X8
1	1	6	3	Tween 80	160	150	4	Precirol
2	0.5	6	1.5	Tween 80	160	150	4	Compritol
3	1	8	3	Cremophore EL	160	120	4	Compritol
4	0.5	8	3	Tween 80	160	120	3	Precirol
5	1	6	3	Tween 80	240	120	3	Compritol
6	0.5	8	1.5	Tween 80	240	120	4	Precirol
7	0.5	6	1.5	Cremophore EL	160	120	3	Compritol
8	0.5	6	3	Cremophore EL	240	150	3	Precirol
9	0.5	8	3	Cremophore EL	240	150	4	Compritol
10	1	8	1.5	Cremophore EL	160	150	3	Precirol
11	1	6	1.5	Cremophore EL	240	120	4	Precirol
12	1	8	1.5	Tween 80	240	150	3	Compritol

2.4.3. Experimental Design:

PB designs are screening designs that involve a large number of factors, which result in relatively fewer experiments. Observed and predicted values for all four responses are shown in Table 2.4. A total of 12 experimental trials involving 8 variables were performed and as shown in Table 2.5 the selected response variables exhibited a wide variation suggesting that the independent variables had a significant effect on the response parameters chosen.

Table 2.4: Actual and predicted value for PS (Y1), PDI (Y2), ZP (Y3) and EE (Y4)

PB Run	Particle Size	Polydispersibility Index	Zeta Potential	Entrapment Efficiency
1	397.00	0.385	-33.24	39.13
2	209.00	0.507	-31.12	51.17
3	289.00	0.463	-35.02	75.01
4	462.00	0.576	-24.42	50.28
5	349.00	0.257	-39.34	60.34
6	674.00	0.765	-22.38	53.18
7	245.00	0.296	-34.04	68.84
8	153.00	0.376	-36.16	62.49
9	125.00	0.284	-39.28	78.46
10	542.00	0.534	-19.49	65.08
11	485.00	0.454	-27.71	62.19
12	325.00	0.625	-32.82	66.24

Table 2.5: Statistical analysis of particle size (Y1), polydispersibility index (Y2), zeta potential (Y3) and entrapment efficiency (Y4) results.

Parameters	Particle size (Y1)		Polydispersibility Index (Y2)		Zeta Potential (Y3)		Entrapment Efficiency (Y4)	
	Coeffici-ent	p-value	Coefficient	p-value	Coeffici-ent	p-value	Coeffici-ent	p-value
Constant b_0	354.58	0.007	0.46	0.042	31.25	0.047	61.0	0.0002
DC (A)	43.25	0.056	-0.01	0.829	0.02	0.981	0.30	0.230
LC (B)	48.25	0.039	0.08	0.019	-2.35	0.045	3.67	0.0003
SC (C)	-58.75	0.020	-0.07	0.032	3.33	0.018	-0.08	0.705
ST (D)	48.08	0.040	0.06	0.056	-0.70	0.396	-7.64	<0.0001
SS (E)	-2.75	0.907	3.752E-017	1.0000	1.70	0.095	2.79	0.0008
BT (F)	-62.75	0.015	-0.01	0.7400	0.77	0.357	-0.61	0.0552
ZA (G)	8.58	0.720	0.16	0.5263	0.21	0.788	-1.18	0.0095
LT (H)	97.58	0.002	0.06	0.0690	-4.02	0.010	-5.64	<0.0001

$Y_1 = +354.58 + 43.25 * X_1 + 48.25 * X_2 – 58.75 * X_3 + 48.08 * X_4 – 2.75 * X_5 – 62.75 * X_6 + 8.58 * X_7 + 97.58 * X_8$ …….eq. 2

$Y_2 = +0.46 – 0.0072 X_1 + 0.081 * X_2 – 0.070 * X_3 + 0.059 * X_4 – 0.00833 * X_6 + 0.016 * X_7 + 0.055 * X_8$ …….eq. 3

$Y_3 = +31.25 + 0.018 * X_1 – 2.35 * X_2 + 3.32 * X_3 – 0.70 * X_4 + 1.70 * X_5 + 0.77 * X_6 + 0.21 * X_7 – 4.02 * X_8$……eq. 4

$Y_4 = + 61.03 + 0.30* A + 3.67 * X_2 – 0.083 * X_3 – 7.64 * X_4 + 2.78 * E – 0.61 * X_6 – 1.18 * X_7 – 5.64 * X_8$……..eq 5

The coefficients in Equations (2) - (5) represent the respective quantitative effect of the independent variables (X_1, X_2, X_3, X_4, X_5, X_6, X_7 and X_8) on the response variables (Y_1, Y_2, Y_3 and

Y_4). The effect of selected independent variables on EE, PS, PDI and ZP is graphically represented from Fig. 2.4-2.7**,** respectively.

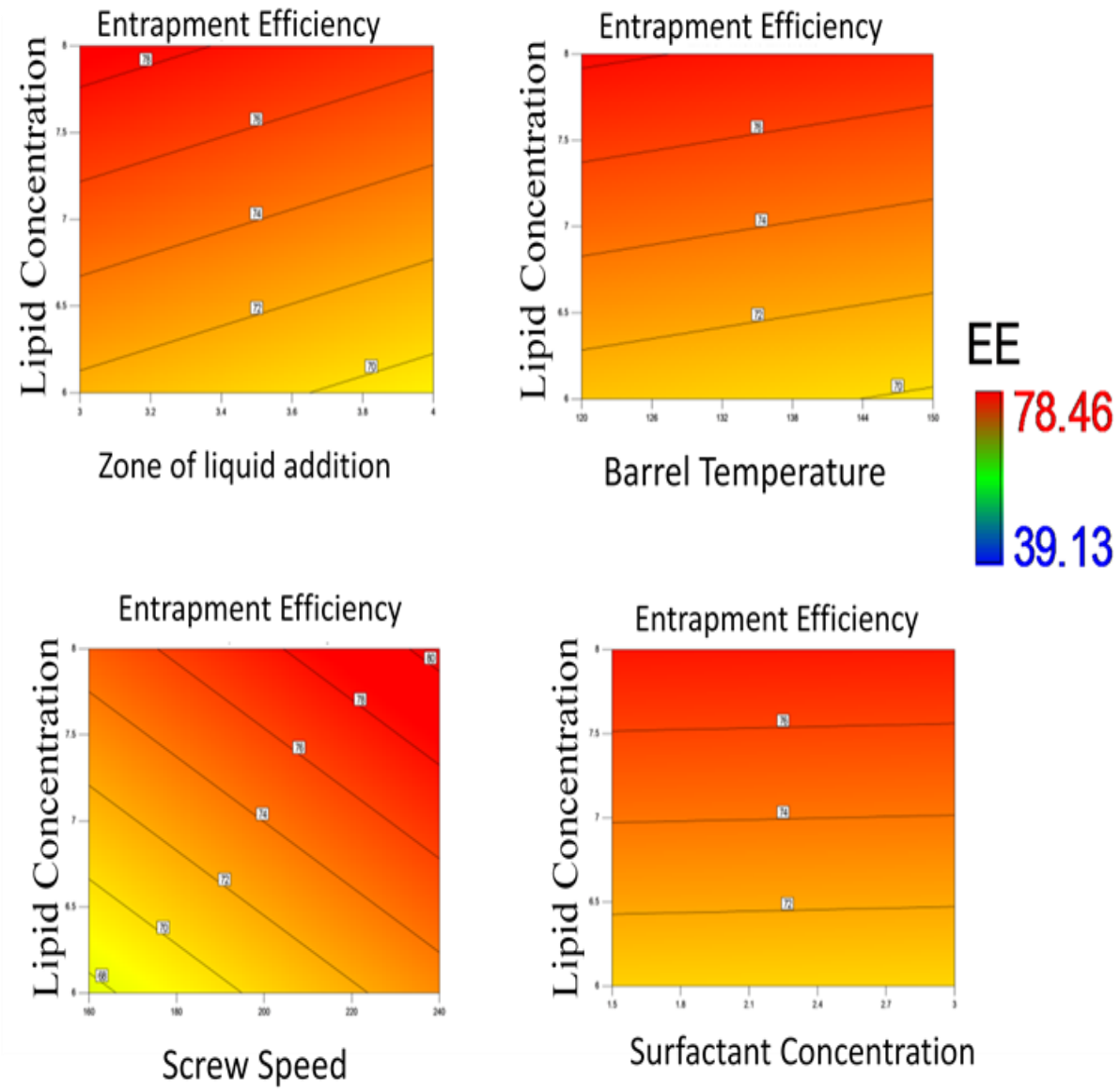

Fig 2.4: Contour plot of EE vs Lipid conc., Surfactant conc., Zone of liquid addition, Screw speed and Barrel temp. (Red color indicates the higher EE, yellow indicates less EE and Blue color indicates lowest EE)

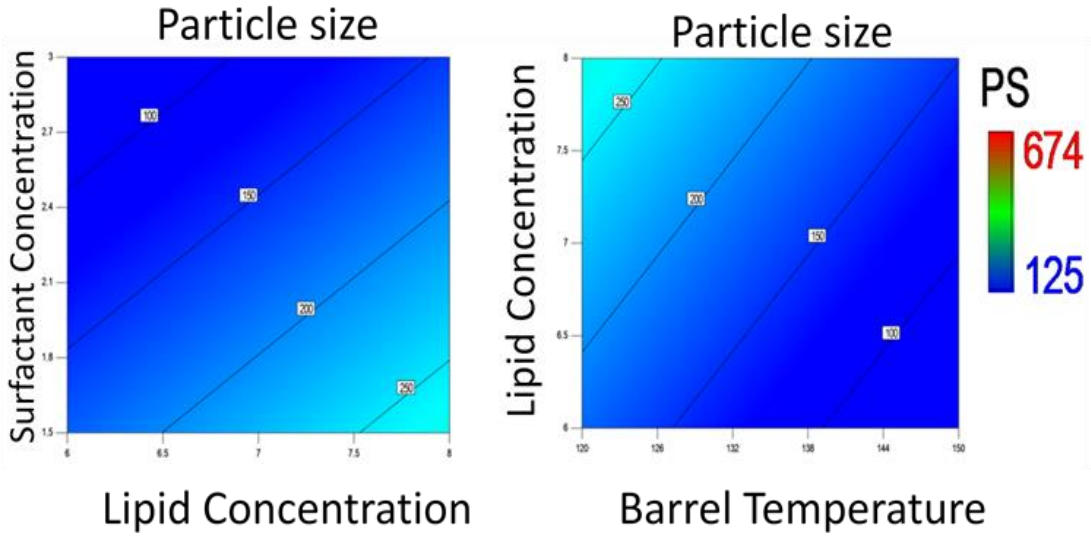

Fig 2.5: Contour plot of PS vs Lipid conc., Surfactant conc. and Barrel temp. (Dark blue color indicates the smaller PS and light blue color indicates larger PS)

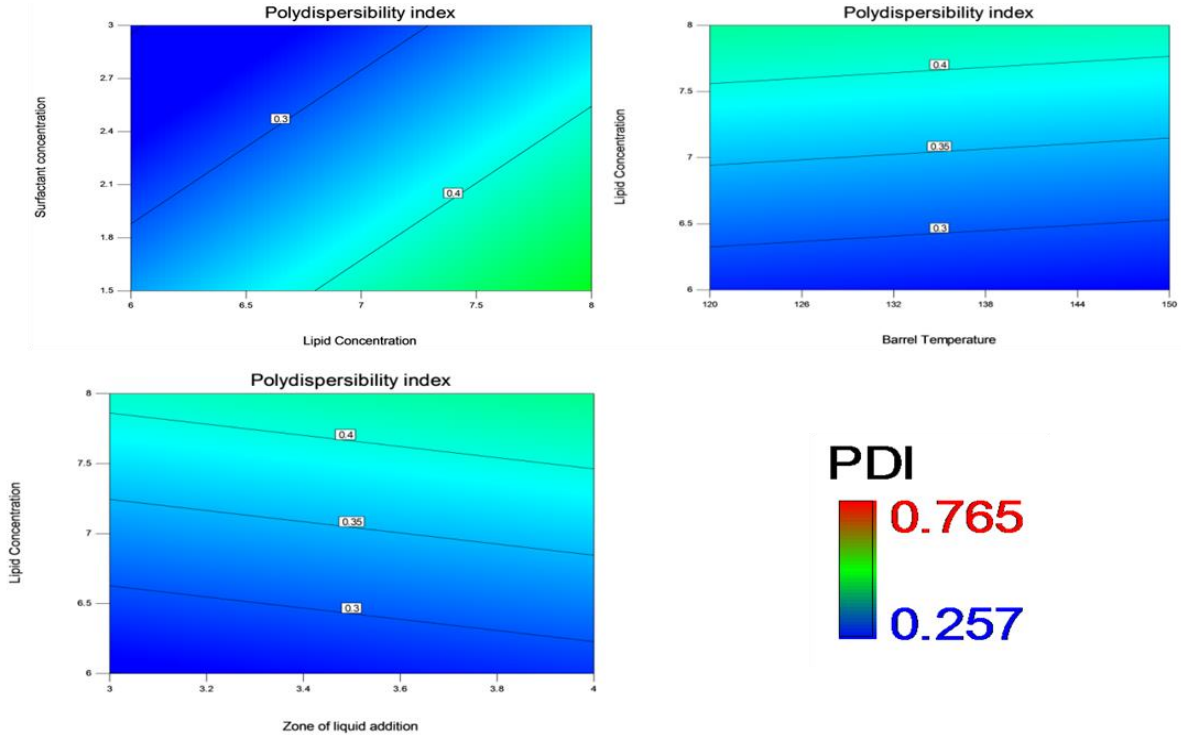

Fig 2.6: Contour plot of PDI vs Lipid conc., Surfactant conc., Zone of liquid addition and Barrel temp. (Color change from Blue to Green indicates increase in PDI)

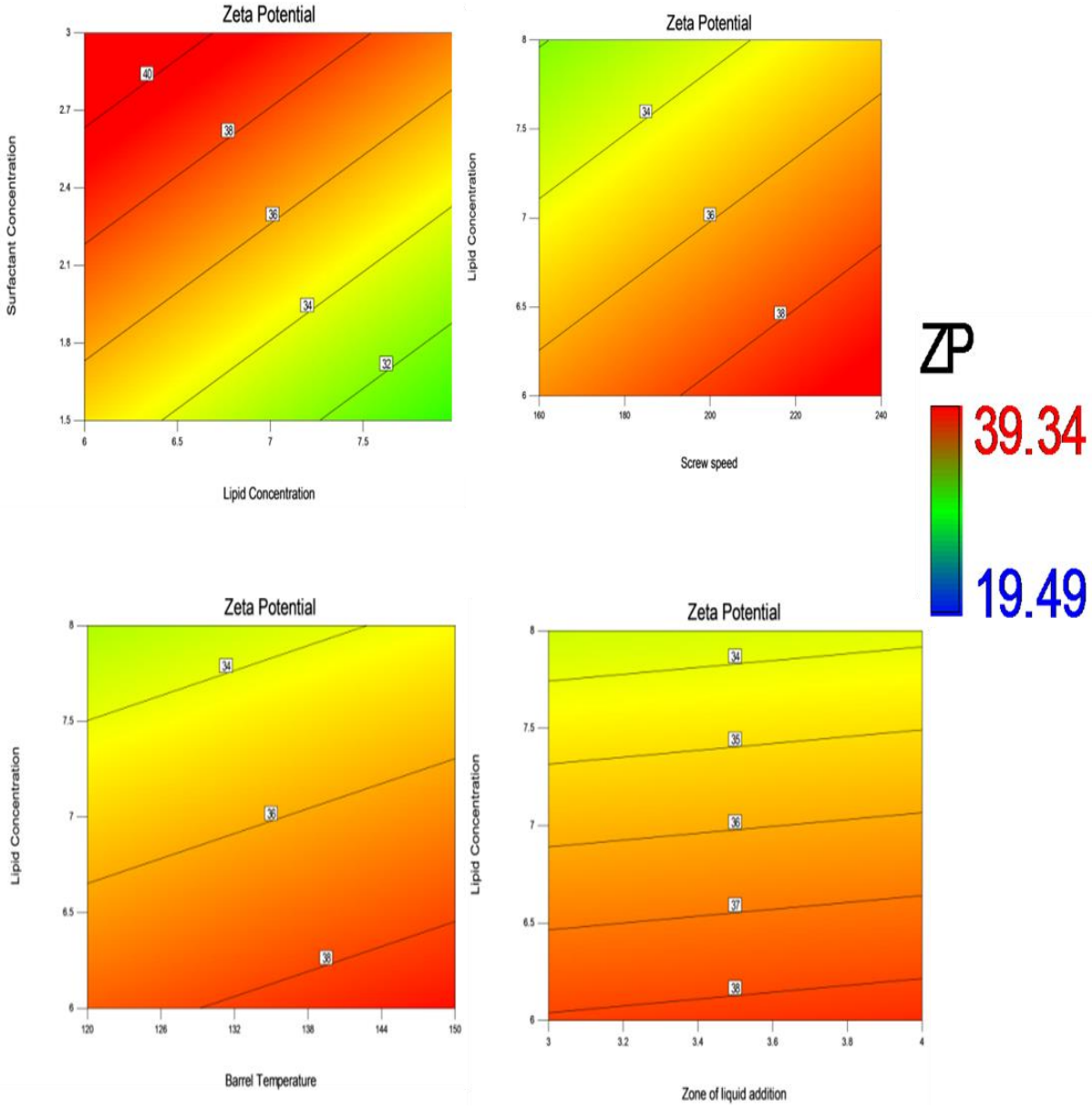

Fig 2.7: Contour plot of ZP vs Lipid Conc., Surfactant conc., Screw speed, Zone of Liquid addition and Barrel temp. (Color change from Red to Green indicates increase in ZP)

2.4.4. Effect of Drug Concentration:

The drug concentration was varied at two levels viz., 0.5 and 1 g. As shown in equations (2, 4 and 5), drug concentration had positive coefficients for PS, ZP and EE but the p value for the drug concentration was found to be more than 0.05 indicating that the drug concentration had insignificant effects on all four responses: PS, PDI, ZP as well as EE. This could be due to the high solubility of FBT in both lipids Compritol® ATO 888 and Precirol® ATO 5, which might result in less variations in the viscosity of the oily phase and therefore there is lower shear generated inside the extruder barrel. Increasing drug concentration results in the increase in drug-to-lipid ratio, which usually decreases EE. Surprisingly, our results showed that increasing drug concentration did not decrease the EE of the drug. This may be due to the range of drug concentration we have used in the formulation. The concentration range from 0.5-1% w/w may be solubilizing the drug completely into the lipid and therefore there is no decrease in EE, as was observed. It may possible that if we increase drug concentration beyond 1% w/w we might see decrease in EE of the drug.

2.4.5. Effect of Surfactant Concentration:

Concentration of surfactant demonstrated a significant influence on particle size and PDI. As shown in eq. (2) the negative value of the coefficient for the surfactant concentration indicates particle size and PDI was decreased with an increase in SC. This might be due to the production and stabilization of smaller lipid droplets at higher SC as enough surfactant was present to reduce interfacial tension between two immiscible phases and stabilize the nano-droplets. Similar results were also reported earlier by Das et al, Hu et al and Liu et al [26, 32, 33]. SC had a significant effect ($p < 0.05$) on ZP. Eq. 5 gives the positive coefficient for SC indicating an increase in SC increases ZP. Generally SC exhibits a huge influence on entrapment efficiency.

As described earlier in Z. Rahman et al [34], a higher amount of surfactant increases the solubility of the drug in the external phase and might be increasing the partitioning of drug from the internal phase to the external phase. Therefore, generally entrapment efficiency increases with an increase in SC as the presence of sufficient SC, which helped the drug to remain within the lipid particles and/or the surface of the particles [26]. Surprisingly, we found that the SC had a negative coefficient but p-value was more than 0.05 indicating SC demonstrated an insignificant effect on EE (as shown in eq. 5).

2.4.6. Effect of Lipid concentration:

Lipid concentration did show a significant effect on all four responses: PS, PDI, ZP and EE. Particle size significantly increased with increasing lipid concentration. Presence of high lipid concentration results increase in the viscosity of the drug-lipid melt. This viscosity increase might cause less homogenization during the initial phase of emulsification and produce larger particles and larger PDI. The negative coefficient of lipid concentration from eq. 4 indicates an increase in LC decreases the ZP of the SLN formulation. This may be due to the negative charge of the lipid. As the amount of negatively charged lipid increases in the formulation, the ZP of formulation decreases. As expected, EE significantly increased with increasing LC. This might be due to availability of a higher amount of lipid to encapsulate more drug, which led to higher EE.

2.4.7. Effect of different surfactant:

Choice of surfactant showed a significant effect on particle size of SLN. Positive coefficient for ST indicates changing ST from Cremophore EL to Tween 80 increases the particle size. Cremophore EL produces SLN with smaller particle size than Tween 80. Similar observations

are reported by other researchers Das et al [26]. This might be due to the difference in HLB value of Cremophore EL and Tween 80. HLB value of 1 and 2 for Compritol® ATO 888 and Precirol® ATO 5, respectively, are closer to the HLB of 12-14 for Cremophore than HLB of 15 for Tween 80. ST showed a huge effect on EE. As mentioned previously, surfactant increases the solubility of the drug in the external phase and might be increasing the partitioning of drug from the internal phase to the external phase. As shown in eq. 5, the negative coefficient for ST indicates that changing ST from Cremophore EL to Tween 80 decreases EE. This may be again due to the high HLB value of Tween 80. EE was significantly low when Tween 80 was used.

2.4.8. Effect of screw speed:

Screw speed produced an insignificant effect ($p > 0.05$) on PS, PDI and ZP. On the other hand it exhibited a significant effect on EE. The positive coefficient for screw speed indicates increase in speed results in the increase in EE. High screw speed generates higher shear inside the barrel, which might result in more homogenization causing more interaction of drug, lipid and surfactant resulting in the formation of a homogeneous emulsion. Thus this may explain the increase in EE.

2.4.9. Effect of barrel temperature:

Barrel temperature only affected particle size of the SLN. The negative coefficient of barrel temperature for particle size demonstrated that increasing barrel temperature reduces the particle size of SLN. This might be because with high barrel temperature, it is possible that the lipids and drug are completely melted resulting in a low viscosity melt without any solid particles. Barrel temperature (zone 2) had insignificant effects on PDI, ZP and EE of SLN.

2.4.10. Effect of zone of liquid addition:

Zone of liquid addition showed an insignificant effect on PS, PDI and ZP. Surprisingly, however, ZA demonstrated a very significant effect ($p = 0.0095$) on entrapment efficiency. Negative coefficient for ZA indicates changing zone of liquid addition from zone 3 to zone 4 decreases EE. This is may be due to the difference in temperature of molten mass at zone 3 and zone 4. The temperature of the molten mass is higher in zone 3 than zone 4 which could affect mixing of the molten mass with the surfactant aqueous solution and droplet formation. Also the other reason to decrease EE by changing the zone of liquid addition could be the length of mixing elements inside the barrel from zone 4 to die is less as compared to the mixing elements from zone 3 to die (Fig. 1.2). If we add surfactant solution at zone 3 then the molten mass of lipid-drug and surfactant solution are exposed to a larger mixing zone, which generates high shear and may enhance entrapment of drug inside the molten lipid. Addition of surfactant solution at zone 4 provides less exposure to the molten lipid-drug mass for mixing with the surfactant solution. Therefore, addition of liquid at zone 4 results in a decrease in EE (39.8%).

2.4.11. Effect of different lipid:

Different lipids exhibited a positive impact on particle size and Compritol® ATO 888 produced smaller SLN when used as the lipid. This may be due to the variations in melt viscosity of Compritol® ATO 888 and Precirol® ATO 5. The positive coefficient for LT for PDI indicates low PDI obtained with Compritol® ATO 888 than Precirol® ATO 5 but p-value for LT was found to be more than 0.05 indicating an insignificant effect on PDI. EE was found higher in the case of Compritol® ATO 888 as compared to Precirol® ATO 5. These observations can be explained by the solubility study that demonstrated the higher solubilization capacity of Compritol® ATO 888 for FBT.

2.4.12. Quantification of drug release *in-vitro*:

As aqueous solubility of FBT is very low, 0.3 % SDS was added to the release media to maintain the sink condition. *In-vitro* release of FBT from the optimized formulation (PB 9) was compared with the release of pure drug and the marketed micronized FBT formulation for a period of 5 h. The amount of FBT released from the SLN dispersion was determined by an *in-vitro* dialysis bag technique. The dialysis bag retained the SLN particles; drug released from SLN and diffused through the dialysis membrane into the release media. *In-vitro* drug release studies (Fig. 2.8) showed approximately 94% drug was released at the end of 5 h for FBT SLN formulation (PB 9) and 62% for the marketed micronized FBT formulation at the end of 5 h, whereas 41% drug was released from pure FBT at the end of 5 h. The increase of the dissolution rate of SLN FBT could be mainly attributed to the obvious reduction of the particle size (from a few microns for the crude FBT and marketed micronized formulation to a few nanometers (125 nm) for SLN). According to Nernst-Noyes-Whitney equation, which described the dissolution rate of drug in a diffusion-controlled process, an increase in the surface area could result in an increase in dissolution rate [34-37].

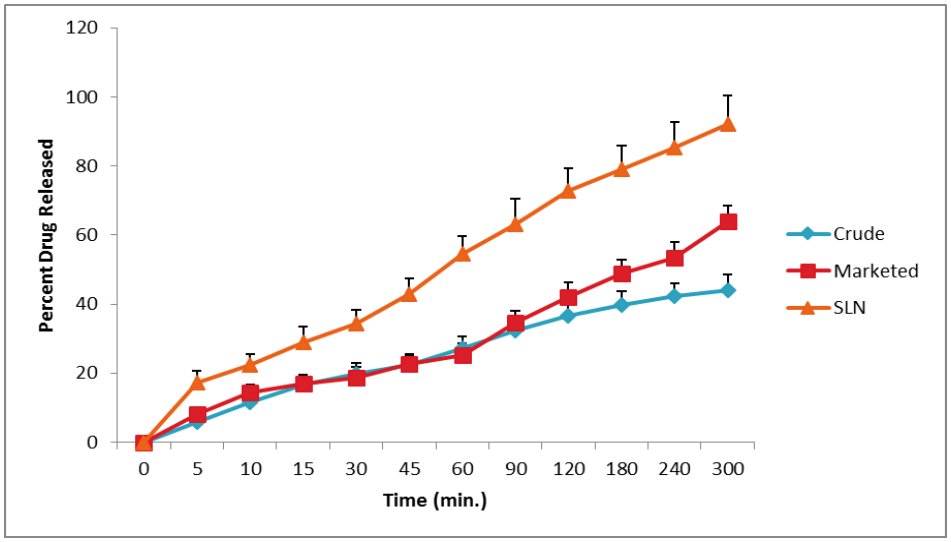

Fig 2.8: Dissolution profile of FBT SLN prepared by novel HME-HPH method marketed micronized FBT formulation (Lofibra) and crude FBT.

2.4.13. Comparison between novel HME-HPH method and conventional method for the preparation of SLN:

The particle size, PDI and ZP of the SLN produced using the novel HME-HPH method and conventional method are presented in Fig. 2.9 (A, B and C). The pre-emulsion prepared by HME and the conventional method compared with each other are emphasized as this is the major contributing difference in these two methods. The quality of the pre-emulsion affects the quality of the final product attributes to a large extent and it is desirable to obtain droplets in the size range within a few micrometers. Pre-emulsions prepared by both the novel method and the conventional method were characterized for PS, PDI and ZP. Particle size of the pre-emulsion prepared by the conventional method was 1643 nm whereas the PS was 653 nm when prepared by the novel method (Table 2.6). It is apparent that if the initial pre-emulsion particle size is significantly higher that it will take more cycles and pressure in the HPH to reduce the particle size to 150-200 nm. However, the particle size of the pre-emulsion prepared by the novel method is itself in nanometers; less downstream processing in the HPH is required. With this novel HME:HPH method high pressure-induced drug degradation that could be caused by HPH can be prevented because of the requirement of fewer number of cycles as well as lower pressure as compared to the conventional SLN preparation method.

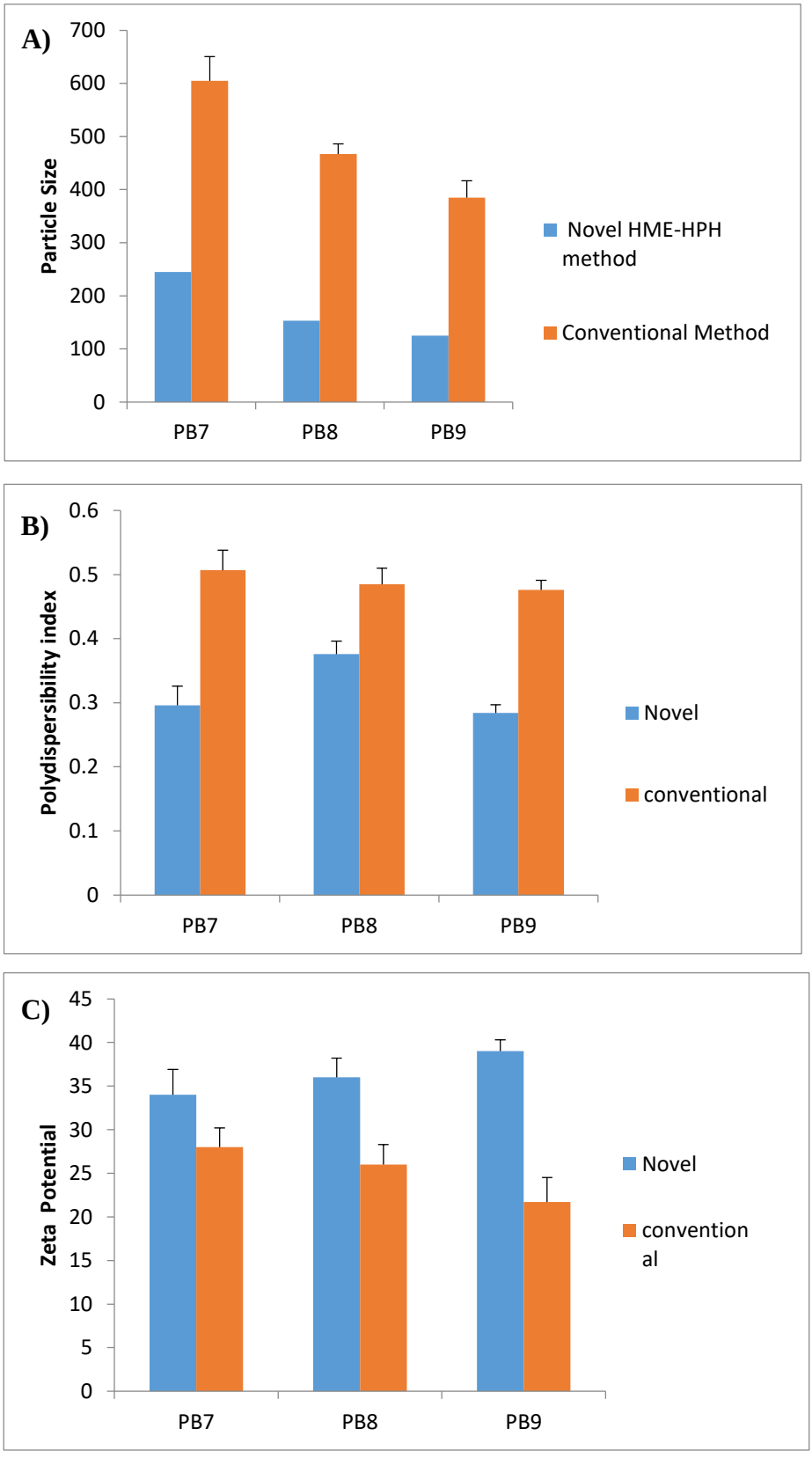

Fig 2.9: Particle size (A) Polydispersibility index (B) and Zeta potential (C) of SLN produced by novel HME-HPH method and conventional method. The error bars in graph indicate 95% confidence interval.

Table 2.6: Comparison between pre-emulsion qualities prepared by HME and conventional method

No.	Method	Particle size (nm)	PDI	Zeta Potential (mV)
1	HME	653	0.63	-24.1
2	Conventional method	1643	1.21	-8.2

2.4.14. *In-vivo* pharmacokinetic study:

In order to determine whether the increase in the dissolution rate helps to improve the oral bioavailability, an *in-vivo* experiment was conducted in the fasted state. The pro-drug FBT, which contains an ester group, undergoes rapid hydrolysis to produce fenofibric acid by intestinal, plasma and tissue esterase, following oral administration. Thus, in the present study the pharmacokinetic analysis of FBT is based on the plasma concentration of fenofibric acid. The plasma drug concentration-time profiles of FBT after oral administration of various formulations to male Wistar rats is shown in Fig. 2.10. The related pharmacokinetic parameters are summarized in Table 2.7. At all-time points, the fenofibric acid plasma concentration was significantly higher ($p < 0.05$) for the rats treated with fenofibrate-SLN than the marketed and crude fenofibrate. The Cmax value of fenofibrate SLN (65.3 ± 7.2 µg/ml) was higher than the marketed (38.05 ± 5.8 µg/ml) and crude fenofibrate (20.0 ± 3.5 µg/ml). Twenty-four hours after oral administration, the fenofibrate-SLN plasma concentration was 10 µg/ml which was higher as compared to the marketed formulation (4 µg/ml) and crude fenofibrate (3 µg/ml). From these results, one can conclude that fenofibrate absorption was enhanced significantly by employing the SLN formulations compared to the marketed and crude fenofibrate [38, 39]. The most

important advantage of SLN formulations over the crude fenofibrate is the lipid protection of drug from chemical as well as enzymatic degradation, thus further delaying the *in-vivo* metabolism by oxidative and conjugative pathways. An increase in the rate of drug absorption from the SLN has been demonstrated compared to the both marketed micronized formulation and crude drug suspension. Reduction in particles size from the micro- to nanometer range increases the surface area and thus increases the dissolution velocity according to the equation of Noyes-Whitney [40, 41].

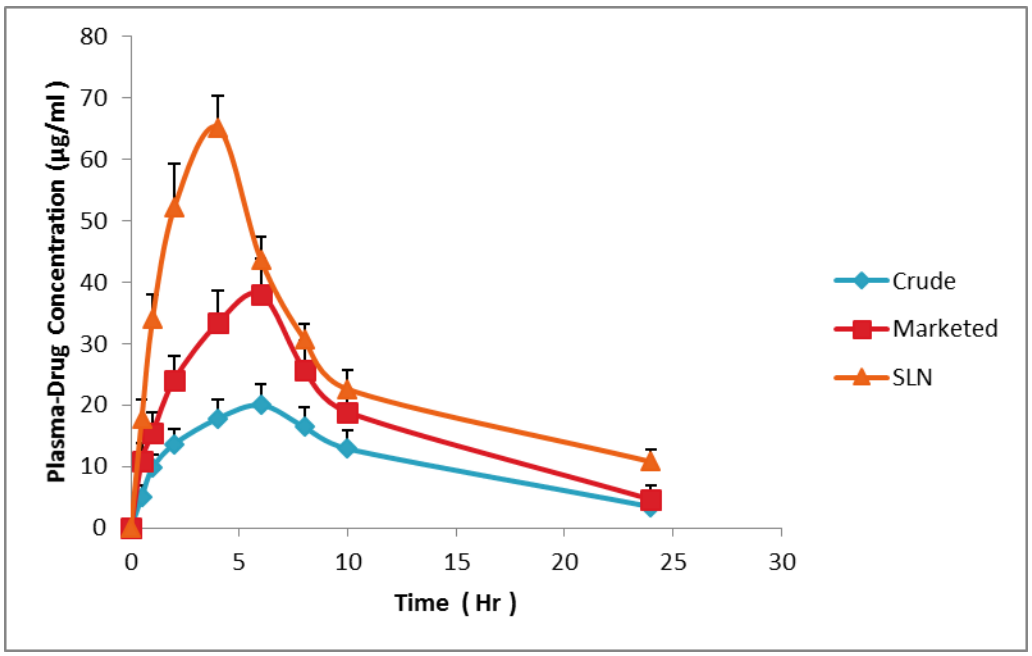

Fig 2.10: Average plasma concentration-time profiles of fenofibric acid following oral administration of 50mg/kg in the rat. Three different formulations were tested: SLN prepared by novel HME-HPH method, marketed micronized FBT formulation (Lofibra) and Crude FBT (means ±S, n=4).

Table 2.7: Pharmacokinetic parameters of FBT formulations in Wistar rats (dose 50 mg/kg, n=4, mean ±SD)

Parameters	SLN Formulation	Crude FBT	Micronized marketed FBT formulation
Tmax (h)	$4.42 \pm 0.4^{*\#}$	6.9 ± 0.54	6.5 ± 0.4
Cmax (µg/ml)	$65.25 \pm 7.2^{*\#}$	20.0 ± 3.5	38.05 ± 5.8
$AUC_{0\text{-}24}$ (h.µg/ml)	$648.23 \pm 85.4^{*}$	266.17 ± 40.9	430.97 ± 70.0
$AUMC_{0\text{-}24h}$ (µg-h_2/ml)	$5342.17 \pm 527.2^{*\#}$	2306.74 ± 221.1	3509.26 ± 324.1
$MRT_{0\text{-}24}$ (h)	8.24 ± 0.5	8.66 ± 1.4	8.14 ± 0.7

* $p < 0.05$ compared with crude FBT

#$p < 0.05$ compared with Marketed FBT

2.4.15. Stability study:

Stability results are shown in Table 2.8. Particle size, PDI and zeta potential studies revealed no significant change ($p > 0.05$). Particle size increased after 6 months storage at 25 °C. Although, not a significant change in particle size. A slight reduction in entrapment efficiency of the FBT SLN was observed after 6 months storage at 25 °C and at 4 °C. However the changes were not significant. Thus it can be concluded that FBT SLN have good physical stability in terms of particle size, PDI, ZP and EE when stored at 4 °C and 25 °C for the 6 month study period.

Table 2.8: Stability after 6 months storage at 4 °C and 25 °C (data represent mean ±SD) (PB 9 Formulation)

Storage	Particle Size (nm)		PDI		Zeta Potential (mV)		Entrapment Efficiency (%)	
	4 °C	25 °C	4 °C	25 °C	4 °C	25 °C	4 °C	25 °C
Fresh	125 ± 0.16		0.284 ± 0.032		39.28 ± 1.21		78.46 ± 1.42	
1 month	124.2 ±0.4	128 ±0.1	0.286 ±0.04	0.284 ±0.04	39.04 ±1.7	38.23 ±1.4	78.13 ±1.3	77.92 ±1.4
3 month	127 ±0.3	133 ±0.5	0.292 ±0.1	0.293 ±0.02	37.74 ±1.5	36.12 ±1.2	77.48±1.9	75.14 ±1.2
6 month	132 ±0.3	139 ±1.4	0.301 ±0.1	0.302 ±0.02	37.22 ±1.3	35.12 ±2.4	76.23 ±2.1	73.47 ±1.5

2.5. Conclusion:

The current study demonstrates that our novel process based on HME-HPH of SLN production is an appropriate continuous technology for producing nano-formulations. The proposed method of HME-HPH was found to be suitable for continuous production of SLN using QbD principles and a DOE approach. This continuous, single step method was found to be a potentially economical, as well as an efficiency benefit for the production of SLN. In addition the process aids to minimize issues associated with the conventional methods of SLN preparation such as pressure-induced drug degradation. Findings of this study demonstrated that selected independent variables significantly affects critical quality attributes of the SLN. Thus, these outcomes of this research have successfully demonstrated the application of QbD principles and a DOE approach to develop a continuous process of SLN production via the HME-HPH technique.

CHAPTER III

FORMULATION AND DEVELOPMENT OF PH-INDEPENDENT/DEPENDENT SUSTAINED RELEASE MATRIX TABLETS OF ONDANSETRON HCL BY CONTINUOUS TWIN-SCREW MELT GRANULATION PROCESS

3.1. Abstract

The objective of the present study was to develop pH-independent/dependent sustained release (SR) tablets of ondansetron HCl dihydrate (OND), a selective 5-HT3 receptor antagonist that is used for prevention of nausea and vomiting caused by chemotherapy, radiotherapy and postoperative treatment. The challenge with the OND API is its pH-dependent solubility and relatively short elimination half-life. Therefore, investigations were made to solve these problems in the current study. Formulations were prepared using stearic acid as a binding agent via a melt granulation process in a twin-screw extruder. The micro-environmental pH of the tablet was manipulated by the addition of fumaric acid to enhance the solubility and release of OND from the tablet. The *in vitro* release study demonstrated sustained release for 24 h with 90% of drug release in formulations using stearic acid in combination with ethyl cellulose, whereas 100% drug release in 8 h for stearic acid-hydroxypropylcellulose matrices. The formulation release kinetics was correlated to the Higuchi diffusion model and a non-Fickian drug release mechanism. The results of the present study demonstrated for the first time the pH dependent release from hydrophilic-lipid matrices as well as pH independent release from

hydrophobic-lipid matrices for OND SR tablets manufactured by means of a continuous melt granulation technique utilizing a twin-screw extruder.

3.2. Introduction

Several approaches has been used to develop sustain release (SR) matrix formulations and among them the most interesting approach is based on melt granulation techniques. Melt granulation is a process by which pharmaceutical powders are efficiently agglomerated by the use of a low melting point binding material, which after melting act as a binding liquid [42]. The advantage of this process over other techniques is that it is a solvent free process, and thus there is no need for a drying step, which consumes time and energy. Also, the percent of fines produced by the melt granulation process is less as compared to the wet and dry granulation process [43]. Several researchers have used melt granulation processes using different kinds of low melting point excipients as binders (polyethylene glycols 3000, 6000 and 8000, various types of waxes and lipids) [44-46]. Over the last few years several techniques have been investigated for melt granulation processes such as high-shear granulation, fluidized bed processing and others. [47, 48]. Hot melt extrusion (HME) is another thermal processing technique that has attracted interest as a novel technique for melt granulation [46, 49]. HME is a continuous, simple, easy to scale up and efficient process [5, 7, 50].

Nausea and vomiting are the common problems in cancer patients undergoing chemotherapy, radiation therapy, and postoperative treatment or due to the advancement in cancer itself. Serotonin (5-Hydroxytryptamine) subtype-3 (5-HT_3) receptor plays an important role in emetogenic pathways in relation to massive release of serotonin from damaged enterochromaffin cells in the gastrointestinal tract following chemotherapy [51, 52]. Serotonin antagonists exert their anti-emetic action via 5-HT_3 receptors located centrally (chemoreceptor trigger zone of the

area postrema and nucleus tractus solitaries) as well as peripherally (enterochromaffin cells of the enteric nervous system) [53, 54]. 5-HT_3 receptor can be antagonized by drugs such as ondansetron, tropisetron, granisetron, dolasetron, palonosetron and ramosetron as well as by certain drugs having prokinetic (increasing gut motility) action such as renzapride, cisapride and metoploramide [52, 55].

Ondansetron, a carbazole derivative, is a potent, highly selective competitive 5-HT_3 receptor antagonist [56]. Intravenous and oral dosage forms of OND are commercially available, for example: oral solutions, orally disintegrating tablets and film-coated tablets. The recommended oral dose regimen of OND is 8 mg, three times a day. Following oral administration OND is well absorbed from the GIT and its bioavailability is approximately 67% and the elimination half-life is relatively short, approximately 3-5 h [57, 58].

The present study has investigated HME techniques to prepare OND granules. Stearic acid is commonly used as a tablet lubricant in oral formulations. Also it has been extensively explored as a binder. In the current study, stearic acid is used as a melt binder in the formulations. Two different polymers were used as matrix formers such as the water-insoluble and almost un-swellable ethyl cellulose [59], and the water-soluble and swellable hydroxypropyl cellulose (HPC) in combination with stearic acid. OND exhibits pH dependent solubility and therefore, it is freely soluble in gastric fluid's low pH [60], but practically insoluble at pH > 6. Several approaches have been used in the past to overcome pH–dependent solubility of weakly basic drugs [61]. The commonly used approach is the addition of acid pH modifiers to the matrix tablets [62]. Therefore, based on preliminary studies, these investigators have used fumaric acid to create a suitable micro-environmental pH, which increased drug solubility at higher pHs.

At present commercially available orodispersible as well as conventional OND tablets are meant for immediate release of the drug and are given 3-4 times a day due to the short half-life (3-5 h) of OND. Therefore, there is a need to develop a sustained release formulation for OND which exhibits pH-independent release profile. The aim of this novel study was to 1. Develop an innovative sustained release OND tablet by continuous twin-screw melt granulation processing. 2. To investigate the influence of formulation parameters on the physical properties of the hot-melt extruded granules and compressed tablets containing stearic acid as a release-retarding agent 3. Study the release kinetics for OND tablets prepared by either hydrophilic or hydrophobic polymers in combination with stearic acid. 4. To study the effect of fumaric acid on drug release behavior from the tablet matrix.

3.3. Materials and methods

3.3.1. Materials

Ondansetron HCl Dihydrate was purchased from Chemscene LLC (New Jersey, USA). Hydroxypropyl cellulose (Klucel® EF) was kindly gifted by Ashland Specialty Ingredients. (Wilmington, DE). Ethyl cellulose (Ethocel® Standard 10) was gifted from Dow chemical company. Fumaric acid and Magnesium stearate was purchased from Spectrum Laboratory Products Inc. (Gardena, CA). Microcrystalline cellulose (Avicel® PH 101) was gifted from FMC Biopolymer (Philadelphia, PA). Stearic acid was purchased from EMD Millipore (Billerica, MA). All the other reagents such as methanol (impurities < 0.1%) used in this study were of the analytical grade.

Table 3.1: Compositions of the investigated granules (all quantities given in percentile)

Formulation	OND	EC	HPC	SA	FA	Magnesium Stearate	MCC
F1	20	37	__	12	__	0.2	30.5
F2	20	__	37	12	__	0.2	30.5
F3	20	37	__	12	2.5	0.2	28
F4	20	37	__	15	2.5	0.2	25
F5	20	40	__	12	2.5	0.2	25
F6	20	40	__	15	2.5	0.2	22
F7	20	__	37	12	2.5	0.2	28
F8	20	__	37	15	2.5	0.2	25
F9	20	__	40	12	2.5	0.2	25
F10	20	__	40	15	2.5	0.2	22

***Magnesium stearate (0.3%) added in all batches extra granularly before compression.**

3.3.2. Compatibility of OND with different excipients

To study the compatibility of OND with the polymers and other excipients, physical mixtures were prepared by mixing the drug with each formulation excipients in the ratio of 1:1. Pure drug (OND) and two physical mixtures were characterized by differential scanning calorimetry (Diamond DSC, Perkin Elmer) using Pyris manager software (PerkinElmer Life and Analytical Sciences, 719 Bridgeport Ave., CT, USA) and Fourier transform infrared spectroscopy (Agilent

Technologies Cary 660, Santa Clara, CA). For the DSC study, samples were prepared by sealing 3-5 mg of pure API and physical mixture in hermetically sealed aluminum pans and the thermal analysis was performed under an inert nitrogen atmosphere at a heating rate of 10 °C/min over a temperature range of 40-250 °C. FTIR studies were conducted in the range of 4000-400 cm^{-1}. The bench was equipped with an ATR (Pike Technologies MIRacle ATR, Madison, WI), which was fitted with a single bounce diamond coated ZnSe internal reflection element.

3.3.3. Hot melt granulation

Ondansetron HCl dihydrate (20% w/w) was blended with other excipients as shown in Table 3.1 using a V-shell blender (GlobePharma, Maxiblend™ New Brunswick, NJ) for 20 min at 25 rpm, after passing through US# 35 mesh screen to remove any aggregates that may have formed. Hot melt granulations were processed without an extrusion die in a fully intermeshing co-rotating twin screw extruder (11 mm Process 11™ Thermo Fisher Scientific) with modified screw design (Figure 3.1). This extruder barrel consists of a total of 8 zones. The first zone (no heating), also known as feeding zone, is where the physical mixture is fed. Based on the preliminary studies zone 2 and zone 3 were set at 110 °C, zone 4 was set at 70 °C and the remaining subsequent zones (zone 5 – zone 8) were heated to 50 °C. The set temperatures of all zones were below the melting point of OND (189 °C). The modified co-rotating screw configuration consists of mixing elements at two places, one at zone 3 and second before the discharge elements. The extruder was allowed to equilibrate at set temperature for 30 min before starting the trials. The physical mixtures were loaded into the volumetric feeder, fed from the extruder feeding zone and further processed through extruder barrel at the set temperatures. Powder feed rate (7.2 g/min) and screw speed (100 rpm) were selected from the preliminary data and kept constant for all batches. Granules were collected from the open end of the extruder after steady state was reached for a

trial condition. At the end of the granulation process the collected granules were stored in a foil-lined sealed bag.

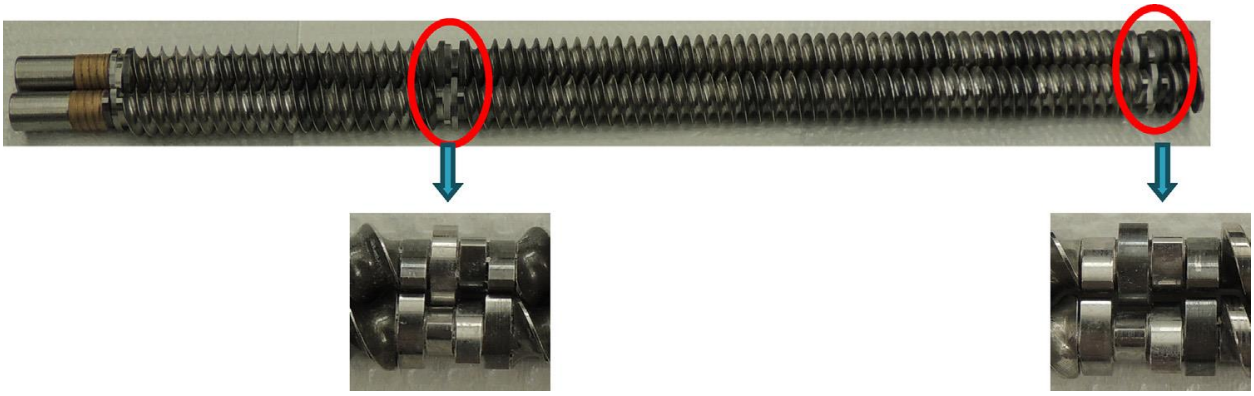

Fig 3.1: Modified screw configuration

3.3.4. Micromeritic properties of granules

Bulk density was calculated by measuring the volume of 5 g granules in a 10 ml graduated cylinder. The cylinder was tapped 100 times until no further reduction in the volume of the granules was observed. Tapped density was calculated using the volume of the granules after tapping. Flow properties of the granules such as angle of repose, Carr's index, and Hausner's ratio were also calculated. The angle of repose was determined by the funnel method. The accurately weighed powder was placed in a funnel. The height of the funnel through which the powder passes was adjusted in such a way that the tip of the funnel just touched the tip of the cone of the powder. The powder was allowed to flow through the funnel freely onto the fixed base. The diameter of the powder cone and height of the cone was measured. The angle of repose (Ɵ) was calculated using the following equation:

$$\text{Tan}\,(\theta) = \frac{h}{r}$$

Where 'h' and 'r' are the height and radius of the powder cone respectively.

Carr's (compressibility) index [63] and Hausner's ratio (HR) was determined according to the following formula:

$$\mathrm{CI} = \frac{(\text{Tapped density} - \text{Bulk density})}{\text{Tapped density}} \times 100$$

$$\mathrm{HR} = \frac{\text{Tapped density}}{\text{Bulk density}}$$

3.3.5. Particle size distribution

Particle size distribution was analyzed by the sieve analysis method. Two standard sieves (U.S.A. Standard Test Sieve) with mesh sizes of 500 µm and 1400 µm were used to conduct the sieve analysis. Three fractions were collected, that is, granule size more than 1400 µm, granule size in-between 1400 - 500 µm and granule size less than 500 µm which are considered as fines and the percentile weight distribution was determined for all three fractions.

3.3.6. Tablet compression

Prior to direct tablet compression, granules were mixed with 0.3% magnesium stearate. Tablets were manually prepared by direct compression on a single punch tablet press (MCTMI, GlobePharma Inc. New Brunswick, NJ), by using an 8 mm flat round punch at a compression force of 130 kg/cm.

3.3.7. Evaluation of tablet properties

Compressed tablets were evaluated for hardness, thickness, friability and drug content uniformity. Ten tablets were randomly selected and tested for their hardness (Hardness tester, Schleuniger). An additional ten tablets were randomly selected and tested for their thickness

using a digital Vernier caliper (Montana). The friability was determined as percentage weight loss of tablets (weighing 6.5 g) using a dual scooping projection Vander Kamp friabilator (Vankel Industries Inc. Chatham, NJ) for 4 minutes at 25 rpm.

3.3.8. Evaluation of Gel Layer pH

To study the effect of fumaric acid, the pH of the tablet surface was measured within 10 h by an Oakton pH meter (pH Spear, Fisher Scientific) equipped with a contact electrode. The dissolution media used to conduct this test was 0.1N HCl (pH 1.2) for the first 2 h, followed by pH 6.8 buffer for the remaining 8 h. The tablets were removed at an interval of 1 h to check the surface pH up to 10 h [64]. Briefly, the tested tablets were removed from the dissolution vessel at set time interval and bathed with purified water to remove residual buffer from the tablet surface. Then the contact electrode was slightly pressed into the gel layer of the tablet to measure the pH.

3.3.9. *In-vitro* drug release

In-vitro drug release was measured using USP dissolution apparatus II (Hanson SR8) set at 50 rpm and equipped with UV-Vis probes (Rainbow Dissolution Monitor, PION) collecting spectra every 2 min for the first 2 h and then for every 25 min until 24 h at 305 nm. The test dissolution media were 700 ml of 0.1N HCl (pH 1.2) with 1% SLS for the first 2 h, then 200 ml of 0.2 M tribasic sodium phosphate (pH 12.5) with 1% SLS to provide a final pH of 6.8 for 24 h (media were maintained at 37 ± 0.5 °C) to simulate the tablet transit from stomach (pH 1.2) to the intestine (pH 6.8) [63, 65]. The drug release studies were conducted in triplicates and the mean values were plotted versus time.

3.3.10. Similarity and dissimilarity factor analysis

The similarity (f_2) and dissimilarity (f_1) factor was used to evaluate pH-independent release patterns of OND from the optimized tablets in the release media pH 1.2 and pH 6.8. Similarity and dissimilarity factors are calculated by using the following Eq. [66]:

$$f2 = 50\, log\left(\frac{1}{\sqrt{1+\left(\frac{1}{p}\right)\sum_{i=1}^{P}(Rt-Tt)^2}} \times 100\right)$$

$$f1 = \{[S_{t=1^n} \; |\mathrm{Rt} - \mathrm{Tt}\;|]\} \times 100$$

Here, R_t and T_t are the cumulative percent of drug dissolved from matrices for the references and test samples at time t and n is the number of time points. The similarity factor values ranges between 0 and 100. The similarity between two profiles increases when f_2 value approaches 100, whereas dissimilarity occurs with a decrease of the f_2 value (less than 50) [67].

3.3.11. Drug Release Kinetics and mechanism

In order to study the mechanism of drug release from the matrix tablets, the experimental data was evaluated kinetically by the following equations [64, 68-70],

Zero order equation: $Q_t = Q_0 + K_0\, t$

First order equation: $In\, Q_t = InQ_0 + \; K_1 t/2.303$

Higuchi equation: $Q_t = K_H t^{1/2}$

Korsmeyer-Peppas equation: $\frac{Q_t}{Q_\infty} = K_{kp} t^n$

where, Q_t is the amount of drug released in time t, Q_0 is the initial amount of the drug in the solution, Q_∞ is the amount of drug released after infinite time, K_0 is the zero order release rate

constant, K_1 is the first order release rate constant, K_H is the Higuchi diffusion rate constant, K_{kp} is the release constant comprised of structural and geometrical characteristics of the tablets and 'n' is the release exponent indicating the mechanism of the drug release.

3.3.12. Statistical Data Analysis

The differences between batches were analyzed by one-way analysis of variance (ANOVA) followed by Student's t-test. A difference of $p < 0.05$ was considered statistical significant. All values were reported as the mean of three recordings.

3.4. Results and Discussion

3.4.1. Compatibility of OND with different excipients

Drug-excipients compatibility studies were performed utilizing DSC and FTIR. Any abrupt or drastic changes in the thermal behavior of either the drug or polymer may indicate a possible interaction between drug and polymer. DSC of drug-polymer physical mixture for both EC-SA and HPC-SA matrices showed a well recognizable endothermic peak of OND at 181.74 °C, the temperature slightly shifted to the lower temperature than corresponding to the melting point of the pure drug (188.58 °C). This result indicates that the drug is compatible with the polymer but due to the presence of stearic acid which is acting as a plasticizer results in lowering the melting temperature of OND. There was no change in the glass transition temperature and melting endotherms of other excipients used in the formulation confirming the absence of any drug-polymer interaction. Also, there were no considerable changes in the IR peaks of OND when mixed with other excipients further confirming the absence of drug-excipient interaction. The FTIR spectra of the pure drug and physical mixture were compared and the characteristic peak for the physical mixture was found to be superimposable to that of the pure drug. This result

indicates that there was no drug polymer interaction. A broad band of bonded –OH of OND was observed from 3481 cm^{-1} to 3245.97 cm^{-1}, and a peak of –CH stretching was found at 2900 cm^{-1} indicating the presence of a methyl group, and at 1680 cm^{-1} (-C=O stretching) indicating a keto group in all of the formulations' physical mixtures (Figure 3.2).

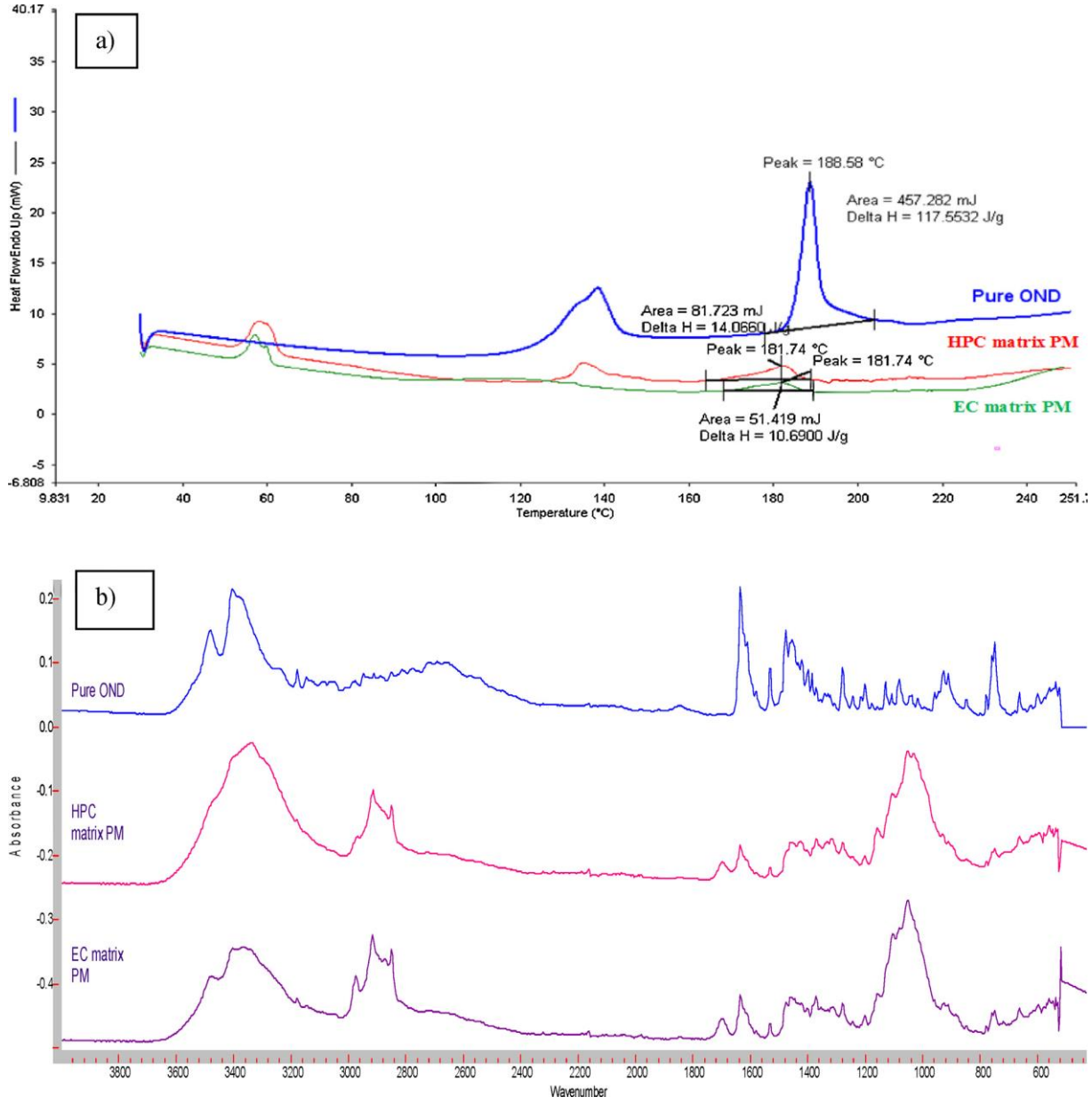

Fig 3.2: (a) DSC and (b) FTIR spectra of pure OND, physical mixture for EC-SA matrix and HPC-SA matrix.

Table 3.2: Granule properties of the different formulations of Ondansetron hydrochloride (OND)

Formulation	Angle of repose (°C)	BD (gm/cm^3)	TD (gm/cm^3)	Carr`s Index (%)	Hausner's Ratio
F1	26	19	16	15.79	1.19
F2	27	19.5	16	17.95	1.22
F3	26	20	17.5	12.5	1.14
F4	27	20	16	20	1.25
F5	27.5	21	18	14.28	1.17
F6	28.5	17.5	14.5	17.14	1.25
F7	27	19	16	15.79	1.19
F8	28	17	14	17.65	1.21
F9	28	15.5	13	16.13	1.19
F10	28.5	18	15.5	13.89	1.16

3.4.2. Micromeritic properties of granules

Granule flowability and compactability affects the die filling and tablet mechanical characteristics; therefore it is essential to study the granule flow properties. Various tests have been performed on all formulations such as bulk density, tapped density, angle of repose, Carr's index and Hausner's ratio. According to the flow property classification of USP, the angle of

repose in a range of 25 to 30 indicates excellent flow properties. All the prepared formulations showed excellent flowability (25 < angle of repose < 30).

As shown in Table 3.2, it is clear that as the amount of the meltable binder and polymer increased, the angle of repose also increased. Carr's index and Hausner's ratio are also the measurement of flow properties and good flowing granules should have a Carr's index between 10.0 to 18.0%, whereas Hausner's ratio should be less than 1.25. When the Carr's index and Hausner's ratio are adequate, the powder flows at minimum bulk density and consolidates to maximum density inside the die, prior to compression [71]. Carr's index and Hausner's ratio in Table 3.2 are between 10.0 to 18.0% and less than 1.25 respectively, confirming the good flow of granules obtained in all the formulations.

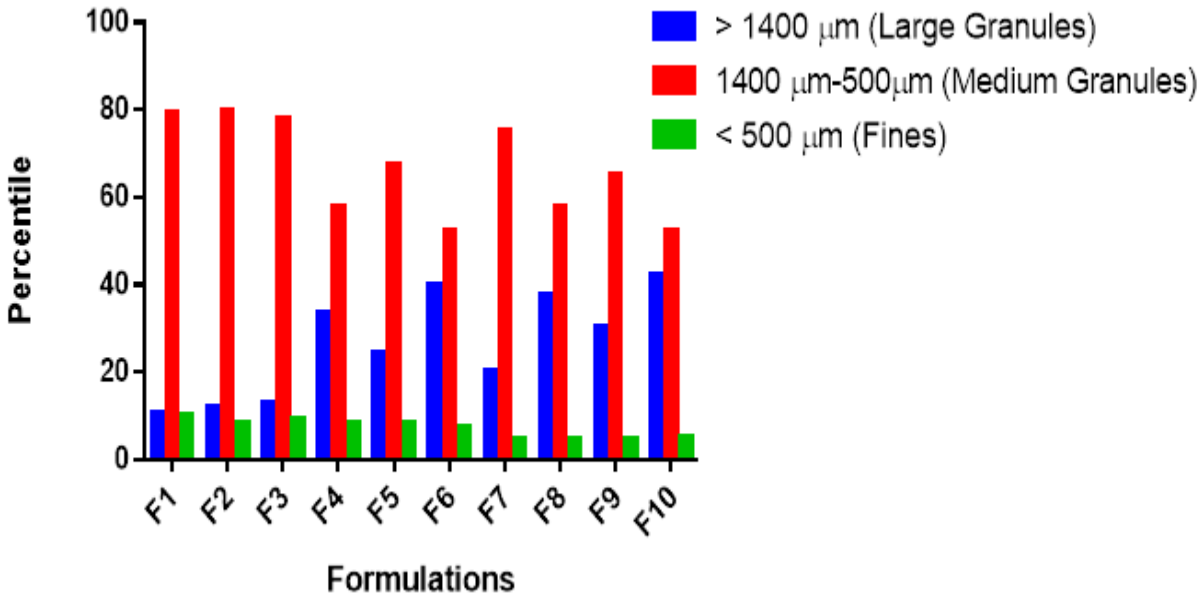

Fig 3.3: Particle size distributions of the OND granules (F1-F10) (determined by sieve analysis)

3.4.3. Particle size distribution

The results of sieve analysis are shown in Figure 3.3. These results were useful to understand the effect of the concentration of stearic acid, EC and HPC on the granule size fractions (F), defined as fines (F < 500 µm), fraction of interest for tableting (500 µm < F < 1400 µm) being the granulation yield, and oversized granules (F > 1400 µm). Large size granules are obtained with the increase in the amount of binder stearic acid or polymer, as a result of increase in the cross-linking inside the matrix granules, which leads to the increase in the matrix density of the granules.

3.4.4. Evaluation of tablets

The formulated tablets were evaluated for hardness, friability, weight variation, and thickness. These parameters were found to be within the acceptable limits as shown in Table 3.3. OND content uniformity in the prepared tablets was determined. Briefly, 20 tablets were selected randomly and triturated with the help of morter and pestle. The amount equivalent to weight of one table was weighed and OND content was determined using UV-Vis Spectrophotometer at λmax 305 nm against blank. All of the formulations possessed exceptional drug content (> 98%) as well as content uniformities (< 2% RSD) after the melt granulation process. This is indicative of a robust formulation and process.

Table 3.3: Comparisons of the physical properties of the matrix tablets containing Ondansetron hydrochloride

Formulation	Hardness (Kp)	Thickness (cm)	Weight (mg)	Friability (%)	Content Uniformity (%)
F1	6.3±0.07	2.40	150.2	0.32	100.5
F2	6.2±0.05	2.38	150.3	0.35	100.2
F3	6.0±0.01	2.37	151.2	0.31	98.46
F4	6.7±0.06	2.39	149.8	0.30	101.3
F5	6.2±0.02	2.40	150.3	0.32	101.7
F6	6.8±0.04	2.37	150.7	0.35	103.4
F7	5.9±0.03	2.39	151.4	0.31	102.6
F8	6.6±0.08	2.41	150.9	0.35	99.8
F9	6.1±0.04	2.40	151.3	0.32	102.4
F10	6.9±0.03	2.38	151.5	0.36	103.8

3.4.5. Tablet Surface pH measurement using contact electrode

To determine the effect of fumaric acid on OND solubility and release characteristics, the tablet surface pH was measured every hour during 10 h of the study using a pH Spear, Oakton pH meter. It was expected that the pH of the tablet surface for all of the samples would be similar to the pH value of the dissolution media. For the first 2 h when 0.1 N HCl (pH 1.2) dissolution

media was used the tablet surface measured a pH of 1.2-1.4, whereas after 2 h when phosphate buffer was added, the dissolution media pH was changed to 6.8, at that time the differences in tablet surface pH were observed between samples during different time intervals. Formulation F1 and F2 (without fumaric acid) indicated pH values the same as pH of the dissolution media (for first 2 h in 0.1N HCl the tablet pH was 1.2-1.4, and in HCl-phosphate buffer pH was 6.8-7.0). Formulation F3 and F7 (with fumaric acid) measured pH 1.2-1.4 for the first 2 h in 0.1 N HCl and after 2 h pH of the tablet surface was changed to 3.5-4.0 in the HCl-phosphate buffer dissolution media of pH 6.8 (Figure 3.4). This indicates that fumaric acid is dissolved inside the tablet microenvironment and thus maintaining the acidity inside the tablet, which assisted in the solubilization of OND in dissolution media with higher pH.

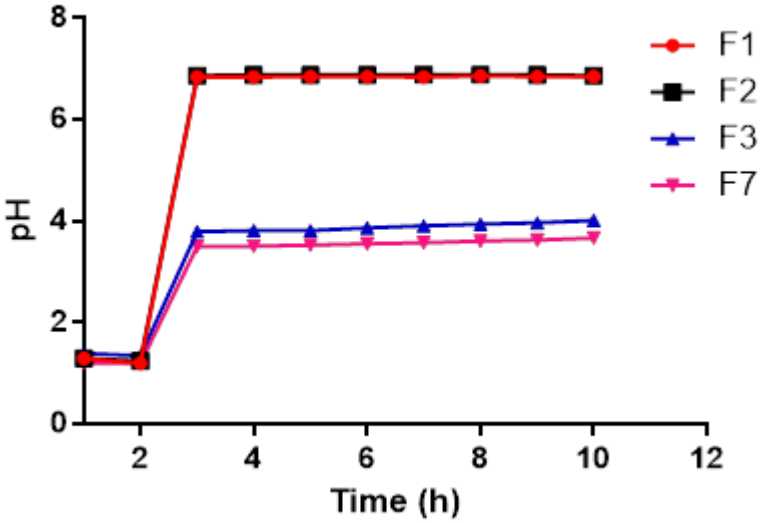

Fig 3.4: Change of gel layer pH within the dissolution test of the matrix tablets (2 h in 1.2 and following 2 h pH changes to 6.8).

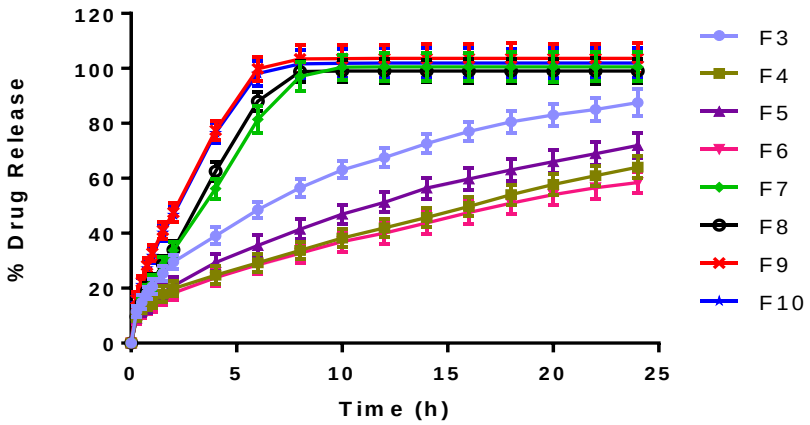

Fig 3.5: In-vitro drug release profile for formulations F3-F10 by two-step dissolution media method

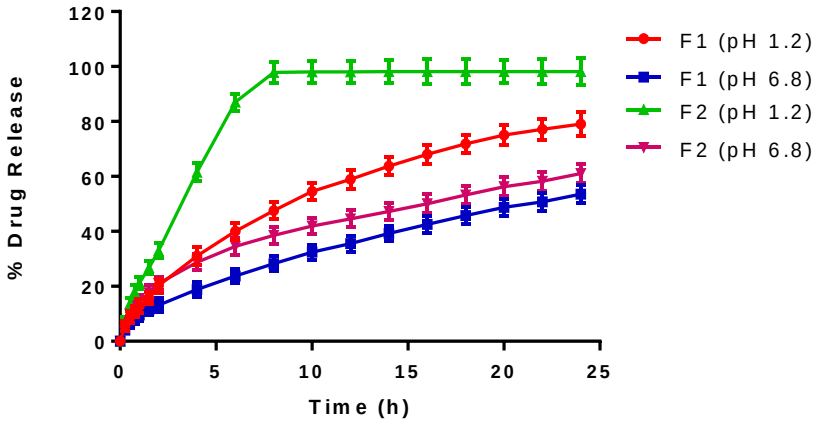

Figure 3.6: Effect of pH of surrounding media on OND release from formulations F1 and F2

3.4.6. Effect of pH of dissolution media, fumaric acid and different polymer matrices on drug release

In-vitro dissolution studies for all formulations were performed using the two-step dissolution method by changing pH, which better corresponds to the real conditions in the gastrointestinal

tract (2 h in pH 1.2 and following 22 h in pH 6.8) [64] (Figure 3.5). Also, *in-vitro* dissolution studies were performed in both 0.1 N HCl and pH 6.8 buffer individually to see the effect of change in the pH of the dissolution media on drug release. As expected, the pH of the dissolution medium was found to significantly affect ($p<0.05$) the release rate of OND from the matrix system. Figure 3.6 showed a lower percentage of OND release at pH 6.8 as compared with the high percentage of OND release in 0.1 N HCl at 24 h, which is due to the very low aqueous solubility of OND at basic pH.

To study the effect of fumaric acid on drug release, *in-vitro* dissolution studies for formulations containing fumaric acid (F3/F7) and formulations without fumaric acid (F1/F2) were conducted in both pH 1.2 and pH 6.8 buffer media. Formulation F3 and F4 composition contained fumaric acid to create a constant acidic micro-environment inside the tablets. Therefore, irrespective of the pH of the surrounding dissolution medium, fumaric acid assisted in the solubilization and release of OND (weakly basic drug) in high pH dissolution medium corresponding to the intestinal pH. These data contribute to solving the pH-dependent solubility problem of OND. Ideally, fumaric acid should dissolve slowly so that it will remain inside the tablet during the entire period of drug release. The dissolution results clearly indicated that the presence of fumaric acid in the matrices increased the dissolution of OND in phosphate buffer pH 6.8. Approximately 90% of drug was released within 24 h from formulation F3 containing fumaric acid in both pH 1.2 and pH 6.8 buffer. The maintenance of a constant and low acidic microenvironment by fumaric acid created the most favorable conditions for OND release. However, formulation F1 and F2 which do not contain fumaric acid demonstrated slower drug release in pH 6.8 as compared to that of pH 1.2 media. These observations indicate that the presence of fumaric acid inside the tablet may affect initial porosity of the tablet as well as

assisting in maintaining the acidic pH inside the tablet, which resulted in the increased drug release. To clarify the important role of fumaric acid in the pH-independent/pH-dependent release of OND in both gastric and intestinal fluid, dissolution profiles of both EC-SA and HPC-SA matrix OND tablets containing fumaric acid (F3 and F7) are compared in Figure 3.7.

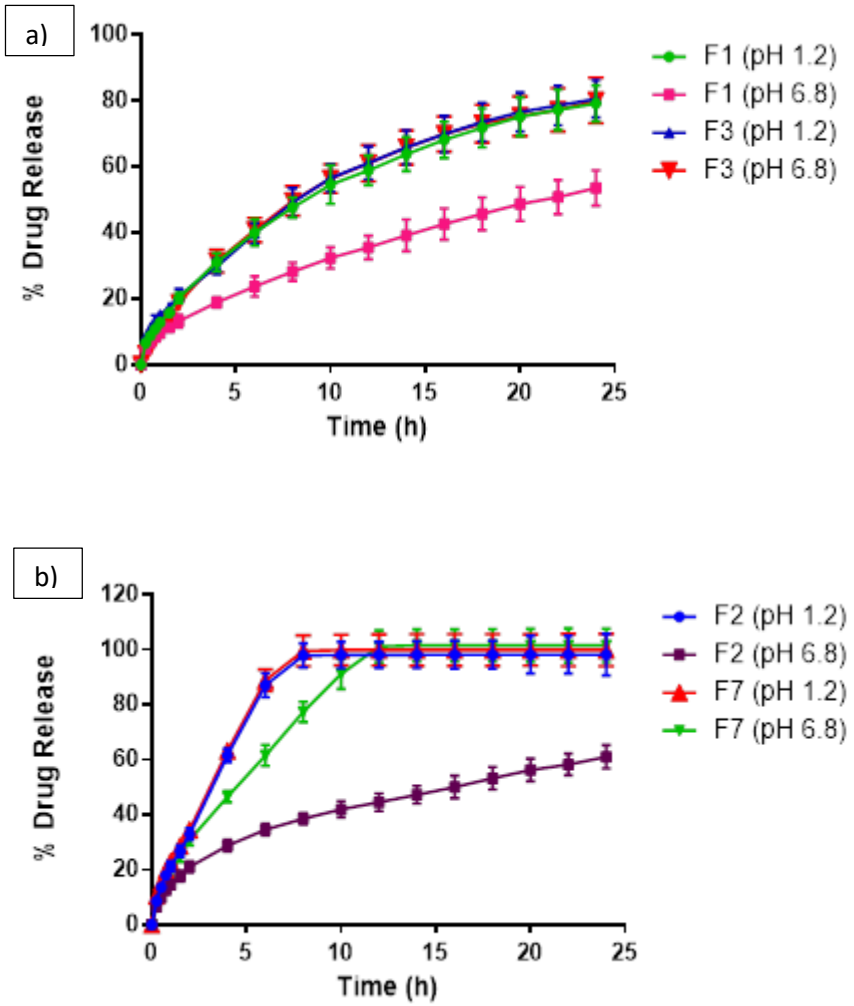

Fig 3.7: Effect of fumaric acid on drug release from a) EC-SA matrix b) HPC-SA matrix

This research group also studied the effect of different types of polymers in combination with stearic acid on the drug release profile. It was observed that the release of the drug depends upon the type of polymer used in the formulation. Ethyl cellulose (hydrophobic polymer) along with

stearic acid sustained the drug release over the period of 24 h (90% drug release). However, hydroxypropyl cellulose (hydrophilic polymer) in combination with stearic acid sustained drug release over a period of 7-9 h (100% drug release) (Figure 3.8). This effect is contributed to the nature of polymer in use. The formulations with EC-SA matrices demonstrated a retarded release of the drug compared to the more hydrophilic matrices. This may be due to the hydrophobic nature of the EC polymer, which prevents the penetration of the dissolution medium into the tablet matrix leading to slower dissolution and diffusion of the drug molecules from the matrix system. These properties sustain the drug release from the matrix of the tablet for a longer period of time as compared to HPC-SA matrix. In formulations with HPC-SA matrices, it was observed that the release of the drug was faster. HPC due to its water-soluble nature dissolves faster and acts as a channeling agent. In our current study, we have used HPC EF, which has low viscosity in water and therefore, it dissolves faster in aqueous media. In the HPC-SA matrix systems, two drug release mechanisms are possible. One mechanism is that after coming in contact with aqueous media HPC EF are hydrated and swelled resulting in formation of a hydrogel through which the dissolved drug diffuses and transfers into the dissolution media. Secondly, dissolution of HPC in dissolution media results in a further increase in drug release. Also, due to the hydroxyl ion (from pH 6.8 media) fumaric acid is dissolved resulting in more pore formation in the HPC matrix as compared to EC-SA matrices. Drug release occurs by mixed mechanisms of diffusion and erosion of the matrix [59, 72]. Thus, the HPC-SA system retarded drug release (< 10 h) as compared to EC-SA matrices.

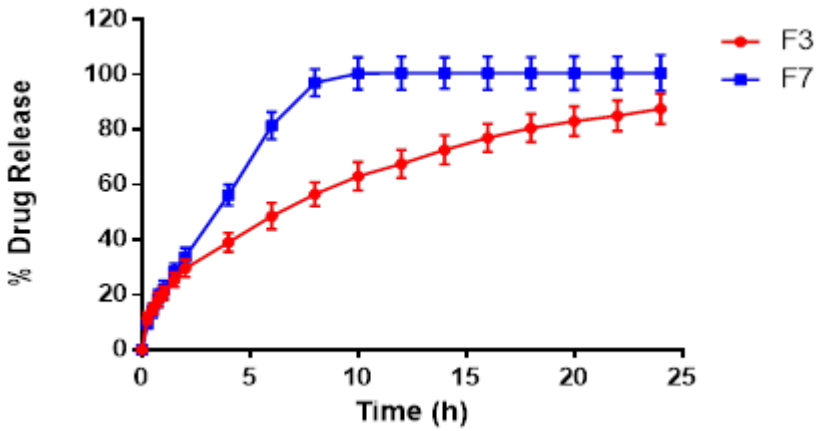

Fig 3.8: Effect of type of polymers (ethyl cellulose and hydroxypropyl cellulose) used in the formulations on drug release profile by two step dissolution method

The *In-vitro* study also revealed that the release of drug was retarded with the proportional increase in the polymer and binder concentration such as in the case of the EC-SA matrix (Figure 3.9a). *In-vitro* drug release decreased from 90% to 64% and 71.9% (F3 to F4 and F5) with the increase in polymer or lipid concentration respectively. In formulation F6, where the percentage of both EC and SA in the tablet composition was increased, the drug release further reduced to 58% at the end of 24 h of dissolution study. On the other hand, the increase in the percentage of HPC and SA in formulation F10 resulted in faster drug release. Complete drug release was obtained within 6.5 h for formulation F10, whereas it was 9.5 h for formulation F7 (Figure 3.9b). The drug release mechanism seen here was the combined effect of diffusion and erosion processes due to the dissolution of HPC and fumaric acid.

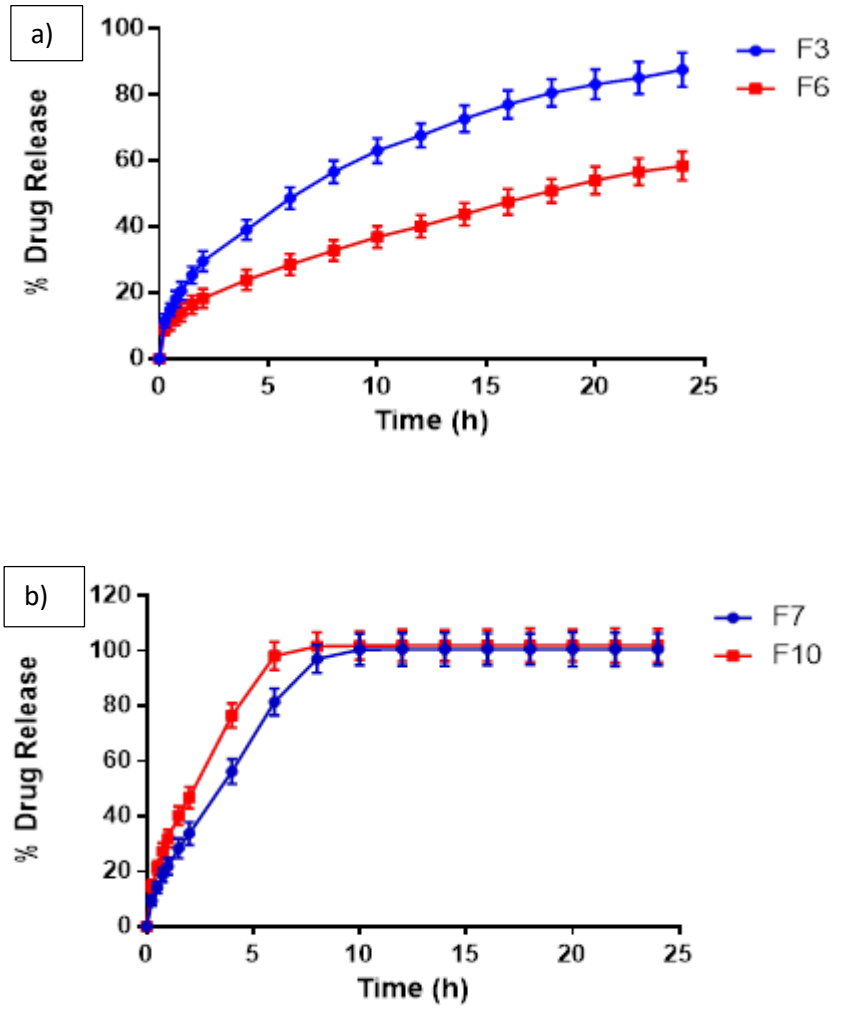

Fig 3.9: Effect of concentration of polymers and binder a) ethyl cellulose (37% and 40%) b) hydroxypropyl cellulose (37% and 40%) used in the formulation on release of OND by two step dissolution method

3.4.7. Similarity and dissimilarity

Similarity factor (f_2) and dissimilarity factor (f_1) were calculated using the release profiles of the formulations in pH 1.2 and 6.8 to see the effect of fumaric acid, pH of surrounding media, and type of polymer used in the formulations.

As shown in Table 4, f_2 value for formulations F1 and F2 in pH 1.2 and 6.8 media were 40 and 29 and, the f_1 values were 36 and 49 respectively. These results indicate that the release profile of

formulation F1 and F2 were not similar as the f_1 value is less that 50 and f_2 value is more than 15. These data indicate that formulation F1 and F2 exhibited pH-dependent release profiles and therefore shows different profiles as change in the pH of the dissolution media. This research group also studied the effect of addition of fumaric acid on the similarity and dissimilarity factor. f_2 value for formulations containing fumaric acid such as F3 and F7 in pH 1.2 and 6.8 were 74 and 44, whereas f_1 value were 6 and 25 respectively, indicating similarity in the dissolution profile for formulation F3, whereas slight dissimilarity in F7. The dissolution profiles and f_1/f_2 values for formulation F3 confirms that it exhibits pH-independent solubility and pH changes do not influence dissolution of this formulation.

Use of different polymers in the formulation composition illustrated different dissolution profiles. As shown in Table 3.4, f_2 values for formulations F3/F7 was 41 and f_1 values was 36 confirming the differences in the dissolution profiles.

Table 3.4: Similarity and Dissimilarity factor analysis

Formulations	Similarity factor	Dissimilarity factor
F1 (pH 1.2 and 6.8)	40	36
F2 (pH 1.2 and 6.8)	29	49
F3 (pH 1.2 and 6.8)	74	6
F7 (pH 1.2 and 6.8)	44	25
F3/F7	41	36

3.4.8. Determination of drug release kinetics

In order to describe the release behavior of OND from different formulations, the dissolution profiles were analyzed according to kinetic equations such as zero-order, first-order, Higuchi and Korsmeyer-Peppas. The regression coefficient values of different release kinetic equations for all developed formulations were compared as shown in Table 3.5. All batches containing EC in combination with stearic acid (F3-F6), showed a very good correlation to the Higuchi equation (r^2=0.9902-0.9985). The Higuchi plot showed high linearity in comparison to other release kinetic equations, which indicates that the drug release is heavily governed by the diffusion process. To confirm the diffusional mechanism, the data were fitted into Korsmeyer–Peppas equation. As shown in Table 4, release exponent (n) found for batches F3-F6 was less than 0.5. Release exponent n<5 is considered consistent with a diffusion-controlled release, whereas values of n between 0.5 – 1 indicates non-Fickian (anomalous) release mechanisms.

Table 3.5: Mathematical modeling and release kinetics of OND from the prepared formulations (F1-F10)

Formulation	Zero order plot Correlation coeff. (R^2)	First order plots Correlation coeff. (R^2)	Higuchi's plots Correlation coeff. (R^2)	Korsmeyer-Peppas plots	
				Correlation coeff. (R^2)	Diffusional exponent (n)
F1	0.9533	0.1383	0.9897	0.9889	0.42
F2	0.9249	0.2162	0.9939	0.9929	0.43
F3	0.9386	0.6328	0.9973	0.9985	0.46
F4	0.9776	0.2201	0.9914	0.9908	0.39
F5	0.9617	0.3551	0.9992	0.9959	0.45
F6	0.9721	0.1789	0.9964	0.9902	0.40
F7	0.7938	0.5678	0.9215	0.9989	0.65
F8	0.765	0.6615	0.9029	0.9991	0.63
F9	0.7243	0.3957	0.8808	0.9997	0.56
F10	0.7221	0.4745	0.8792	0.9987	0.57

The mechanism of drug release through matrices containing water soluble and swellable polymers in combination with lipophilic binders is a more complex process. Formulations containing HPC in combination with stearic acid (F7-F10) demonstrated a good fit to the Korsmeyer–Peppas equation, indicating combined effects of diffusion and erosion mechanisms for drug release. Moreover, the release exponent n was within the range of 0.50-0.89, indicating a non-Fickian diffusion mechanism and that drug release was governed by both diffusion and matrix erosion. Thus, drug release was controlled by more than one process in the case of the HPC-SA matrices.

Conclusion

It can be concluded from this study that the continuous melt granulation technique within a twin-screw extruder is a viable method to develop a sustained release tablet of OND. The granules prepared with the melt granulation binder (stearic acid) exhibited good flowability as well as good compressibility with a fewer amount of fines. Stearic acid in combination with EC (F3) demonstrated prolonged release of OND for 24 h with 90% drug release, whereas stearic acid in combination with HPC (F7) showed 100% drug release over a period of 9 h. The incorporation of fumaric acid in the formulation led to the improvement of OND release from both EC-SA and HPC-SA systems. Thus, this work formulated a sustained release OND matrix tablet that was not influenced by pH in dissolution testing. In conclusion, the novel aspect of the current study is its demonstration of the feasibility to continuously manufacture ready-to-compress melt granules of OND by a twin-screw extruder that can be processed into tablets to provide pH-dependent/pH-independent sustained release of the drug.

CHAPTER IV

NOVEL DRY-GRANULATION PROCESS FOR CONTROLLED RELEASE FORMULATIONS OF ONDANSETRON HYDROCHLORIDE DIHYDRATE USING TWIN SCREW EXTRUDER

4.1. Abstract

The aim of this study was to apply a quality by design (QbD) approach based on design of experiments as a risk-based proactive approach to achieve predictable critical quality attributes (CQAs) to develop a dry-granulation process for controlled release formulation of Ondansetron sustained release tablets by twin-screw extruder. Optimization of formulation and process parameters reduces the variability and thus results in the quality improvement, risk reduction and productivity enhancement. Preliminary studies were conducted to select screw design, ratio of polymers and barrel temperature to achieve dry granulation via twin-screw extruder. Further, the effect of screw speed, feed rate and amount of fumaric acid on the particle size and flow properties of the granules and time required for complete and controlled release of the drug from the dosage was optimized by 2^3 factorial design. Based on the design of experiment (DOE) results, a formulation comprising of 2.5% (w/w) fumaric acid extruded at high screw speed (100 rpm) and low feed rate (1%) was found to fulfill requisites of an optimum formulation. The optimized formulation Z8 showed High percentage of medium size granules (89%), low angle of repose (25), and the formulation showed sustained release of OND over the period of 15.5 h with

100% drug release. This study introduces the novel dry granulation process for the development of OND controlled release formulation via twin-screw extruder as well as highlights the level of understanding that can be accomplished through a well-designed study based on the approach of QbD.

4.2. Introduction

Granulation is a process in which the small particles are made to cohere into larger, multi-particle masses, so called granules i.e. a process of small particle enlargement by agglomeration phenomena. This process is routinely utilized in the pharmaceutical industries in order to reduce dust of the small particles thus preventing the potential health and environmental hazard, to prevent segregation, granules are easy to handle and transport, and also they are free flowing therefore useful for dosage filling (capsules) and compression process (tablets) [73-75]. Granulation process can be divided into two types: wet and dry granulation. Wet granulation process which utilizes some form of solvent to bind the small particles together and dry granulation process is performed without adding any solvent. The methods utilized for wet granulation are either low-shear mixing, high-shear mixing, extrusion-spheronization or fluid-bed processing, whereas dry granulation process involves either slugging or roller compression [73]. The obtained compacts in the dry granulation process is known as briquettes, flakes or ribbons and in order to obtain the desired granules, the compaction process is further followed by a milling step. Apart from these granulation methods, twin-screw extruder has now been extensively utilized for granulation process.

Twin-screw extrusion is a continuous solvent-free process, in which the physical mixture is introduced into the extruder through the feeder and the extrudate is collected through the die

block under the controlled feeding rate, temperature, mixing (kneading with the help of different screw configuration), and pressure. Whereas, in case of granulation process in order to collect the granules continuously, the twin-screw extruder is used without the die block in order to prevent the immoderate densification of material inside the barrel. As per the literature, till now only wet and melt granulations were prepared by twin-screw extruder. The continuous production of dry granules via twin-screw extruder has not previously been demonstrated.

Therefore, the objective of this study was to develop a continuous twin-screw dry granulation process to prepare dry granules using a model drug ondansetron (OND) for formulating sustained release tablets. OND, a carbazole derivative, is a competitive and selective serotonin (5-HT3) receptor antagonist recommended for preventing nausea and emesis in the patients undergoing cancer chemotherapy and radiation therapy, and it is also used to prevent post-operative nausea and episodes of emesis. OND is commercially available in both oral and injectable forms. OND has a relatively short terminal elimination half-life of approximately 3-5 h following the oral administration and therefore, sustained release formulation is needed for this drug.

The final goal of this study is to apply QbD approach to the optimization of OND sustained release formulation prepared via twin-screw dry granulation process. The important part of this approach is to understand how formulation and process parameters affect the product performance and following optimization parameters with respect to final stipulation.

4.3. Materials and Methods:

4.3.1. Materials

Ondansetron HCl dihydrate was purchased from Chemscene LLC (New Jersey, USA). Hydroxypropyl cellulose (Klucel EF) was generously gifted by Ashland Specialty Ingredients (Wilmington, DE). Ethyl cellulose (Ethocel Standard 10) was kindly gifted by Dow chemical company. Fumaric acid and Magnesium stearate was purchased from Spectrum Laboratory Products Inc. (Gardena, CA). All the other reagents used in this study were of the analytical grade.

4.3.2. Methods:

4.3.2.1. Drug-excipient interaction studies

In order to study the interaction of OND with the polymers and other excipients used in this study, physical mixture was prepared in 1:1 ratio by mixing the OND with each of the formulation excipients. Differential scanning calorimetry (Diamond DSC, Perkin Elmer Life and Analytical Sciences, 710 Bridgeport Ave., Connecticut, USA) equipped with Pyris manager software (Shelton, CT, USA) and Fourier transform infrared spectroscopy (FTIR, Agilent Technologies Cary 660, Santa Clara, CA) was utilized to study the compatibility of OND with other excipients. In brief for DSC study, samples were prepared by hermetically sealing approximately 3-5 mg of pure API and physical mixture in an aluminum pans. These samples were then heated over a temperature range of 40-250 ^{o}C at a linear heating rate of 10 ^{o}C/min under an inert nitrogen atmosphere. Whereas mid- infrared spectra in the range of 4000-650 cm^{-1} were collected on FTIR bench equipped with an MIRacle ATR (Pike Technologies, Madison, WI), which was fitted with a single bounce diamond coated ZnSe internal reflection element.

4.3.2.2. Preliminary screening for the selection of formulation variables and process variables

Preliminary studies were conducted to determine the process parameters, screw configuration and barrel temperature as well as formulation parameters such as ratio of polymers, type and amount of acidifier and lubricant required for the successful dry granulation process. The effect of all these parameters on the quality of granules was studied. As well as the API form (crystalline/amorphous) present in the granules were determined.

Table 4.1: Formulation composition

Formulations	**Ondansetron (%)**	**EC (Ethocel® 10P) (%)**	**HPC EF (%)**	**Fumaric acid (%)**	**Mg.S. (%)**
Formulation A	20%	36.25%	36.25%	7.5%	0.2% intragranule plus 0.3% extragranule
Formulation B	20%	37.5%	37.5%	5%	0.2% intragranule plus 0.3% extragranule
Formulation C	20%	38.75%	38.75%	2.5%	0.2% intragranule plus 0.3% extragranule

Table 4.2: Barrel Temperature Setting

Barrel Temperature								
Feed Zone	Zone 2	Zone 3	Zone 4	Zone 5	Zone 6	Zone 7	Zone 8	Die
°C								
N/A	70	70	80	90	80	70	70	40

4.3.2.3. Twin-screw extrusion process for the dry granulation

Formulation composition and the processing parameters are as shown in the Table 4.1 and 4.2, respectively. Briefly, ondansetron HCl dihydrate and other inactive ingredients were passed through US mesh # 35 (500 µM) in order to remove any aggregates that may have formed. Organic acid (Fumaric acid) was added in the formulation composition in order to solve the pH-dependent solubility of the OND. Magnesium stearate was also added in the formulation composition as a lubricant to prevent squeaking noises generated by the extruder while extruding these formulations. Further, the physical mixture (OND (20% w/w) and other inactive ingredients) was mixed using a V-shell blender (GlobePharma, Maxiblend^{TM} New Brunswick, NJ) at 25 rpm for 20 min. Dry granulation process was performed without an extrusion die block in a fully intermeshing co-rotating twin-screw extruder (11 mm Process 11^{TM} Thermo Fisher Scientific) with modified screw configuration design (Fig 4.1). The prepared physical mixture was fed to the extruder with the help of volumetric feeder through the first zone (no heating). Temperature for all barrel zones were selected based upon the preliminary study optimization

and was below the melting point of OND (189 ^{o}C) (Table 4.2). Also the powder feed rate (g/min) and the screw speed (rpm) were set at two levels, low and high and were selected based on the preliminary study and varied according to the process parameter. As soon as the steady state was reached the granules were collected at the end of discharge element of the extruder (without the die block). The collected granules were stored in sealed aluminum pockets for further analysis.

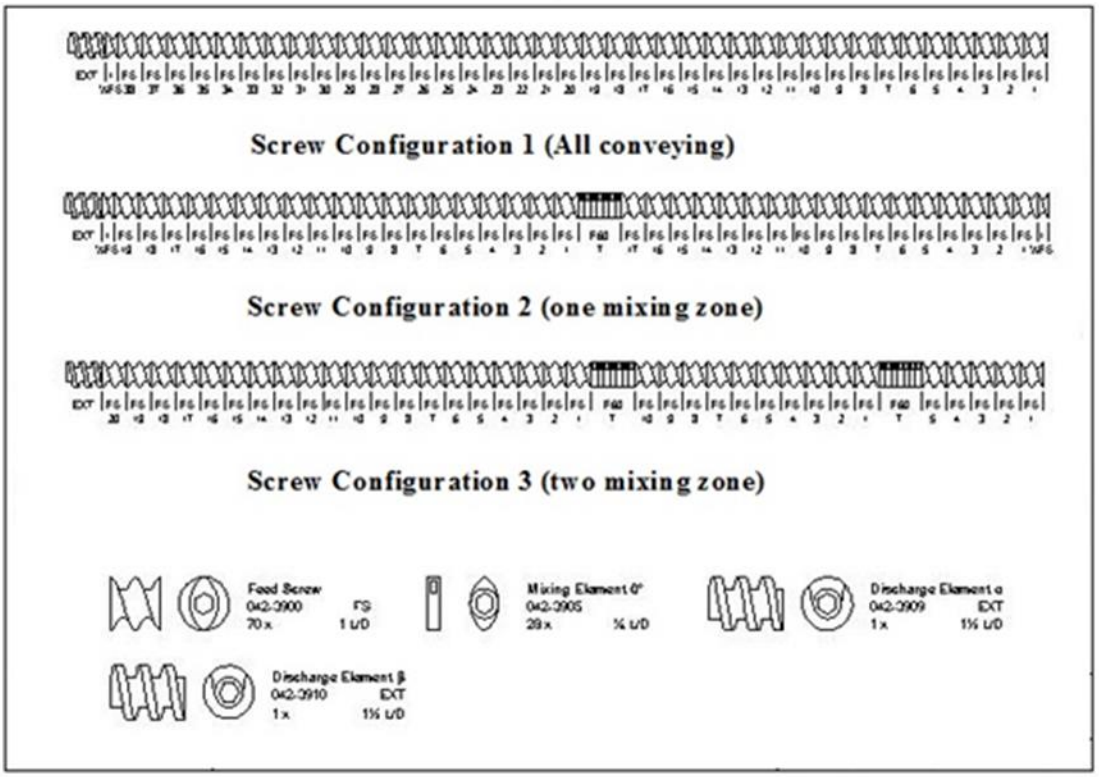

Fig 4.1: Screw design

Table 4.3: Quality target product profile

QTPP Element	Target	Justification
Dosage form	Tablet	Pharmaceutical equivalence requirement: same dosage form
Route of administration	Oral	Pharmaceutical equivalence requirement: same route of administration
Dosage strength	30 mg	
Pharmacokinetics	*In-vitro* dissolution – 12-15hrs 80% release	
Stability	At least 6 months 40C/75RH accelerated stability	
Drug Product quality attributes	Physical Attributes	Tablets (size, color, shape)
	Identification	Positive identification for ondansetron HCl dihydrate
	Assay	90.0-110.0 (Compendial requirement)
	Content Uniformity	AV $\leq$ 15.0 (USP<905>)
	Degradation Products	Monitor and report (CQA)
	DSC	Monitor and report (CQA)
	TGA	Monitor and report (CQA)

	XRPD	Monitor and report (CQA)
	NIR	Monitor and report (CQA)
	Residual Solvents	Will not be monitored for this study
	Drug Release	ER
	Microbial Limits	Will not be monitored for this study
	Water Content	Will not be monitored for this study
Container Closure System	NA	
Administration/concurrence with labeling	NA	
Alternate methods of administration	NA	

4.3.2.4. QbD approach for the development of dry granules via twin-screw extruder

QbD study involves several key elements in it such as quality target product profile, determination of critical quality attributes (CQAs), and relationship between formulation/process parameters with CQAs and based on it, determines the risk assessment and development of design space for the optimization of formulation. Quality target product profile were set for the desired formulation and given in Table 3. Primary determinants of OND sustained release formulation prepared by twin-screw dry granulation process were selected as CQAs for the

formulation and process optimization. The CQAs and their acceptance limits are listed in table 4.4.

Table 4.4: Quantification of CQAs

CQAs	Desired target value
Particle size	1.4 mm – 500 μm
Angle of Repose	25-31
Dissolution time (100% drug release)	12-16 h

Table 4.5: Initial risk assessment

Drug Product CQAs	Process steps		
	Twin Screw extrusion	Milling	Compression
Particle Size	Low	Low	High
Assay	High	Low	Low
Content Uniformity	High	Low	Low
Drug Release	High	High	High
Drug release –alcohol-induced dose dumping	High	High	High

Initial risk assessment was determined to identify potentially high risk formulation and process variables and to determine which studies were necessary to achieve product and process understanding in order to develop a control strategy (Table 4.5).

Table 4.6: 2^3 Full Factorial Design (with 2 center points)

Factor (independent variables)	**Level-1**	**Level+1**	**Responses (dependent variables)**
Screw Speed (RPM)	25	100	1. Particle size 2. % Dissolution 3. Flow properties
Feed Rate (%)	1	3	
Fumaric acid (%)	2.5	7.5	

4.3.2.5. Experimental design

A full 3 factor, 2 level (2^3) factorial design was used to optimize the process and formulation parameters (Table 4.6 and 4.7). A total 10 trial formulations were proposed by the 2^3 factorial designs for three independent variables (factors) namely, feed rate, screw speed and amount of fumaric acid, which were varied at two levels (low and high). Particle size distribution (PSD),

dissolution time and flow properties (angle of repose) were selected as the response variables. The linear equation of the model is as follows:

$$Y = b0 + b1X1 + b2X2 + b3X3 + b4X4 + b5X5 + \cdot\cdot\cdot + bnXn \quad \text{Eq. 1}$$

where Y is the dependent variable, b0 is the arithmetic mean response, b1, b2, b3, b4 and b5 are the estimated co-efficient for the factor X1, X2 and X3. The statistical analysis of the factorial design formulations was performed using Design-Expert® (Version 9.0.5, Stat-Ease Inc., Minneapolis, MN).

Table 4.7: Design of experiments

Screw Speed (RPM)	Batch	Feed Rate (g/hr)	Fumaric Acid (%)	Torque (%)	Specific Energy (kw hour /kg)
25	**Z1**	40	7.5	15.83	0.009
	Z2	40	2.5	16.66	0.01
	Z3	120	2.5	33.33	0.01
	Z4	120	7.5	41.66	0.01
62	**Z5**	80	5	28.33	0.02
	Z6	80	5	30	0.02
100	**Z7**	120	2.5	35	0.03
	Z8	40	2.5	20	0.04
	Z9	120	7.5	35.83	0.03
	Z10	40	7.5	20	0.04

4.3.2.6. Physicochemical properties of granules

4.3.2.6.1. Particle size distribution

Sieve analysis method was used to determine the particle size distribution. Two USA standard test sieve, # 35 (500 µm) and # 14 (1.4 mm) were used and the amount of granules retained on each sieve were weighed. Three fractions were collected, first the granules size of more than 1.4 mm retained at the topmost sieve (# 14), second the granules size of between 1.4 mm – 500 µm retained at the second sieve (# 35), finally fines were collected at the bottom having granules size less than 500 µm. Percentile weight distribution was determined for all of the three fractions.

4.3.2.6.2. Flow Properties

The bulk volume (V_o) of 5 g of granules was measured in 10 ml of graduated glass cylinder. The bulk density (ρ_b) was calculated by the following equation:

$$Bulk\ density\ (\rho_b) = \frac{amount\ of\ granules\ weighed\ (5\ g)}{bulk\ volume\ (V_o)} \ldots\ldots\ldots\ldots Eq.2$$

The graduated glass cylinder was tapped manually 100 times until no further reduction in the volume of the granules was observed. Tapped density (ρ_t) was calculated by using the volume of the granules after tapping 100 times (V_{100}) by the following equation:

$$Tapped\ density\ (\rho_t) = \frac{amount\ \ of\ granules\ weighed\ (5\ g)}{tapped\ volume\ (V_{100})} \ldots\ldots\ldots\ldots \text{Eq. } 3$$

Carr's (compressibility) index (CI) and Hauser's ratio (HR) was calculated by the following equations:

$$CI = \frac{(\rho_t - \rho_b)}{\rho_t} \times 100 \ldots\ldots\ldots\ldots Eq.4$$

$$HR = \frac{\rho_t}{\rho_b} \ldots\ldots\ldots Eq.5$$

Angle of repose was determined by funnel method. The height of the funnel above the horizontal plane surface, on which the wax paper was placed, was adjusted in such a way that the tip of the formed cone of the granules just touched the tip of the funnel. The accurately weighed granules were freely poured through the funnel on the wax paper. The diameter and the height of the cone were measured and the angle of repose (θ) was calculated by the following equation:

$$Tan\,(\theta) = \frac{h}{r} \ldots\ldots\ldots Eq.6$$

Where, 'h' and 'r' are the height and radius of the formed cone, respectively.

4.3.2.6.3. True Density and Surface Area

The true density of the granules was measured (n=3) with the help of helium pycnometer (AccuPyc II 1340 Pycnometer, Micromeritics, USA). The surface area of the granules was determined (n=3) using Gemini VII 2390 (Micromeritisc, USA).

4.3.2.7. Tablet Compression

The obtained granules were mixed with 0.3% magnesium stearate just prior to manual direct compression on a single punch tablet press (MCTMI, GlobePharma Inc., New Brunswick, NJ), by using an 8 mm flat round punch at a compression force of 140 kg/cm.

4.3.2.8. Tablet Evaluation

The prepared compressed tablets were evaluated for hardness, thickness, friability and drug content uniformity. For hardness test, ten tablets were randomly selected and were tested with Schleuniger-hardness tester. The thickness of the tablets (n=10, randomly selected) were measured by digital Vernier caliper (Montata). The tablet friability was determined using a dual scooping projection Vander Kamp friabilator (Vankel Industries Inc., Chatham, NJ) at speed of 25 rpm for 4 min. The percentage weight loss of tablets (weighing 6.5 g) was expressed as the tablet friability. For drug content uniformity, tablets (n=10, randomly selected) were accurately weighed and average weight was calculated. Briefly, they were grounded with the help of mortar and pestle, and powder equivalent to 10 mg of OND was accurately weighed and dissolved in 0.1 N HCl. The absorbance was measured at λmax 305 nm using UV-VIS Spectrophotometer and the percentage drug content was calculated using calibration curve of OND.

4.3.2.9. *In-vitro* drug release

In-vitro drug release from the compressed tablets was measured using USP dissolution apparatus type-II (Hanson SR8 Plus), set at a paddle speed of 50 rpm and equipped with UV-Vis probes (Rainbow dissolution monitor, PION). The UV spectra were collected at λmax 305 nm every 2 min for first 2 h and then for every 25 min until 24 h. For the first 2 h the dissolution media consisted of 700 ml of 0.1 N HCl (pH 1.2) with 1% sodium laurly sulfate (SLS), after that 200 ml of 0.2 M tribasic sodium phosphate (pH 12.5) with 1% SLS (maintained at 37 ± 0.5 ^{o}C) was added to achieve final pH of 6.8 for 24 h, in order to simulate the tablet transit from the stomach (pH 1.2) to the intestine (pH 6.8). *In-vitro* drug release study was performed in triplicate and the mean % drug release was plotted against time (h).

4.3.2.9.1. Computation of release kinetics of 30 mg ondansetron HCl dihydrate matrix tablet

In order to study the mechanism of drug release kinetics from the optimized formulation of 30 mg ondansetron HCl dehydrate matrix tablet, the *in-vitro* drug release dissolution data was evaluated kinetically by the following equations:

$$Zero - order\ equation: Q_t = Q_0 + K_0 t \ldots\ldots\ldots Eq.7$$

$$First - order\ equation: log\ Q_t = log\ Q_0 + \frac{K_1 t}{2.303} \ldots\ldots\ldots Eq.8$$

$$Higuchi\ equation: Q_t = K_H \sqrt{t} \ldots\ldots\ldots Eq.9$$

$$Korsmeyer - Peppas\ equation: \frac{Q_t}{Q_\infty} = K_{kp} t^n \ldots\ldots\ldots Eq.10$$

where, Q_t is the amount of drug released in time t, Q_0 is the initial amount of the drug in the solution (most of the time $Q_0 = 0$), Q_∞ is the amount of drug released after infinite time, K_0 is the zero order release rate constant, K_1 is the first order release rate constant, K_H is the Higuchi diffusion rate constant, K_{kp} is the kinetic release constant incorporating structural and geometrical characteristics of the tablets and 'n' is the diffusion release exponent indicating the drug release mechanism. The mechanism of drug release is dependent on the value of 'n'.

4.4. Result and discussion

4.4.1. Compatibility testing (Drug-excipient interaction):

The selected DSC curve of OND and physical mixture is shown in the Fig 2. The DSC curves represent a well-recognized melting point endothermic peak of pure drug (OND) in the range of 185.2-188.58 ^{o}C. DSC results also indicated that OND is compatible with polymers used in this study as there was no change in the glass transition temperature and melting endotherms of other excipients used in the formulation. This was further confirmed by FTIR, as there was no change in the IR of the OND when mixed with other excipients, thus indicating the absence of drug-excipient interaction.

Table 4. 8: DOE Results

Batch	>1.4 mm % (14 Mesh)	Medium %	< 500 microm % (35mesh)	Hausner's Ratio	Carr's Index	Angle of Repose	Dissolution Time for 100% Drug Release (h)
Z1	40.77381	53.21621	6.009985	1.09	8.69	34	6.5
Z2	26.04511	65.20301	8.75188	1.22	18.18	36	6.5
Z3	70.39839	24.6483	4.953304	1.13	11.53	33	7.5
Z4	81.45596	14.66561	3.878434	1.08	8	43	7.5
Z5	46.61275	48.99556	4.391686	1.13	11.53	30	9.5
Z6	37.40889	57.97194	4.619169	1.13	11.53	31	10.5
Z7	37.91596	57.76051	4.323537	1.13	11.53	36	9.5
Z8	5.575453	89.6525	4.772045	1	0	25	15.5
Z9	46.101	49.33976	4.559243	1.22	18.51	31	12.5
Z10	28.5657	68.91675	2.517553	1.04	4	27	15.5

4.4.2. Preliminary study

4.4.2.1. Screw configuration

Different screw configurations were tried to produce dry granules by using twin-screw extruder. Conveying screw configuration without any mixing zone resulted in the generation of 20% granules and more than 80% materials were remained as un-granulated fine powders, even under high temperature processing. Screw configuration with increase in mixing zone resulted in the generation of more granules and less fines. However, there were lots of big particles formed when the two and three mixing zones were utilized in the screw configuration. Also, screw configurations more than one kneading zone results in the formation of rubbery texture granules which were hard to break while passing through sieve. One kneading zone yielded good quality granules and the particle size distribution was good with around 89% granules of the desired particle size range (500 μm – 1.4 mm) with few big particles as shown in Table 8. Therefore, for further investigation of the dry granulation process, one kneading zone screw configuration was fixed.

4.4.2.2. Barrel temperature

Different barrel temperatures were tried to optimize the barrel temperature in order to produce dry granules of OND. High temperature resulted in the melting of HPC polymer and formation of big agglomerated granules. Due to the melting of HPC polymer the big granules formed were rubbery in texture and were difficult to break easily. Based on the preliminary study results, barrel temperature of around 70-90 ^{o}C showed promising results and therefore this barrel temperature was kept constant for the further experiments. Digital images are shown in Fig.3 for the granules prepared with different screw configurations and at different temperatures.

4.4.2.3. Ratio of polymer

1:1 and 3:1 ratio of EC and HPC were studied to optimize the ratio of polymers. Among these two, 1:1 ratio showed the larger percentage of medium size granules. From these preliminary study results, screw configuration having one kneading zone, 1:1 ratio of EC and HPC and barrel temperature (70-90 ^{o}C) was selected as constant parameters for further optimization of other process and formulation parameters.

4.4.2.4. Addition of acidifier:

It was observed that the formulations without organic acid were unable to release the drug in intestinal pH media due to its weakly basic nature. Presence of organic acid in the tablet creates a constant acidic micro-environment inside the tablets. Therefore, irrespective of the pH of the surrounding dissolution medium, organic acid assisted in the solubilization and release of OND in high pH dissolution medium corresponding to the intestinal pH. Among the three organic acids (citric acid, adipic acid and fumaric acid), fumaric acid showed promising results as it was able to release 100% drug at intestinal pH.

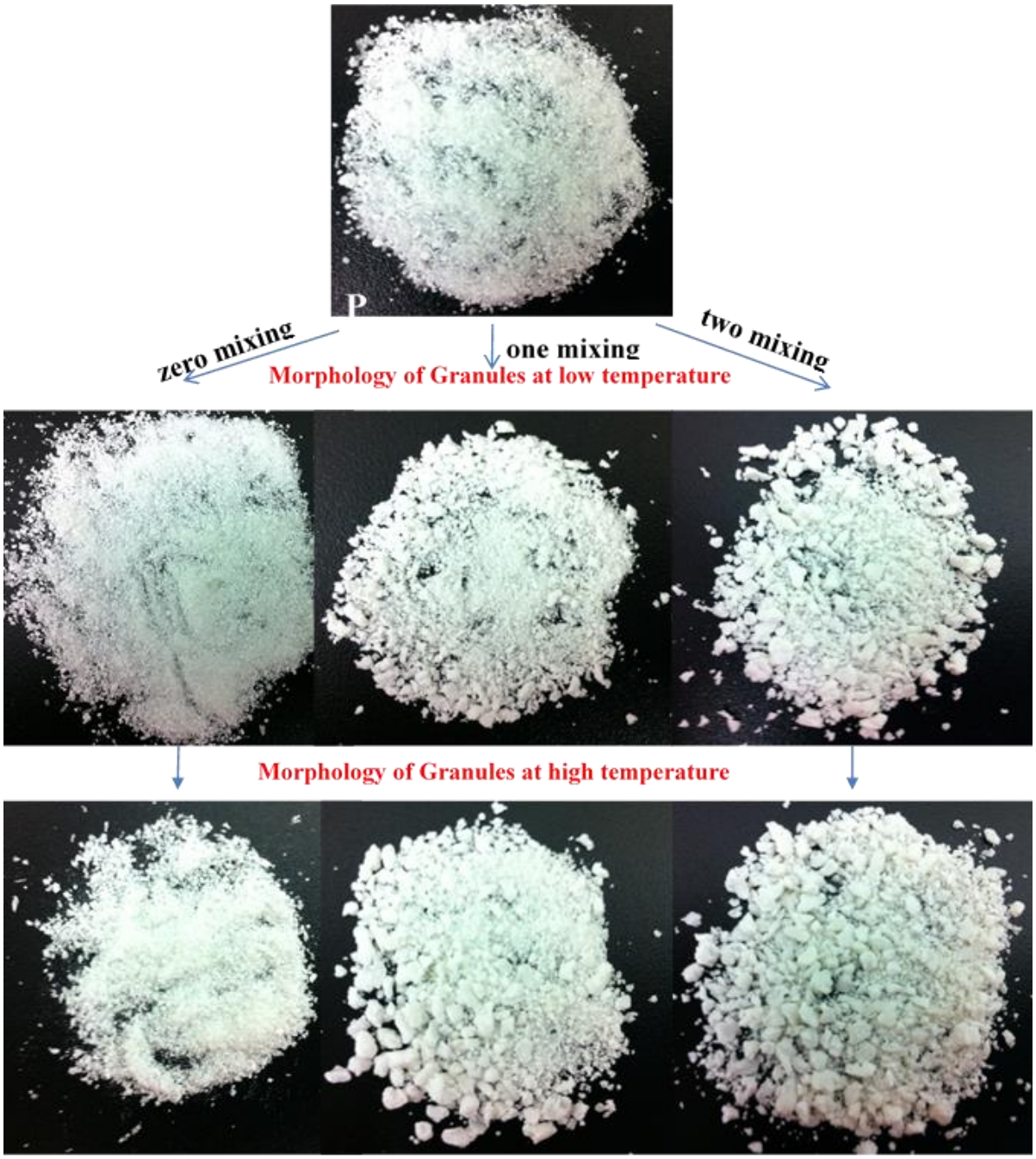

Fig 4.2: Digital images showing pre-screening effects of screw configuration and barrel temperature on granules size

4.4.2.5. Addition of Lubricant:

As this is the dry granulation process all the material remain in a solid state throughout the process and therefore, lubrication step is essential in order to reduce the friction between the surfaces of manufacturing equipment that is in this case twin-screw extruder and that of organic solids as well as to ensure the continuation of an operation (appropriate torque values). Magnesium stearate was used in the formulation composition as the lubricant. Although magnesium stearate act as a lubricant and ease the dry granulation extrusion process, too much magnesium stearate will have adverse effects on tablet hardness and dissolution because it is non-soluble in water. Therefore, generally the recommended amount to be used in the formulation should be less than 1%. To avoid the adverse effects 0.2% of magnesium stearate was used to prepare the dry granules via twin-screw extruder.

4.4.3. Design of experiments

2^3 factorial design was implemented to evaluate the main effects and interaction effects of independent variables screw speed, feed rate and amount of fumaric acid on the dependent variables to obtain the desired granule size, flow properties for the granules prepared by twin-screw dry granulation process and sustained drug release profile of the drug from tablets containing dry granules.

4.4.4. Characterization of Granules

Yields of granulation process were found to be high (97-99%). It was observed that as the process was dry granulation no excipients as well as API was melted at the set process parameters and therefore, no loss of material was seen in the process. After experiment get over when the barrel top was opened, no sticking of material was observed inside the barrel walls or

screws itself. The granules of different formulations were evaluated for crystallinity, particle size, flow properties, true density and surface porosity.

4.4.4.1. Crystallinity

DSC was conducted for pure drug and dry granules prepared by twin-screw extruder. DSC curve of pure OND shows a melting endothermic peak at 189 ^{o}C and for all formulation Z1-Z10, an endothermic peak was observed in the range of 185 - 191 ^{o}C. From DSC data it can be inferred that at the employed twin-screw extruder process parameters as well as formulation parameters for all the formulations, crystalline structure of OND was not lost.

4.4.4.2. Particle size distribution:

Granule particle size distribution results for all the formulation have been shown in Table 8. Three granule size factions were collected that is big granules (> 1.4mm), Medium size granules (fraction between 1.4 mm- 500 μm) and un-granulated fines (< 500μm). For the tableting purpose medium size granules, fraction between 1.4 mm- 500 μm is the important fraction along with the requirement of 10-15% fines in order to get good compressibility. And it is desirable to get maximum percent of granules of medium size. Therefore, particle size between 1.4 mm – 500 μm was selected as the one of the dependent variable (response) in 2^3 factorial design.

The following polynomial equation was generated for granule size prepared by twin-screw dry granulation process:

Particle size = +53.03 + 13.49 *A -16.32 *B -6.39 *C + 3.45 *AB + 1.79 *BC ……Eq. 11

Where, A, B and C are the screw speed, feed rate and amount of fumaric acid respectively. A positive or negative sign of the polynomial terms indicates increase or decrease effect on

response by different level combination of independent variables. ANOVA of the equation suggested the Model F-value of 40.23 implies the model is significant. The “Lack of Fit F-value” of 0.24 implies the Lack of Fit is not significant ($p > 0.0001$). The model was statistically significant for the response particle size with “R-squared” of 0.9852, "Pred R-Squared" of 0.7971 and "Adj R-Squared" of 0.9336 which are close to unity. The "Pred R-Squared" is in reasonable agreement with the "Adj R-Squared". The adequacy/precision ratio was 24.026 indicating signal adequacy. All three independent factors feed rate, screw speed and amount of fumaric acid were found to have significant effect on the particle size of granules. The most significant factor among these three was feed rate. Highest percentage of medium size granules were obtained at lower feed rate (1%). Feed rate showed negative coefficient for response particle size indicating increase in feed rate from 1 to 3 results in the decrease in the percentage of medium size granules. In order to achieve higher percentage of medium size granules it is preferred to keep low feed rate this may be attributed by the amount of material present inside the barrel affects the agglomeration step and with high feed rate high amount of material forcing to pass through the barrel resulting in more dense and big particles.

Screw speed was found to be another factor with the significant influence on particle size. Positive coefficient for the factor screw speed indicates that it has positive effect on the particle size. Increasing screw speed from 25 to 100 rpm resulted in the increase in the percentage of medium size granules at all three levels of amount of fumaric acid. Increase in screw speed results in the decrease in the residence time as well as high shear generation which might be the reason for formation of granules but with the more percentage of medium size granules.

The third independent variable, amount of fumaric acid showed negative coefficient indicating high fumaric acid content in the formulation gives low percentage of medium size granules. This

may be due to the differences in the particle size of fumaric acid and other formulation composition utilized in this process. Hence it may be concluded that to maximize the percentage of medium size granules, low feed rate, high screw speed and low amounts of fumaric acid should be used to get the optimum response. The Eq. 11 is presented in the form of a contour plots and response surface graphs to visualize the effect of all changing independent variables on granule size (Fig. 4.3).

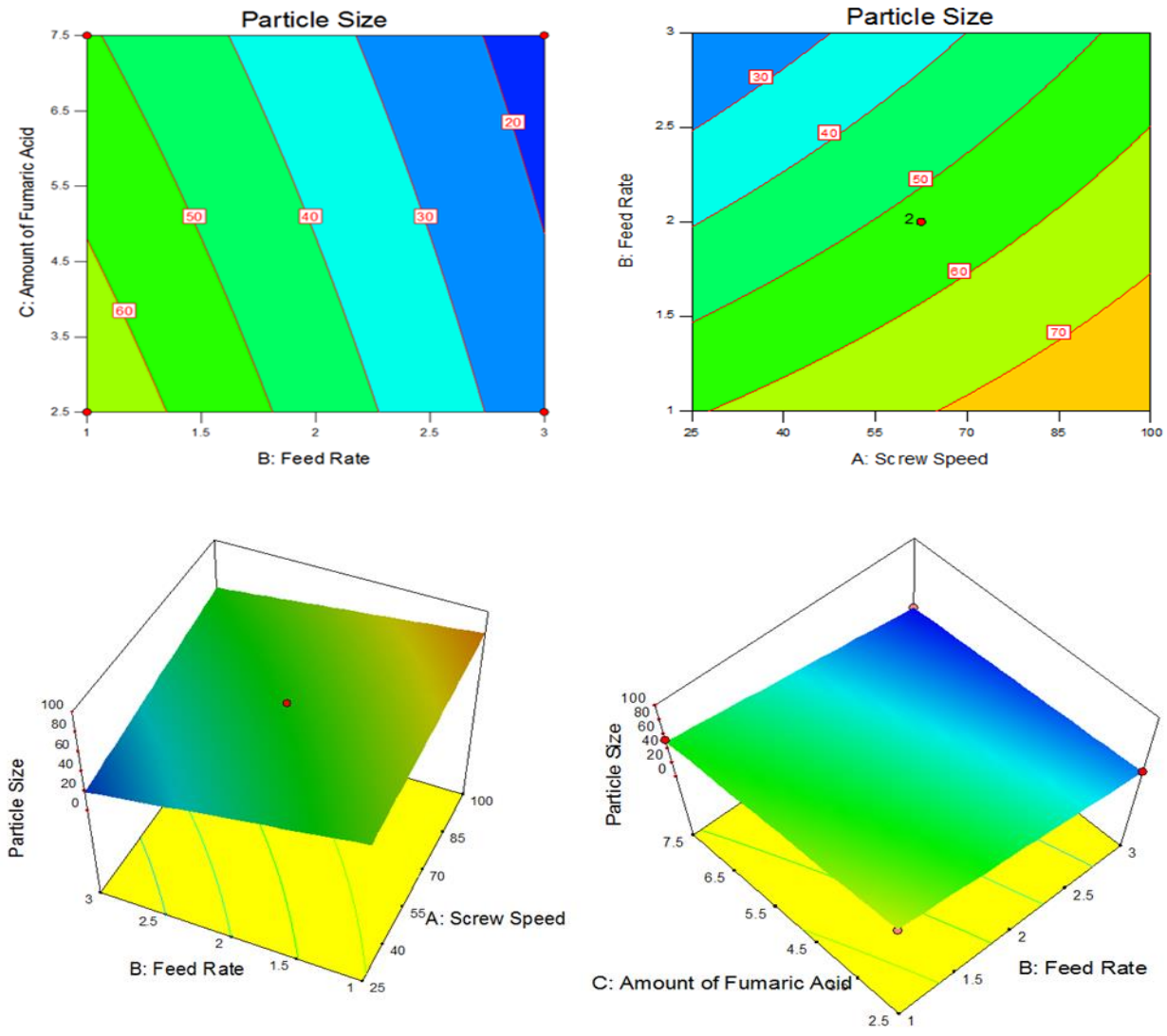

Fig 4.3: Response particle size Contour plot and Response surface graph

4.4.4.3. Flow properties:

Granule flow properties are critical to mixing, die filling and tableting, which may significantly affect dosage uniformity, content and tablet mechanical characteristics. Granule flowability have been assessed by measuring Hausner's ratio, Carr's index and Angle of repose for all the formulations and results are summarized in Table 8. A Hausner's ratio less than 1.25 is considered an indication of good flowability. All the formulations Z1-Z10 showed Hausner's ratio value less than 1.25. A Carr's index below 15 is considered an indication of good flowability (reference). All the formulations showed Carr's index value less than 15 except formulation Z2 and Z9. The angle of repose in a range of 25 to 30 indicates excellent flow properties (USP reference). Formulations Z5, Z8 and Z10 showed excellent flow (angle of repose < 30) and other formulations showed angle of repose more than 30.

Based on 2^3 factorial design, screw speed and feed rate was found to be the significant factors affecting flowability of granules. A polynomial regression equation to describe the response variation to the three variables within the design space was generated. The reduced equation after correction for insignificant terms (in coded units) was:

Angle of Repose = +32.60 - 3.37 *A + 2.63 *B + 1.12 *AB – 1.38 *AC -2.37 *ABC……Eq. 12

Model F-value of 19.26 for the adjusted model implies the model is significant. Lack of fit F-value of 6.25 indicates that the lack of fit is not significant. The adequacy/precision ratio was 10.258 indicating signal adequacy. Screw speed showed the most significant effect on angle of repose of granules. Negative coefficient for screw speed factor indicates the increase in screw speed results in the decrease in the angle of repose that means improving flowability of granules with increase in screw speed. Whereas, feed rate showed positive coefficient which implies

increase in feed rate will result in increase in angle of repose that is poor flowability of granules. These results are well correlated with the particle size of the granules. High screw speed and low feed rate gives the higher percentage of medium size granules that is improving the flowability of granules and therefore lowering the angle of repose. The effect of selected independent variables on angle of repose of granules is represented in contour plots and response surface graphs (Fig. 4.4).

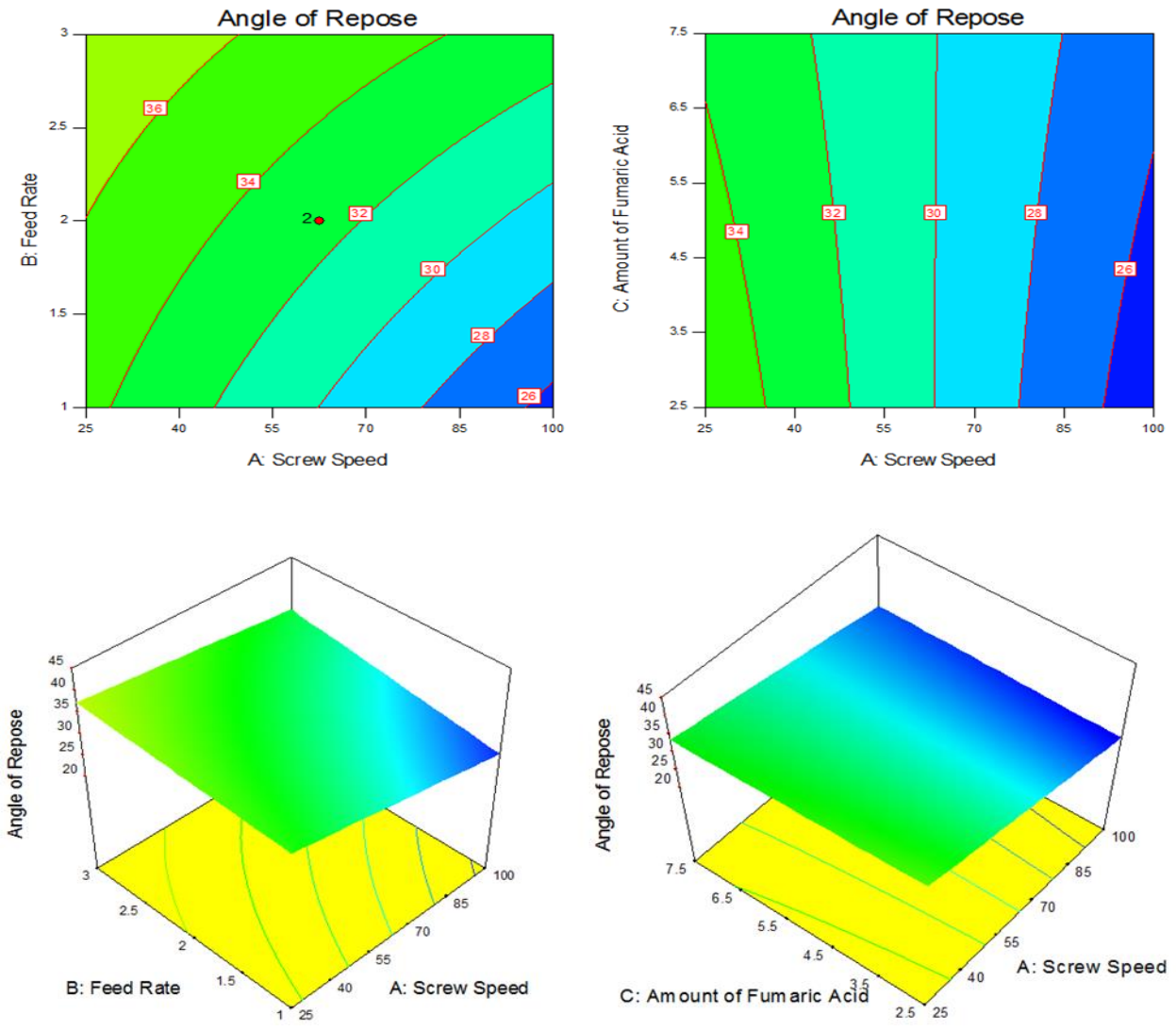

Fig 4.4: Response Angle of Repose Contour plot and Response surface graph

Table 4.9: True density and surface area of twin-screw dry granules

Formulation	True density	Surface area (m2/g)
Z1	1.2419±0.0013	0.2747±0.0021
Z2	1.2421±0.0024	0.2015±0.0046
Z3	1.2490±0.0014	0.2804±0.0023
Z4	1.2643±0.0011	0.1717±0.0023
Z5	1.2801±0.0012	0.3347±0.0080
Z6	1.2786±0.0013	0.1278±0.0034
Z7	1.2227±0.0017	0.3579±0.0093
Z8	1.2246±0.0055	0.3239±0.0079
Z9	1.2163±0.0014	0.3904±0.0094
Z10	1.2185±0.0008	0.2565±0.0061

4.4.4.4. True density and Surface Area:

The true density and surface area of granules for all the formulations has been reported for the granule size between 1.4 mm – 500 μm in Table 4.9.

4.4.5. Characterization of tablets:

4.4.5.1. Physicochemical properties

All the formulations showed uniform weight, thickness and hardness. The average percentage deviation of 20 tablets of each formula was less than ± 5% and hence all formulations passed the test for uniformity of weight as per USP official requirements. Good uniformity content was found among three different batches of tablets.

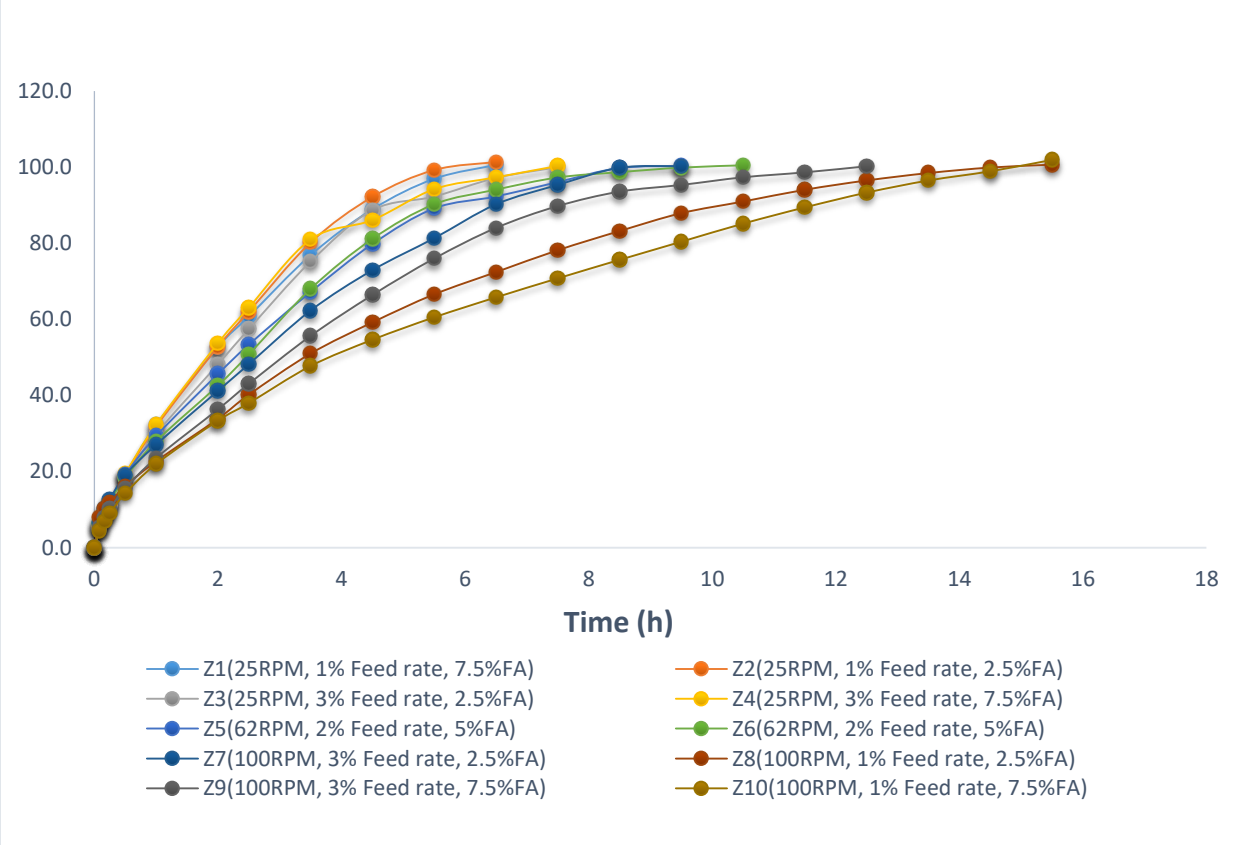

Fig 4.5: Drug Release Profile

4.4.6. *In-vitro* release study

The *in-vitro* release of the drug from all of the formulations has been investigated in gastric fluid (pH 1.2) during first 2 h and then in intestinal fluid (pH 6.8) for the next 22 h. For all the formulations, 100% drug release was achieved but at different time points (Fig. 4.5). The equation derived by best fit mathematical model for dissolution time response with independent variable was:

Dissolution time = +10.10 + 3.13 *A -0.88 *B + 0.38 *C – 1.38 *AB + 0.38 *BC…….Eq. 13

ANOVA analysis of the model equation suggests the F value 26.49 ($p < 0.0001$) indicating the significance of model. The adequacy/precision ratio was 13.950 indicating signal adequacy. It was observed that screw speed is the dominant factor affecting drug release profile. Positive coefficient of screw speed indicates the high screw speed requires more time to release 100% drug from the dosage resulting in slower drug release as compared to medium and low screw speed. This might be due to the increase in screw speed results in high shear generation which results in more binding between drug and polymer resulting in slower release of drug from granules. No differences in dissolution profile were observed at low screw speed. Center point formulations that are Z5 and Z6 showed intermediate dissolution profiles as compared to low and high screw speed batches.

A negative interaction was also observed for AB which has significant effect on dissolution time. Increasing the screw speed expectedly increased the interaction between drug and polymer resulting in the slower drug release from the dosage. At low feed rate the amount inside the material is less and therefore high screw speed at low feed rate resulting in more shear generation on the material.

The Eq. 13 is presented in the form of a contour plots and response surface graphs to visualize the effect of all changing independent variables on dissolution time (Fig. 4.6).

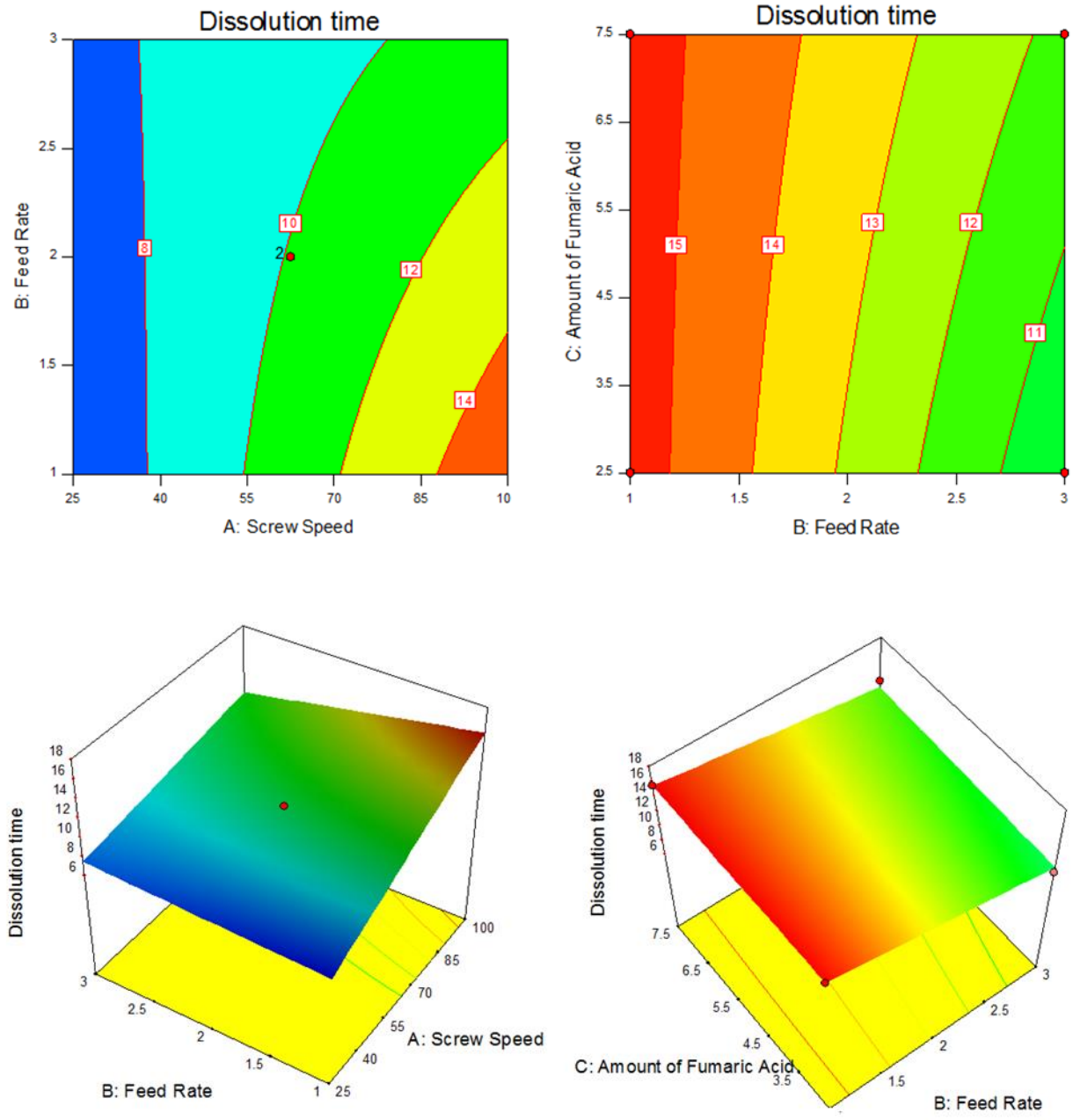

Fig 4.6: Response Dissolution time Contour plot and Response surface graph

Table 4.10: Drug release kinetics

Formulation	Zero Order	First order	Higuchi	Krosmeyer peppas	
	R^2	R^2	R^2	R^2	N
Z1	0.9509	0.9444	0.991	0.9995	0.75
Z2	0.9481	0.878	0.9878	0.999	0.72
Z3	0.9342	0.9708	0.9818	0.9993	0.69
Z4	0.9139	0.9808	0.979	0.9983	0.70
Z5	0.9168	0.8568	0.9822	0.9993	0.63
Z6	0.894	0.9066	0.9777	0.9973	0.62
Z7	0.947	0.8014	0.9843	0.9985	0.58
Z8	0.919	0.8323	0.9926	0.9982	0.59
Z9	0.9151	0.9754	0.9761	0.9986	0.63
Z10	0.9433	0.9011	0.9988	0.9997	0.62

4.4.7. Kinetic modelling of cumulative drug release data

To understand the drug release mechanism from all the 10 formulations Z1-Z10, the *in-vitro* release data were analyzed according to kinetic equations such as zero-order, first-order, Higuchi and Korsmeyer-Peppas. The release rate kinetic data for all the models can be seen in Table 4.10. As shown in Table 4.10, kinetic modeling of the release data for all the formulations were best fitted to Korsmeyer-peppas model. The diffusion coefficient value (n) for all the formulations are within the ranges of 0.59 - 0.72, indicating a non-Fickian diffusion mechanism and that drug release was governed by both diffusion and matrix erosion.

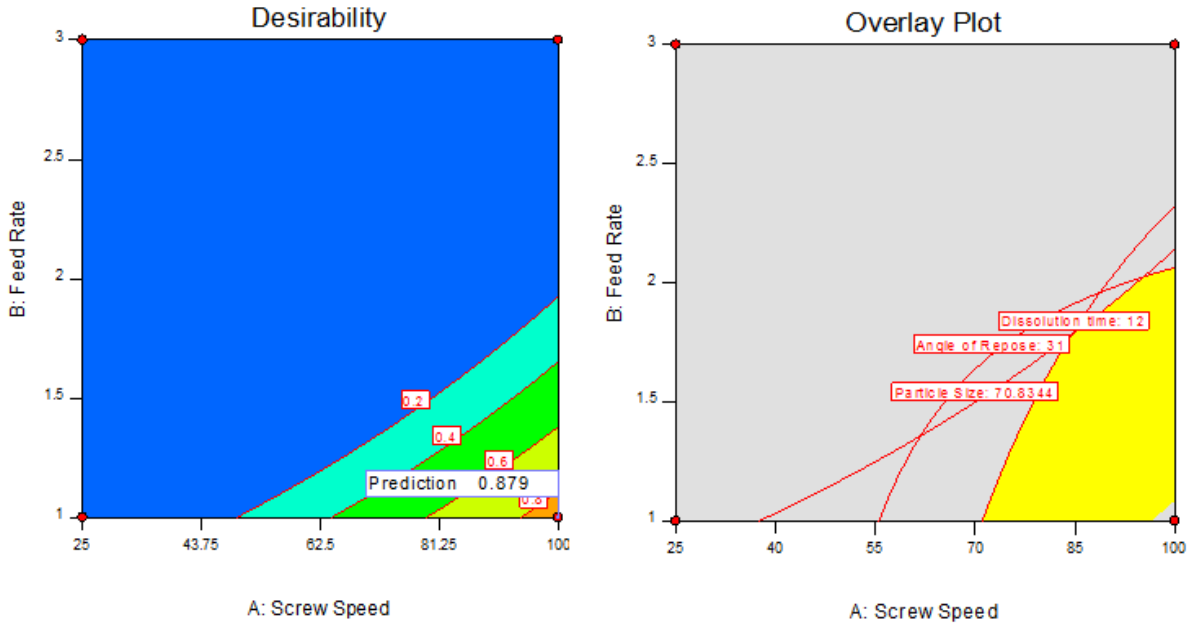

Fig 4.7: Numerical and graphical optimization: Desirability plot and overlay plot

4.4.8. Numerical and graphical optimization

The optimized formulation was selected based on the set criteria of the desired CQA's in the formulation. The percentage of medium size granules and dissolution time required for attaining the complete and controlled drug release were set at maximum, whereas angle of repose was set at minimum level. Desirability plot was constructed to understand the relationship between independent variables and response values (Fig. 4.7). In order to achieve the goal of best formulation, granules should possess good flow properties (lower angle of repose, 25-31), higher percentage of medium size granules (70-90%) and more time should be required for dissolution of dosage (12-16 h). The calculated desirability value for the formulation Z8 is 0.880 which indicated suitability of the designed factorial model. Along with desirability plot, graphical optimization overlay plot for the set response variables is also analyzed (Fig 4.7). It was observed that the optimized formulations with the desired set goals can be achieved at high screw speed (100 RPM), low feed rate (1% or 80 g/hr) and low amount of fumaric acid (2.5%) in the formulation.

4.5. Conclusion

To the best of our knowledge this is the first study in which twin-screw extruder is utilized to develop a novel continuous dry granulation process. QbD approach was successfully used in the preparation of OND sustained release formulation via twin-screw dry granulation process. Free flowing granules with angle of repose 25, medium particle size percentage around 89% and the drug release from the tablet was achieved 100% over the period of 15.5 h. Therefore, the optimized formulation was able to achieve the set target goals of CQAs. The information obtained from this study introduces third method of dry granulation process via twin-screw extruder which can be an adequate method in terms of its overall simplicity as compared to the

currently available methods for dry granulation as well as the feasibility to control and optimize crucial factors more easily, such as particle size. In conclusion, the novel aspect of the current study is its demonstration of the feasibility to continuously manufacture ready-to-compress dry granules of OND by a twin-screw dry granulation process to provide sustained release of the drug.

CHAPTER V

HOT-MELT EXTRUSION PROCESSING INDUCED SOLID-PHASE TRANSFORMATION OF LABILE ACTIVE PHARMACEUTICAL INGREDIENT: PREVENTIVE MEASURES

5.1. Abstract

Hydrates of active pharmaceutical ingredients may undergo dehydration during the manufacturing process and/or storage. This can affect the physiochemical properties of the formulation including solubility, dissolution rate, bioavailability and stability. Ondansetron (OND), a serotonin 5-HT_3 receptor antagonist is a first choice of drug used to treat and prevent chemotherapy/radiotherapy/cancer surgery induced nausea and vomiting, exists in a dihydrate form. The main objective of this study was to understand the dehydration behavior of OND during hot-melt extrusion (HME) process. Differential scanning calorimetry (DSC), thermogravimetric analysis (TGA), dynamic vapor sorption (DVS) and hot stage microscopy (HSM) were used to investigate the solid state phase transformation of OND formulation due to HME process.

5.2. Introduction

A large number of active pharmaceutical ingredients (API) are crystalline in nature and the crystalline solids can exist in different sub-phases such as polymorphs, hydrates, solvates and co-crystals [76]. Understanding the nature of drug molecule crystalline sub-phases, helps in determining the relative physical stability in the solid state, its solution properties and its

absorption [77]. For example the stability and behavior of hydrates can vary widely and this may affect the solid state of API during the processing or storage, by phase transformation such as hydration, dehydration or re-hydration state. Therefore, the knowledge of crystalline sub-phases of API and other pharmaceutical excipients is considered to be an extremely important factor in the preformulation stage, in order to develop a stable pharmaceutical formulation.

Polymorphism in the material science is the ability of a compound or element to exist in more than one crystalline form. The manufacturing process can induce solid state phase transformation which occurs due to changes in process and formulation parameters such as humidity, temperature, solvent and pressure. Therefore, polymorphism of the API is the major problem in the pharmaceutical industry as this can affect the physicochemical properties of API and thus can lead to poor drug absorption, decrease the rate of dissolution and the stability of the formulation [78, 79].

Ondansetron (OND) (Fig 1) is a potent, highly selective, competitive 5-hydroxytryptamine (5-HT_3) receptor antagonist, commonly used to prevent nausea and vomiting caused by chemotherapy, radiotherapy and postoperative treatment. OND has been also listed in "WHO Model List of Essential Medicines" for basic health system [80]. Lacer et al., (1999) reported ondansetron polymorphs, under different experimental conditions such as pH, temperature, pulverization and solvents. The factors which influenced the formation of polymorphs were heating the sample of ondansetron over a range of temperature (40 ^{o}C to 170 ^{o}C) at various time intervals (5 min to 24 h), and the use of different solvents such ethanol and methanol [78].

Hot-melt extrusion (HME) is a well-established technology in non-pharmaceutical industries such as plastic, food, metal and medical devices (sutures). In last 3 decades the application of

HME in pharmaceutical industry has gained lot of attention due to its advantages over a conventional manufacturing process such as has a potential to convert a batch process into a continuous process, less number of processing steps, solvent-free process, easy to scale-up process, etc. Therefore, HME has emerged as an alternative platform technology to other conventional process for manufacturing wide range of pharmaceutical dosage forms such as granules, pellets, mini-tablets, tablets, films, implants etc [4]. HME being a thermal process, despite of the above mentioned advantages, it has few limitations. The main disadvantage is that this process cannot be utilized for heat-labile compounds as this can contribute to stability issue of the API. Therefore, it is essential to study the effect of different HME process parameters (barrel temperature, screw speed, screw configuration and feed rate) on labile active compounds. Till now in the literature, it has only mentioned that HME process cannot be used for sensitive, labile compounds, but no study has been reported to show how HME process parameters induce the phase transformation in active molecules. Along with this it is also important to study how we can optimize the HME processing parameters to prevent such a phase transformation and maintain the stability of the active molecule. In this study, the authors have made an attempt to clarify the effect of HME processing parameters on the dehydration behavior of a labile active pharmaceutical compound OND in the solid state. Therefore, studying the dehydration behavior of an active compound is crucial to predict the physicochemical properties during storage and in order to prevent physicochemical instability of the active compound in the formulation during storage optimizing the HME processing parameters is essential.

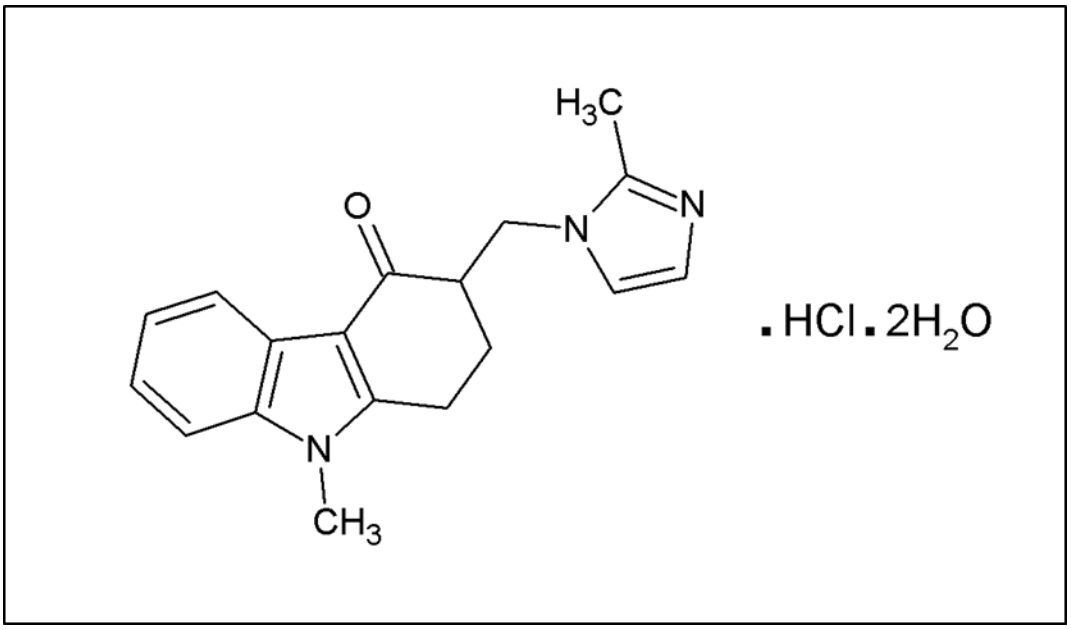

Fig 5.1: Ondansetron Hydrochloride Dihydrate

5.3. Material and Methods

5.3.1. Material

Ondansetron HCl Dihydrate was purchased from Chemscene LLC (New Jersey, USA). Hydroxypropyl cellulose (Klucel^{TM} EF) was generously gifted by Ashland Specialty Ingredients. (Wilmington,DE). Ethyl cellulose (Ethocel Standard 10) was kindly gifted by Dow chemical company. All other reagents used in this study were of the analytical grade.

5.3.2. Methods

5.3.2.1. Design of experiment to prepare drug-polymer extrudates via hot-melt extrusion process:

Physical mixture of drug-polymer containing 20% drug, polymer ethlycellulose (EC) and hydroxylpropyl cellulose (HPC) in a ratio of 1:1 and magnesium stearate (0.5%, as a lubricant) was prepared by using a V-shell blender (GlobePharma, Maxiblend^{TM} New Brunswick, NJ) for

20 min at 25 rpm, after passing through US# 35 mesh screen to remove any aggregates that may have formed. The prepared physical mixture was fed into the co-rotating twin-screw extruder (11 mm Process 11^{TM}, Thermo-Fisher Scientific Karlsruhe, Germany) using a volumetric feeder.

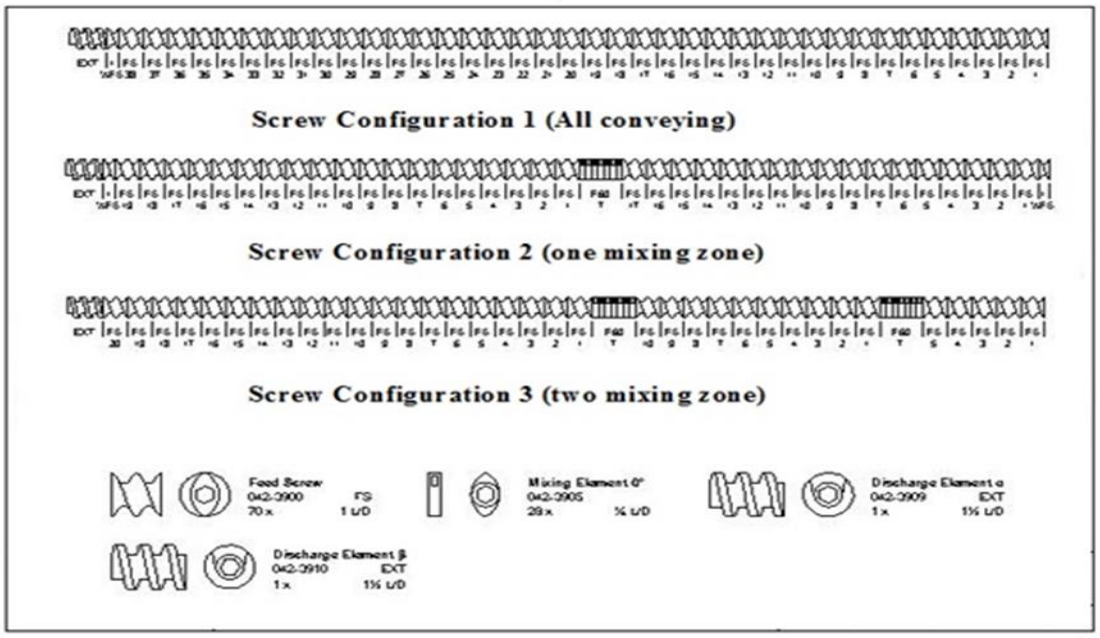

Fig 5.2: Different Screw configurations

To study the effect of screw configuration, screw speed and barrel temperature on dehydration of OND, the authors have designed the experiments as shown in Table 5.1 and 5.2. Briefly, three screw configurations (SC) were used to see the effect of shear stress on the phase transformation of OND that is SC with zero mixing zone, i.e. all conveying elements, second SC contain one mixing zone along with conveying elements and the third SC containing two mixing zones along with the conveying elements (Fig 5.2). Three barrel temperatures (low, medium and high) were utilized to prepare the drug-polymer extrudates at two screw speeds, 25 and 100 rpm. The prepared extrudates with the above mentioned process parameters were then characterized to observe the solid-state phase transformation of OND.

Table 5.1: Extruder process parameters (Barrel Temperature, Screw speed and Feed rate)

Setting No.	Extruder Parameters										
1	Feed Zone	Zone 2	Zone 3	Zone 4	Zone 5	Zone 6	Zone 7	Zone 8	Die	Screw Speed	Feed Rate
	°C									rpm	g/hr
	N/A	140	140	140	140	50	50	50	40	25 or 100	80
2	Feed Zone	Zone 2	Zone 3	Zone 4	Zone 5	Zone 6	Zone 7	Zone 8	Die	Screw Speed	Feed Rate
	°C									rpm	g/hr
	N/A	110	110	110	110	50	50	50	40	25 or 100	80
3	Feed Zone	Zone 2	Zone 3	Zone 4	Zone 5	Zone 6	Zone 7	Zone 8	Die	Screw Speed	Feed Rate
	°C									rpm	g/hr
	N/A	90	90	90	90	50	50	50	40	25 or 100	80

Table 5.2: Design of experiments

Batch #	Screw Configuration (# of Mixing zones)	Barrel Temp (℃)	Screw speed (rpm)
A1	2	90	100
A2	2	90	25
A3	2	110	100
A4	2	110	25
A5	2	140	100
A6	2	140	25
A7	0	90	25
A8	0	90	100
A9	0	110	25
A10	0	110	100
A11	0	140	25
A12	0	140	100
A13	1	90	25
A14	1	90	100
A15	1	110	25
A16	1	110	100
A17	1	140	25
A18	1	140	100

5.3.3. Characterization of HME extrudates:

5.3.3.1. Differential Scanning Calorimetry (DSC)

Diamond DSC (Perkin Elmer Life and Analytical Sciences, Waltham, MA, USA) was used to study the phase transformation of OND in HME extrudates. 3-5 mg of pure API, physical mixture and HME extrudates were weighed and hermetically sealed in aluminum pans and the thermal analysis was performed over a temperature range of 25-250 °C at a heating rate of 10 $^{\circ C}$/min, under an inert nitrogen atmosphere at a flow rate of 20 mL/min. Endothermic onset and peak temperature of melting were calculated from the obtained thermogram using Pyris™ Manager software (PerkinElmer Life and Analytical Sciences, 719 Bridgeport Ave., CT, USA).

5.3.3.2. Thermogravimetric Analysis (TGA)

TGA (Pyris 1 TGA Perkin Elmer) was utilized to determine the weight loss of the pure OND. Weighed sample of OND was heated from 25 ^{o}C to 300 ^{o}C at a rate of 20 ^{o}C/min. in a platinum pan under an inert nitrogen atmosphere purge of 20 ml per minute

5.3.3.3. Dynamic Vapor Sorption (DVS)

The DVS (Surface Measurement Systems, London, UK) is a commercially available water sorption balance, which allows a sample to be weighed during exposure to defined temperature and humidity conditions and was employed to measure the mass change of OND during the isotherm dehydration studies. Approximately, 14 mg of the OND was weighed onto the aluminum pan. To study the phase transformation of OND under the influence of humidity, the DVS apparatus was programmed to run from 0% to 90% RH with the increment of 10% RH and then again going from 90% to 0% RH with the 10% RH increment. This allowed investigations

into the effects on OND after the exposure 0-90-0% RH. All experiments were run at 25 ^{o}C and in triplicates. The accuracy of the system is ±1.0% for the RH and ±0.2 ^{o}C for the temperature.

5.3.3.4. Hot Stage Microscopy (HSM)

Thermal events of OND HCl $2H_2O$ samples were evaluated using hot-stage microscopy (HSM). A glass slide with a small amount of the sample was inserted into a hot-stage system (FTIR 600, Linkam Scientific Instruments, Surrey, UK). The sample was examined by dispersing it in silicone oil heated from 35 °C to 150 °C temperature range at a constant rate of 2 °C/min. A camera-mounted optical microscope (Cary 620 IR, Agilent Technologies, Santa Clara, CA, USA) equipped with a hot-stage was used to capture images at different stages of the transformation.

5.4. Result and discussion

5.4.1. DSC

a. Effect of Screw Configuration on the easily-dehydrated drug Ondansetron:

Effect of different screw configuration on OND phase transformation was studied by DSC (Fig 5.3). When drug-polymer physical mixture was processed under screw configuration with all conveying elements, the DSC curves exhibited the melting peak of OND HCl $2H_2O$ at 189 ^{o}C which is same as physical mixture corresponding to the melting peak of dihydrate form. For one mixing zone screw configuration, the melting peak shifted from 189 ^{o}C (black arrow) to 179 ^{o}C (pink arrow) and there is occurrence of new endothermic peak at high temperature was seen at 214 ^{o}C. The same results were obtained when two mixing zone screw configuration was used. The melting endothermic peak corresponding to dihydrate form shifted to lower temperature (at 169 ^{o}C) and new dehydrated form endothermic peak was observed at 223 ^{o}C. The increase in

number of mixing zone results in intense mixing and high shear mechanical energy exerted on the material. In the HME process, there are two components responsible for melting of material that is energy from the heater and applied shear stress. Therefore, the design of the screw has a significant impact on the process and can be selected to meet particular requirements such as high or low shear. From the results it can be concluded that an increase in number of mixing zone results in further dehydration on OND HCl $2H_2O$. And therefore, the high shear generated during HME process should have an important role in OND dehydration.

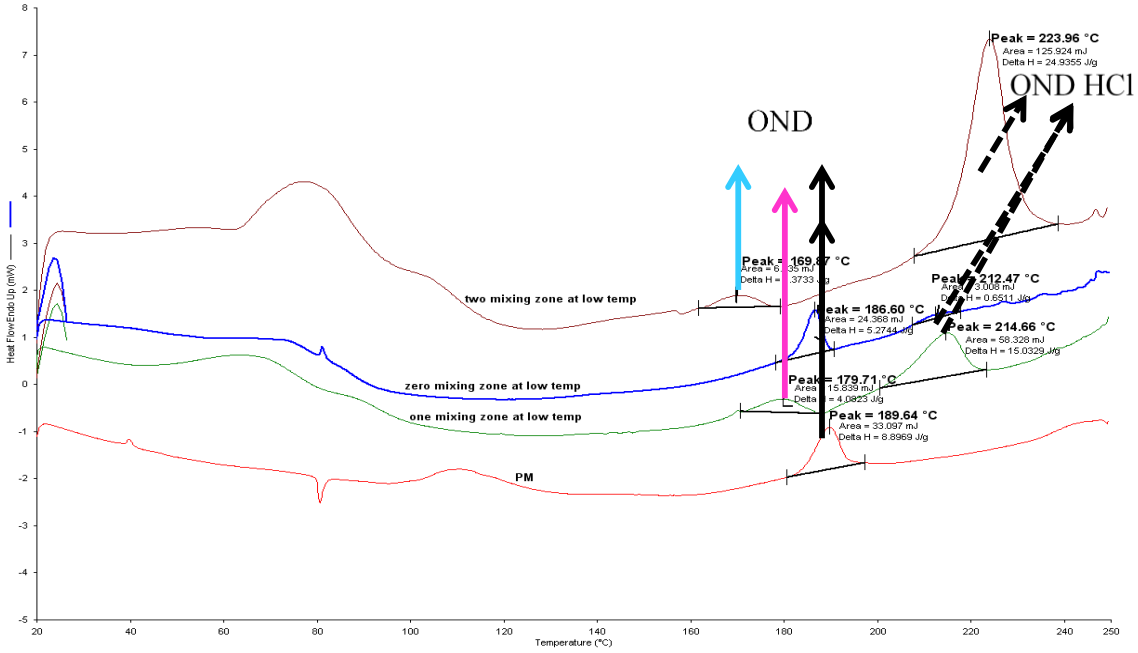

Fig 5.3: DSC thermogram - screw configuration effect on dehydration of OND

b. Effect of Barrel temperature

In order to check the effect of barrel temperature on OND dehydration, the samples extruded from all conveying screw configurations under low and high temperatures were scanned by DSC (Fig 5.4). The DSC results showed that there was no shift in the melting peak of OND between different processing temperatures when all conveying element screw configurations was utilized,

but with high temperature there was an appearance of new endothermic peak at 219 ^{o}C corresponding to dehydration peak of OND. However, with two mixing zone screw configuration at high temperature, there was only one endothermic peak observed at 217 ^{o}C confirming that the OND undergone complete phase transformation due to high shear as well as high temperature. It looks like increasing process temperatures did not generate much interaction between the drug and polymers. The high shear should be the main issue for drug-polymer interaction. For the drug dehydration, barrel temperature along with shear stress also played a key function generating more dehydration.

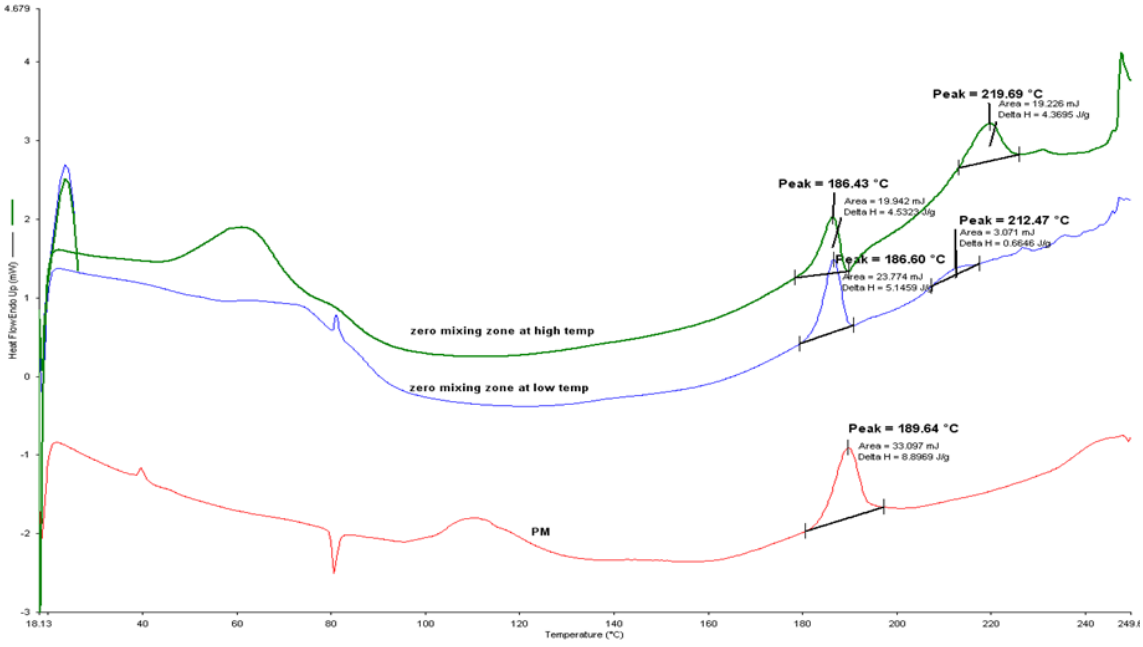

Fig 5.4: DSC thermogram - temperature effect on dehydration of OND

c. Effect of screw speed

DSC thermogram of the extrudates prepared with high and low screw speed with one mixing zone SC both at high and low temperature is shown in Figure 5.5 and 5.6. From the thermogram it was observed that screw speed do not affect the dehydration process of OND as such when compared to the other factors SC and barrel temperature. For both screw speeds the melting endothermic peak for Ondansetron was observed at 190 ^{o}C indicating no change in the DSC thermogram due to the change in the screw speed process parameter.

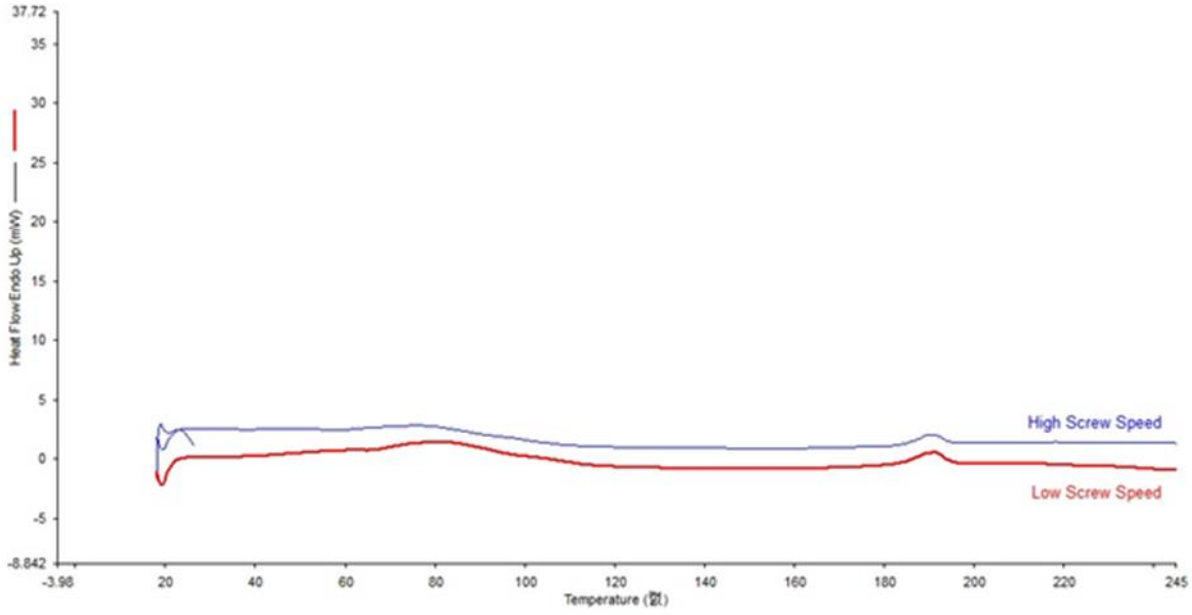

Fig 5.5: One mixing zone SC at low temperature – effect of screw speed on dehydration of OND

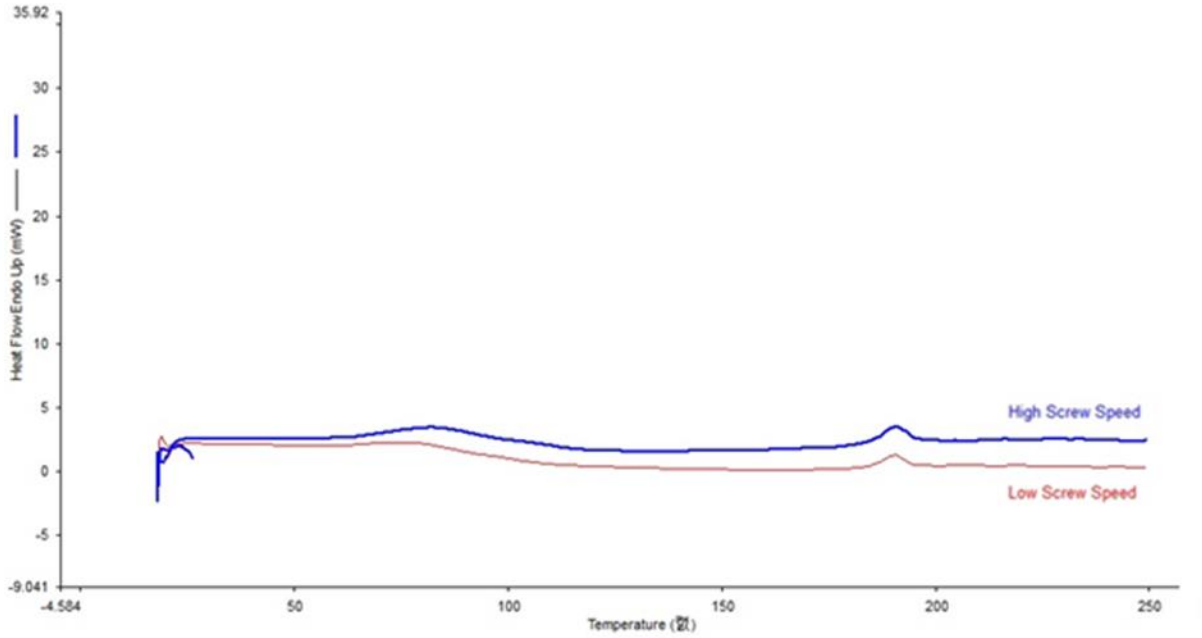

Fig 5.6: One mixing zone SC at high temperature – effect of screw speed on dehydration of OND

5.4.2. TGA

TGA thermogram of OND is presented in Fig 5.7. It is clearly illustrated from TGA results that heating of OND results in the loss of 2 moles of loosely bound water. As shown in Figure 6, ~10 % of weight was lost when OND heated from 60-105 ^{o}C. This value is in agreement with the theoretical value for 2 moles of water in OND.

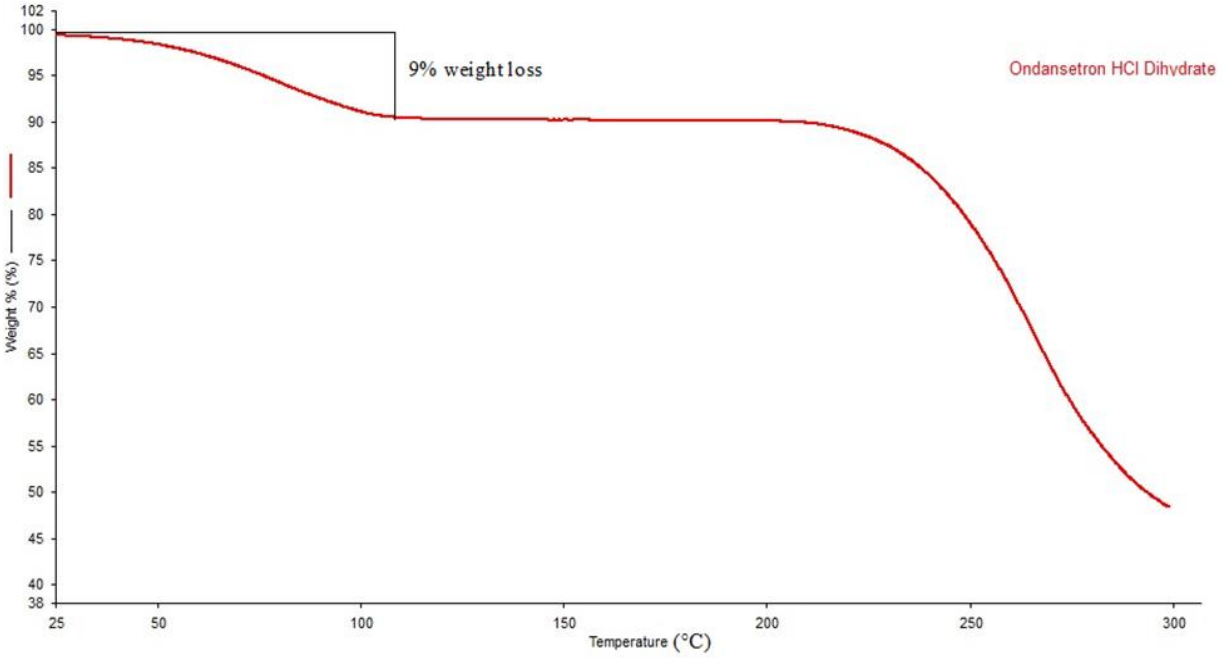

Fig 5.7: Thermogravimetric analysis of OND

5.4.3. DVS

Drying curve and DVS mass plot of OND is shown in Fig 5.8 and 5.9. The DVS data showed a significant change in mass at 0% RH for the period of 100 min. The weight loss of 9.5% at 0% RH is corresponding to the loss of two water molecules resulting in the dehydration of OND. As the RH increased from 0% to 10% and then to 20%, there was a 2.67% and 8.9% weight gain was observed respectively in the DVS graph. There was a very slight gain in the weight (from 8.9% to 9.2%) observed with the increase in RH beyond 20% upto 90%. In the DVS study, decreased RH only caused a slight decrease in the sample mass over 90% to 20% RH range. At 10% RH, dihydrate starts to lose its crystal water and its weight largely decreases upto 4.44% corresponding to one water molecule. When humidity was further reduced, DVS data showed a rapid decrease in water content, indicating loss of a second water molecule from the API at 0%

RH. The weight at 0% RH reached to the original weight of the sample indicating complete dehydration of OND.

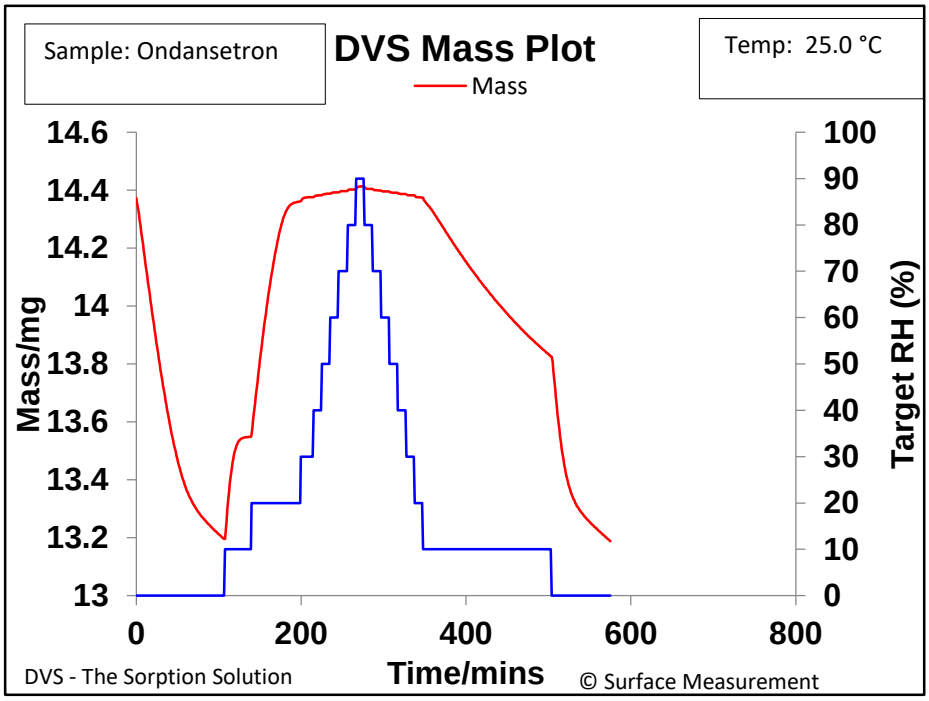

Fig 5.8: DVS mass plot

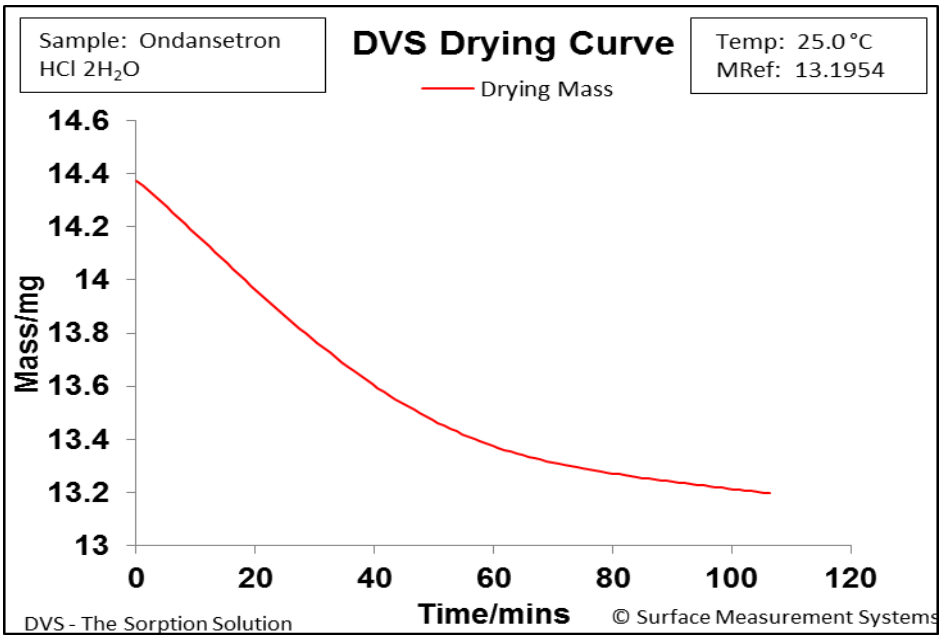

Fig 5.9: DVS Drying curve of Ondansetron HCl $2H_2O$

5.4.4. HSM

The transition of pharmaceutical polymorphs can be visually and semi-quantitatively detected by hot-stage microscopy. HSM thermal events are presented in Fig 5.10. HSM results revealed that the dehydration event as a gradual appearance and disappearance of water bubbles starting from 90 ^{o}C till 104 ^{o}C. Temperatures below 90 ^{o}C there was no water bubbles seen in HSM images. Around 156 ^{o}C, the HSM images got foggy due to the condensation of water evaporated from the sample on the glass surface. After cleaning the condensation on the top glass, the image was much clearer at temperature 179 ^{o}C. Around temperature 192 ^{o}C, drug particles started to melt and at 196 ^{o}C it almost completely melted. The present HSM images indicated that OND crystals were first dehydrated and then started to melt at temperature 192 ^{o}C. These HSM results are well correlates with the TGA thermogram where dehydration event was seen between the temperature ranges of 60-105 ^{o}C.

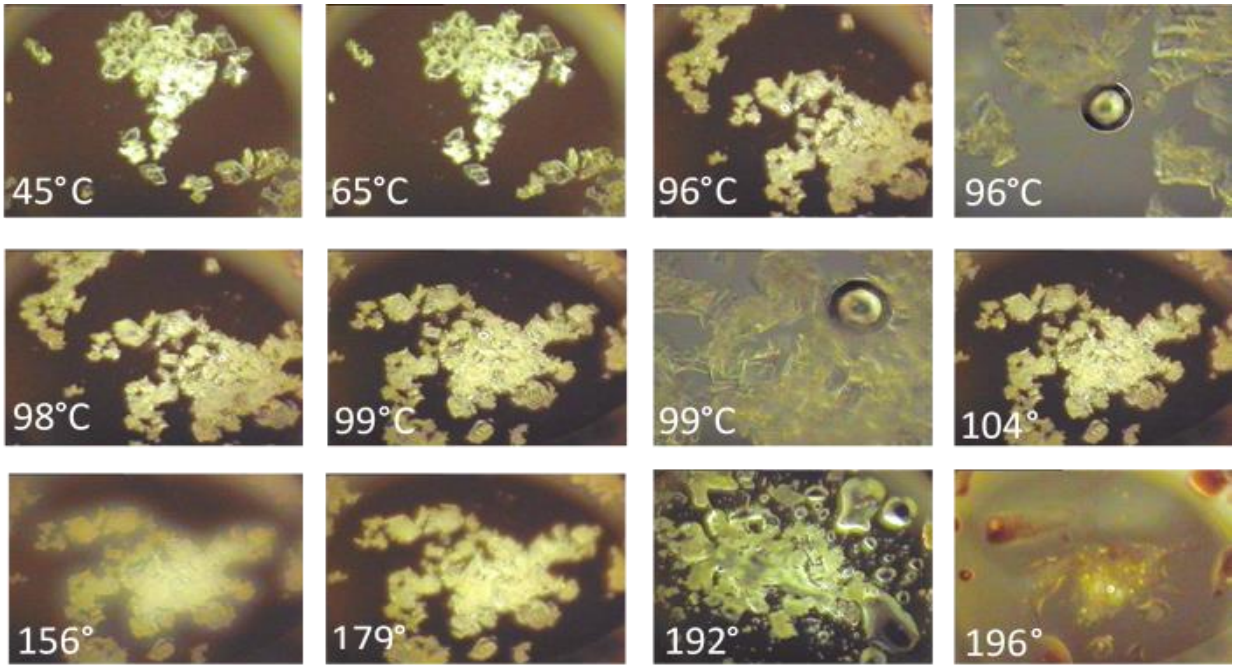

Fig 5.10: Hot stage microscopy images

5.5 Conclusion:

Verification and screening stability in solid state methods proposed in this paper provide full and detailed information about the dehydration behavior of Ondansetron hydrochloride dihydrate. The thermal-dependent dehydration process of ondansetron hydrochloride dihydrate in the solid state was effectively studied using thermal techniques DSC and TGA. Also, hot stage microscopy and dynamic vapor sorption techniques were successfully used to confirm dehydration process of OND. In the solid state, phase transformation due to dehydration process induced by processing parameters may lead to the production of metastable or intermediate form of API. Hot melt extrusion is a thermal and shear generating process. Therefore, it is essential to do preliminary study to see the effect of temperature and shear on the solid state phase transformation of API in-order to formulate a stable product via hot melt extrusion process. From the results, it confirms that both shear as well as temperature is significant factor responsible for the dehydration of OND. It was found that screw speed do not affect dehydration process of OND. In conclusion, to produce stable optimized formulation of OND via HME, low shear and low temperature should be the choice of process parameter.

BIBLIOGRAPHY

REFERENCES

1. el-Egakey, M.A., M. Soliva, and P. Speiser, *Hot extruded dosage forms. I. Technology and dissolution kinetics of polymeric matrices.* Pharm Acta Helv, 1971. **46**(1): p. 31-52.
2. McGinity, J.W., et al., *Hot-melt extrusion as a pharmaceutical process.* Am Pharm Rev, 2001. **4**: p. 25-37.
3. Breitenbach, J., *Melt extrusion: from process to drug delivery technology.* Eur J Pharm Biopharm, 2002. **54**(2): p. 107-17.
4. Crowley, M.M., et al., *Pharmaceutical applications of hot-melt extrusion: part I.* Drug Dev Ind Pharm, 2007. **33**(9): p. 909-26.
5. Patil, H., et al., *Continuous manufacturing of solid lipid nanoparticles by hot melt extrusion.* Int J Pharm, 2014. **471**(1-2): p. 153-6.
6. Patil, H., et al., *Formulation and development of pH-independent/dependent sustained release matrix tablets of ondansetron HCl by a continuous twin-screw melt granulation process.* Int J Pharm, 2015. **496**(1): p. 33-41.
7. Repka, M.A., et al., *Pharmaceutical applications of hot-melt extrusion: Part II.* Drug Dev Ind Pharm, 2007. **33**(10): p. 1043-57.
8. Repka, M.A., et al., *Applications of hot-melt extrusion for drug delivery.* Expert Opin Drug Deliv, 2008. **5**(12): p. 1357-76.
9. Repka, M.A., et al., *Melt extrusion: process to product.* Expert Opin Drug Deliv, 2012. **9**(1): p. 105-25.
10. Shah, S., et al., *Melt extrusion with poorly soluble drugs.* Int J Pharm, 2013. **453**(1): p. 233-52.
11. Shah, S. and M.A. Repka, *Melt extrusion in drug delivery: three decades of progress*, in *Melt Extrusion*. 2013, Springer. p. 3-46.
12. Chokshi, R. and H. Zia, *Hot-melt extrusion technique: a review.* Ira J Pharm Res, 2010: p. 3-16.
13. Patil, H., R.V. Tiwari, and M.A. Repka, *Hot-Melt Extrusion: from Theory to Application in Pharmaceutical Formulation.* AAPS PharmSciTech, 2016. **17**(1): p. 20-42.
14. Patil, H., R.V. Tiwari, and M.A. Repka, *11 Encapsulation via Hot-Melt Extrusion.* 2016.
15. Leister, D., T. Geilen, and T. Geissler, *Twin-screw Extruders for Pharmaceutical Hot-melt Extrusion: Technology, Techniques and Practices.* Hot-melt Extrusion: Pharmaceutical Applications, 2012: p. 23-42.
16. Basalious, E.B., W. El-Sebaie, and O. El-Gazayerly, *Application of pharmaceutical QbD for enhancement of the solubility and dissolution of a class II BCS drug using polymeric surfactants and crystallization inhibitors: development of controlled-release tablets.* AAPS PharmSciTech, 2011. **12**(3): p. 799-810.
17. Maltesen, M.J., et al., *Quality by design - Spray drying of insulin intended for inhalation.* Eur J Pharm Biopharm, 2008. **70**(3): p. 828-38.
18. Patil-Gadhe, A. and V. Pokharkar, *Single step spray drying method to develop proliposomes for inhalation: a systematic study based on quality by design approach.* Pul Pharmacol Ther, 2014. **27**(2): p. 197-207.
19. Yerlikaya, F., et al., *Development and Evaluation of Paclitaxel Nanoparticles Using a Quality-by-Design Approach.* J Pharm Sci, 2013. **102**(10): p. 3748-3761.

20. Hanafy, A., et al., *Pharmacokinetic evaluation of oral fenofibrate nanosuspensions and SLN in comparison to conventional suspensions of micronized drug.* Adv Drug Deliv Rev, 2007. **59**(6): p. 419-26.
21. Chandra Sekhara Rao, G., et al., *Nanosuspensions as the most promising approach in nanoparticulate drug delivery systems.* Pharmazie, 2004. **59**(1): p. 5-9.
22. Niu, X., et al., *Mesoporous carbon as a novel drug carrier of fenofibrate for enhancement of the dissolution and oral bioavailability.* Int J Pharm, 2013. **452**(1-2): p. 382-9.
23. Sanganwar, G.P. and R.B. Gupta, *Dissolution-rate enhancement of fenofibrate by adsorption onto silica using supercritical carbon dioxide.* Int J Pharm, 2008. **360**(1): p. 213-218.
24. Mehnert, W. and K. Mader, *Solid lipid nanoparticles: production, characterization and applications.* Adv Drug Deliv Rev, 2001. **47**(2-3): p. 165-96.
25. Wishart, D.S., et al., *DrugBank: a comprehensive resource for in silico drug discovery and exploration.* Nucleic Acids Res, 2006. **34**(Database issue): p. D668-72.
26. Das, S., et al., *Formulation design, preparation and physicochemical characterizations of solid lipid nanoparticles containing a hydrophobic drug: effects of process variables.* Colloids Surf B Biointerfaces, 2011. **88**(1): p. 483-9.
27. Dong, Y., et al., *Solid lipid nanoparticles: continuous and potential large-scale nanoprecipitation production in static mixers.* Colloids Surf B Biointerfaces, 2012. **94**: p. 68-72.
28. Raza, K., et al., *Systematically optimized biocompatible isotretinoin-loaded solid lipid nanoparticles (SLNs) for topical treatment of acne.* Colloids Surf B Biointerfaces, 2013. **105**: p. 67-74.
29. Shah, R.M., et al., *Physicochemical characterization of solid lipid nanoparticles (SLNs) prepared by a novel microemulsion technique.* J Colloid Interface Sci, 2014. **428**: p. 286-94.
30. Luo, Y., et al., *Solid lipid nanoparticles for enhancing vinpocetine's oral bioavailability.* J Control Release, 2006. **114**(1): p. 53-9.
31. Wang, S., et al., *Emodin loaded solid lipid nanoparticles: preparation, characterization and antitumor activity studies.* Int J Pharm, 2012. **430**(1-2): p. 238-46.
32. Hu, L., X. Tang, and F. Cui, *Solid lipid nanoparticles (SLNs) to improve oral bioavailability of poorly soluble drugs.* J Pharm Pharmacol, 2004. **56**(12): p. 1527-35.
33. Liu, J., et al., *Isotretinoin-loaded solid lipid nanoparticles with skin targeting for topical delivery.* Int J Pharm, 2007. **328**(2): p. 191-5.
34. Rahman, Z., et al., *Understanding the quality of protein loaded PLGA nanoparticles variability by Plackett-Burman design.* Int J Pharm, 2010. **389**(1-2): p. 186-94.
35. Huang, Q.P., et al., *Preparation of ultrafine fenofibrate powder by solidification process from emulsion.* Int J Pharm, 2009. **368**(1-2): p. 160-4.
36. van Drooge, D.J., W.L. Hinrichs, and H.W. Frijlink, *Anomalous dissolution behaviour of tablets prepared from sugar glass-based solid dispersions.* J Control Release, 2004. **97**(3): p. 441-52.
37. Galli, C., *Experimental determination of the diffusion boundary layer width of micron and submicron particles.* Int J Pharm, 2006. **313**(1-2): p. 114-22.

38. Jia, Z., et al., *A novel nanomatrix system consisted of colloidal silica and pH-sensitive polymethylacrylate improves the oral bioavailability of fenofibrate.* Eur J Pharm Biopharm, 2011. **79**(1): p. 126-34.
39. Müller, R.H. and K. Peters, *Nanosuspensions for the formulation of poorly soluble drugs: I. Preparation by a size-reduction technique.* Inter J Pharm, 1998. **160**(2): p. 229-237.
40. Borkar, N., et al., *Investigating the correlation between in-vivo absorption and in-vitro release of fenofibrate from lipid matrix particles in biorelevant medium.* Eur J Pharm Sci, 2014. **51**: p. 204-10.
41. Noyes, A.A. and W.R. Whitney, *The rate of solution of solid substances in their own solutions.* J Am Chem Soc, 1897. **19**(12): p. 930-934.
42. Perissutti, B., et al., *Formulation design of carbamazepine fast-release tablets prepared by melt granulation technique.* Int J Pharm, 2003. **256**(1-2): p. 53-63.
43. Tan, D.C., et al., *Effect of binders on the release rates of direct molded verapamil tablets using twin-screw extruder in melt granulation.* Int J Pharm, 2014. **463**(1): p. 89-97.
44. Voinovich, D., et al., *Melt pelletization in high shear mixer using a hydrophobic melt binder: influence of some apparatus and process variables.* Eur J Pharm Biopharm, 2001. **52**(3): p. 305-13.
45. Voinovich, D., et al., *Screening of high shear mixer melt granulation process variables using an asymmetrical factorial design.* Int J Pharm, 1999. **190**(1): p. 73-81.
46. Yang, D., et al., *Effect of the melt granulation technique on the dissolution characteristics of griseofulvin.* Int J Pharm, 2007. **329**(1-2): p. 72-80.
47. Aoki, H., et al., *Fine granules showing sustained drug release prepared by high-shear melt granulation using triglycerin full behenate and milled microcrystalline cellulose.* Int J Pharm, 2015. **478**(2): p. 530-9.
48. Campisi, B., et al., *Melt granulation in a high shear mixer: optimization of mixture and process variables using a combined experimental design.* Chemo Intel Lab Sys, 1999. **48**(1): p. 59-70.
49. Liu, J., F. Zhang, and J.W. McGinity, *Properties of lipophilic matrix tablets containing phenylpropanolamine hydrochloride prepared by hot-melt extrusion.* Eur J Pharm Biopharm, 2001. **52**(2): p. 181-90.
50. Maniruzzaman, M., et al., *A review of hot-melt extrusion: process technology to pharmaceutical products.* ISRN Pharm, 2012. **2012**: p. 436763.
51. Harris, D.G., *Nausea and vomiting in advanced cancer.* Br Med Bull, 2010. **96**: p. 175-85.
52. McManis, P.G. and N.J. Talley, *Nausea and Vomiting Associated With Selective Serotonin Reuptake Inhibitors.* CNS drugs, 1997. **8**(5): p. 394-401.
53. Glare, P.A., et al., *Treatment of nausea and vomiting in terminally ill cancer patients.* Drugs, 2008. **68**(18): p. 2575-90.
54. Hesketh, P.J. and D.R. Gandara, *Serotonin antagonists: a new class of antiemetic agents.* J Natl Cancer Inst, 1991. **83**(9): p. 613-20.
55. Warr, D.G., *Chemotherapy-and cancer-related nausea and vomiting.* Curr Oncol, 2008. **15**(Suppl 1): p. S4-9.
56. Ye, J.H., R. Ponnudurai, and R. Schaefer, *Ondansetron: a selective 5-HT(3) receptor antagonist and its applications in CNS-related disorders.* CNS Drug Rev, 2001. **7**(2): p. 199-213.

57. Gungor, S., et al., *Ondansetron-loaded biodegradable microspheres as a nasal sustained delivery system: in-vitro/in-vivo studies.* Pharm Dev Technol, 2010. **15**(3): p. 258-65.
58. Rojanasthien, N., et al., *Pharmacokinetics and bioavailability studies of generic ondansetron, and the innovator preparation, in healthy Thai male volunteers.* J Med Assoc Thai, 1999. **82**(7): p. 713-20.
59. Siepe, S., et al., *Microenvironmental pH and microviscosity inside pH-controlled matrix tablets: an EPR imaging study*. J Control Release, 2006. **112**(1): p. 72-8.
60. Venkatesh, G., et al., *Drug delivery systems comprising weakly basic drugs and organic acids*. 2009, Google Patents.
61. Streubel, A., et al., *pH-independent release of a weakly basic drug from water-insoluble and -soluble matrix tablets.* J Control Release, 2000. **67**(1): p. 101-10.
62. Gabr, K., *Effect of organic acids on the release patterns of weakly basic drugs from inert sustained release matrix tablets.* European journal of pharmaceutics and biopharmaceutics, 1992. **38**(6): p. 199-202.
63. Corti, G., et al., *Sustained-release matrix tablets of metformin hydrochloride in combination with triacetyl-beta-cyclodextrin.* Eur J Pharm Biopharm, 2008. **68**(2): p. 303-9.
64. Dvorackova, K., et al., *The effect of acid pH modifiers on the release characteristics of weakly basic drug from hydrophlilic-lipophilic matrices.* AAPS PharmSciTech, 2013. **14**(4): p. 1341-8.
65. He, W., et al., *Matrix tablets for sustained release of repaglinide: Preparation, pharmacokinetics and hypoglycemic activity in beagle dogs.* Int J Pharm, 2014. **478**(1): p. 297-307.
66. Moore, J.W. and H.H. Flanner, *Mathematical comparison of dissolution profiles.* Pharm Technol, 1996. **20**(6): p. 64-74.
67. Pillay, V. and R. Fassihi, *Evaluation and comparison of dissolution data derived from different modified release dosage forms: an alternative method.* J Control Release, 1998. **55**(1): p. 45-55.
68. Bose, A., T.W. Wong, and N. Singh, *Formulation development and optimization of sustained release matrix tablet of Itopride HCl by response surface methodology and its evaluation of release kinetics.* Saudi Pharm J, 2013. **21**(2): p. 201-13.
69. Higuchi, T., *Mechanism of Sustained-Action Medication. Theoretical Analysis of Rate of Release of Solid Drugs Dispersed in Solid Matrices.* J Pharm Sci, 1963. **52**: p. 1145-9.
70. Korsmeyer, R.W., et al., *Mechanisms of solute release from porous hydrophilic polymers.* Int J Pharm, 1983. **15**(1): p. 25-35.
71. Wells, J.I., *Pharmaceutical preformulation: the physicochemical properties of drug substances*. 1988: Ellis Horwood Chichester.
72. Espinoza, R., E. Hong, and L. Villafuerte, *Influence of admixed citric acid on the release profile of pelanserin hydrochloride from HPMC matrix tablets.* Int J Pharm, 2000. **201**(2): p. 165-73.
73. Parikh, D.M., *Handbook of pharmaceutical granulation technology*. Drugs and the pharmaceutical sciences;, 2005. **154**(Second edition): p. 1-6.
74. Sandler, N. and R.F. Lammens, *Pneumatic dry granulation: potential to improve roller compaction technology in drug manufacture.* Expert Opin Drug Deliv, 2011. **8**(2): p. 225-36.

75. Shanmugam, S., *Granulation techniques and technologies: recent progresses.* Bioimpacts, 2015. **5**(1): p. 55-63.
76. Seton, L., et al., *Processing induced transformations: Phase impurities introduced during hydration/dehydration.* Chem Eng Sci, 2012. **77**: p. 57-64.
77. Zhu, H.J., *Dehydration behavior and structural characterization of the GW275919X monohydrate.* Int J Pharm, 2006. **315**(1-2): p. 18-23.
78. Llacer, J.M., et al., *Formation of ondansetron polymorphs.* Int J Pharm, 1999. **177**(2): p. 221-9.
79. Singhal, D. and W. Curatolo, *Drug polymorphism and dosage form design: a practical perspective.* Adv Drug Deliv Rev, 2004. **56**(3): p. 335-47.
80. Organization, W.H., *WHO model list of essential medicines: 18th list, April 2013.* 2013.

VITA

Hemlata Patil was born in Navi Mumbai, MH, India on July 19th, 1984. She got her Bachelor degree in Basic Pharmaceutical Sciences from University of Pune, India, in May 2006 and Master degree in Industrial Pharmaceutics from SNDT College of Pharmacy at Mumbai, India, in October 2008. In 2012, she joined Dr. Michael A. Repka's laboratory, Department of Pharmaceutics and Drug Delivery, The University of Mississippi as a graduate assistant to pursue her doctoral degree. She successfully completed a summer internship at Boehringer Ingelheim pharmaceuticals, Ridgefield, CT, USA in 2013. She was awarded a Doctor of Philosophy degree in Pharmaceutics in the May of 2016.